DEPARTMENT OF CIVIL ENGINEERING

AN INVESTIGATION OF THE EFFECT OF DYNAMIC AND STATIC LOADING TO GEOSYNTHETIC REINFORCED PAVEMENTS OVERLYING A SOFT SUBGRADE

Candidate:
Dennis K. Kiptoo

Supervisors:
Dr. Denis Kalumba
Dr. Felix Okonta

A thesis submitted to the University of Cape Town in partial fulfilment of the requirement for the degree of Master of Science in Civil Engineering, specialising in Geotechnical Engineering.

May 2016

PLAGIARISM DECLARATION

1. I know that plagiarism is wrong. Plagiarism is to use another's work and to pretend that it is one's own.

2. I have used the Harvard Convention for citation and referencing. Each significant contribution to and quotation in this report form the work or works of other people has been attributed and has been cited and referenced.

3. This report is my own work.

4. I have not allowed and will not allow anyone to copy my work with the intention of passing it as his or her own work

Date: _____18th MAY 2016_____

Signature:_____Signed by candidate_____

DENNIS KIPNGETICH KIPTOO

DEDICATION

To Dad, Mum, Lagoo, Stella, Betty

The utmost to the most high.

ACKNOWLEDGEMENTS

Thus far, I have been uniquely privileged to sit side by side and also stand upon the shoulders of giants. My utmost gratitude to my research supervisor, teacher, and mentor Dr Denis Kalumba, for believing in me and affording the opportunity to work with him. To my co-supervisor Dr Felix Okonta for such an infectious passion in Geotechnical Engineering, and for providing excellent support during my testing at the University of Johannesburg. I am grateful for my exchange advisor at the University of Massachusetts-Amherst, Dr Guoping Zhang, for his constant encouragement during my writing. Geotechnical Lecturer Faridah Chebet, for always being willing to share her knowledge and reading resources. In the course of my two years, I have also gotten immense feedback from Prof Christian Moormann and Johannes Aschrafi of the University of Stuttgart and Gerard Dirks of Fibertex. I would also like to thank Dr Eduard Vorster of Aurecon for his input and Johnny Oriokot for setting the foundation for my study. Special thanks to Macaferri Southern Africa for the financial support in this project and Edoardo Zannoni for his constructive feedback.

I am thankful for the camaraderie of my Geotech (G)-Unit crew: Vincent Oderah, Lita Noluthshungu, Byron Mawer, Joan Ong'ondia, Samuel Jjukko, Angela Lekea, Sam Wagener, Dercio Chim Jin, Sanelisiwe Buthelezi, Vuyiseka Mapangwana, Laxmee Sobhee and Paul "Pichana" Wanyama. The demanding daily banter in research was less daunting and a lot of fun because of you. My Nyumba Kumi friends Job King'ori, Rose Jeptoo, Jackie Gachiri and Ruth Nekura, for the many evenings we shared dreaming. And to my friends Valentin and Mburu, for the constructive distraction while writing my dissertation. My Cape Town buddies, Godfrey, Big Mike, Su, Dr Chao, Lulama and Ria, for always lending a listening ear, and for the opportunity to do life together.

Sincere thanks to my friends in Kenya: Dennis Otieno, Gideon Sang, Henry Bett, Morgan Chirchir, Ken Kulei, Anthony Mbatia and Benjamin Mandela, for never lacking an encouraging word. To Phyllis, the mere thought of you ignited a desire to see you again and pushed me to the completion of my thesis. My cousin, Robon for challenging me to commence my masters.

Finally, I am most grateful to Greg Bukasa, Fhatuwani Sinngu, Lerato Moatlhodi, Moahlala Edwin, Sicelo Thumbathi and Hermen Kalula for their assistance in conducting the experiments. Lastly, I am thankful to God, for provision, joy and peace of mind.

ABSTRACT

Construction of roads over soft soils can lead to design and construction related problems linked to the soil's compressibility characteristics and low strength. Failure, in terms of bearing capacity can occur when pavements are constructed over such soft soils. When road pavements, which are constructed over soft soils, are subjected to cyclic traffic loading (dynamic in nature), rapid deterioration of the base layer material and progressive permanent deformation of the surface will occur. This not only reduces the serviceability of the pavement structure but also its design life.

In this study, reinforcement geosynthetics (geogrids and geotextiles) were used as reinforcement inclusions within a granular base overlying a soft subgrade of California Bearing Ratio (CBR) less than 2% in a 1.0 m^3 steel test box. Firstly, a geotextile/geogrid was placed at the interface between the base layer and subgrade. Thereafter, a combination of the geotextile at the interface (of the base and subgrade) and geogrid within the base layer. Bench scale plate load tests (static and cyclic) were conducted on a 305 mm diameter circular steel plate on the two layer system using a Universal Compression Machine. Static loading was applied at a rate of 1.2 mm/min. Dynamic sinusoidal load wave was applied with a 4 kN seating load that was linearly increased with an incremental load of 4 kN for every 8 cycles at a frequency of 0.2 Hz on a 305 mm circular plate. For both tests, settlement failure of the composite system was considered at a deformation of 75 mm as defined for unpaved roads.

The results obtained from the pavement model showed that there was a significant improvement in bearing capacity and reduction in settlement accruing from geosynthetic inclusion as shown by the Bearing Capacity Ratio (BCR) of 1.21, 1.29 and 1.63 for geogrid, geotextile and geogrid-geotextile combinations respectively. Additionally, a Settlement Reduction Factor (SRF) of 18% for geogrid, 23% for geotextile and 31% for the geogrid-geotextile combination resulted. There was also an improvement in extended pavement life as depicted by the Traffic Benefit Ratio (TBR) greater than 1 for all reinforced base layers. An improved performance was realised with the double combination of geotextile at the interface, geogrid at the base.

The observed benefits were considered in using the AASHTO pavement design equation, and the resulting geosynthetic reinforced pavements were capable of supporting more than twice the Equivalent Standard Axles (ESALs) of an unreinforced pavement. Furthermore, cost savings of up to 55% in base thickness reduction were realised with the use of geotextile and geogrid in pavements.

TABLE OF CONTENTS

LIST OF TABLES

LIST OF FIGURES

ABBREVIATIONS

AASHO	-	American Association of State Highway Officials
AASHTO	-	American Association of State Highway and Transportation Officials
ASTM	-	American Society of Testing and Materials
BCR	-	Bearing Capacity Ratio
CBR	-	California Bearing Ratio
CMD	-	Cross Machine Direction
E	-	Modulus of elasticity
EGG	-	Extruded Geogrid
ESAL	-	Equivalent Standard Axle Load
GG	-	Geogrid
GTX	-	Geotextile
HDPE	-	High Density Polyethylene
Kg	-	Kilogram
Km	-	Kilometer
kN	-	Kilo Newton
kPa	-	Kilopascals
LL	-	Liquid Limit
LVDT	-	Linear Variable Displacement Transducer
MD	-	machine direction
MDD	-	Maximum Dry Density
m	-	Meter
mm	-	millimeter
MC	-	moisture content
NGTX	-	Non-woven Geotextile
OMC	-	Optimum Moisture Content
PET	-	Polyester
PI	-	Plastic Index
PL	-	Plastic Limit
PP	-	Polypropylene
SAPEM	-	South African Pavement Engineering Manual
SAMDM	-	South African Mechanistic-Empirical Design Method
SRF	-	Settlement Reduction Factor
TIF	-	Traffic Impact Factor
TBR	-	Traffic Benefit Ratio
TSP	-	Total Stress Path
USCS	-	Unified Soil Classification System
WGx	-	Woven Geotextile
XMD	-	cross-machine direction

1.0 INTRODUCTION

1.1 BACKGROUND OF THE STUDY

Due to the wide spread of problematic soils in South Africa (Paige-Green, 2004), pavements have had to be built over soft clay subgrade soils which are often associated with design and construction difficulties because of the compressible nature of such soils. During construction, placing an aggregate base on top of the soft subgrade will result in significant aggregate loss caused by intrusion, which is triggered by construction traffic loads. Moreover, roadways constructed over subgrades with significant fines experience migration of fines into the aggregate base. The contamination of the base by subgrade fines and the aggregate loss into the subgrade causes localised failures, hence leading to increased maintenance costs and a shortened life cycle. Yoder & Witczcak (1975) determined that about 20% by weight of the subgrade soil when mixed into the aggregate will significantly reduce the bearing capacity of the base layer. The American Association of State Highway and Transportation Officials (AASHTO) noted that approximately 20% of pavement failure is due to insufficient structural strength (Pokharel 1997; Tencate, 2014).

The typical traditional approaches to constructing in weak soils include: 1) replacing the top of the subgrade soils with better quality fill that exhibits superior strength properties; 2) increasing the thickness of the pavement layers, both the unbound base and asphalt concrete; 3) treating/stabilising the subgrade with a binder such as cement or lime or incorporating a reinforcement media within the soil in order to create a working platform by improving the engineering properties of the subgrade. All of these methods have a scope of applicability but are disadvantaged because of being either expensive, time consuming or both. The inclusion of geosynthetics such as geotextile and geogrids within the pavement structure can be used to address this problem. This is because these materials possess better qualities comparatively through their reinforcement and separation functions that enhance performance. Furthermore, the use of geosynthetic reinforcement has become a common solution for problems in geotechnical engineering due to their simplicity of construction (Tuna & Altun, 2012).

1.2 JUSTIFICATION OF THE STUDY

According to the South Africa Department of Transportation (2012), it is estimated that 79% of all roads in South Africa are unpaved, with only 21% representing the paved roads. The construction of new roads sometimes necessitates the traversing of pavements in regions with problematic soils such as soft clays that form the subgrade. This translates to a bearing capacity and settlement problem.

Subgrades that change their volumetric and/or stiffness properties significantly over the service life of the pavement are undesirable. This is because the performance of constructed road pavements depends not only on the pavement's structural capacity but also on the subgrade support conditions. Hence, such subgrades exacerbate the deformation and cracking of the road surface. Consequently, this eventually culminates in a deterioration of the performance and service provided by the pavement, leading to premature failure. This translates into significant losses in extra maintenance requirements (Paige-Green, 2008).

For an adequate pavement, the two primary considerations are its ability to support heavy traffic loads and its resilience to the repeated and dynamic traffic loads without failure. Unbound aggregates forming the base are normally subjected to repeated application of stress with each wheel pass. The moving wheel loads are dynamic, whose repetition results in permanent deformation of the surface. In addition, sufficient bearing capacity is an important characteristic of a pavement and it is even more critical when the structure is expected to carry heavy traffic loads. Therefore, this study investigated the potential benefits and effectiveness of including geotextile and geogrid within a road pavement subjected to static and dynamic loads. The model pavement constitutes a granular base material overlying a soft clay subgrade in a 1.0 m^3 square steel box.

1.3 RESEARCH OBJECTIVES

The main objective of this study was to investigate the effect of the use of geogrid and geotextile within a pavement structure underlain by a soft subgrade soil when subjected to static and dynamic loading.

In order to fulfil the primary objective, secondary objectives were established as follows:

1.) Determine the effect of compaction density to the performance of unreinforced and geosynthetic reinforced pavements.
2.) Determine the effect of type of loading to geosynthetic reinforced and unreinforced pavements.
3.) Determine the improvement in bearing capacity resulting from the inclusion of the reinforcement geosynthetics within the pavement.
4.) Determine the reduction in settlement within the composite system.
5.) Determine the resilience of the pavement to cyclic loading under reinforced and unreinforced conditions.
6.) To draw a comparison in performance between the geogrid, geotextile and geotextile-geogrid combination reinforced pavements.

1.4 THESIS OUTLINE

Chapter 1 introduces the topic investigated, provides the context of the problem, background and justifications for undertaking this study.

Chapter 2 gives a general outlook of road pavements to inform the reader of the theories behind the functioning, behaviour and design.

Chapter 3 discusses the problematic soils in the field upon which road pavements have had to be constructed on with an emphasis on soft clays. Different improvement methods have also been exploited that could address the underlying difficulty in constructing on such soils.

Chapter 4 is a review of different types of geosynthetics, with a focus on geotextiles and geogrids with their potential benefits when used within the road pavement. Additionally, a literature review of previous studies on the use of geosynthetics as reinforcement components is conducted.

Chapter 5 gives an overview of flexible pavement design, whereby the design methods associated with geosynthetic reinforced pavements are discussed in detail.

In Chapter 6, the research materials and the methodology applied to undertake this investigation are presented. Data collected from the experimental testing are presented in Chapter 7 and discussed in Chapter 8. The results obtained are incorporated in pavement design equations and equivalent pavement layers designed for in Chapter 9. Chapter 10 gives the conclusions and recommendations for future works to be undertaken.

2.0 ROAD PAVEMENTS

2.1 INTRODUCTION

The movement of people and goods in South Africa is dependent on the transportation networks consisting of roadways, with more than 85% of freight being transported by road (Nordengen, 2009). The surface of these roadways, referred to as pavements, must have sufficient smoothness and skid resistance to allow a reasonable speed of travel as well as ensure the safety of people and cargo. Once the pavement is in service, the economies depending on it will be burdened if the pavement is taken out of service for repair or maintenance. Therefore, pavements are designed to be long lasting and with minimum maintenance requirements.

The pavements are usually constructed with one or more compacted granular material of appropriate quality in layers over the subgrade. The long term satisfactory performance of these pavements depends on the repeated loading response of the granular material. Also, sufficient bearing capacity to support the traffic loads is required, especially when heavy wheel loads are involved. To this end, the two most important characteristics in any soil material are its strain and deformation response to traffic loads. This makes stiffness and strength as the most critical parameters in roadways.

There are two distinct categories of pavements based on the surfacing material and stress distribution, namely:

- Rigid pavement and
- Flexible pavement.

Most of the paved roads in South Africa are flexible pavements, with 90% being thinly paved (< 50mm) with an asphalt layer or surface seals for an all-weather surface (de Beer, Fisher, & Kannemeyer, 2004). Moreover, design considerations for unpaved roads are the same as flexible pavements, but with lower load levels. Also, stage construction in flexible pavements allows for the pavement to be trafficked (construction traffic) prior to construction of the surface layer. This study is limited to flexible pavements.

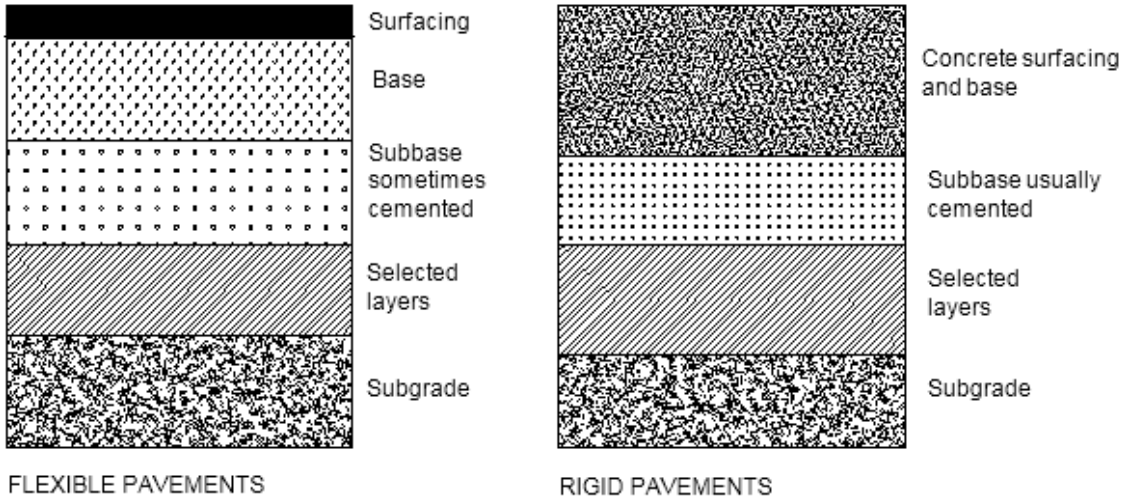

Figure 2-1 Typical cross sections of pavement structures (Ntirenganya, 2014)

The stresses, strains and distresses in flexible pavements are detailed in this chapter. The magnitude of the discussed stresses is influenced by the tire pressure and the total load on the tire; this is discussed in Section 2.4.2. Furthermore, the mechanism through which the stresses are distributed into the pavement is highlighted in Section 2.4.3. The stresses have a significant depth at which pressure is felt most, and this concept is explored in Section 2.4.4. Additionally, road pavements when subjected to traffic cyclic loading undergoes different phases in behaviour, from elastic to plastic and finally the shakedown limit, beyond which there is an excessive accumulation of deformation. These are expounded in Section 2.4.5.

2.2 COMPARISON BETWEEN RIGID PAVEMENT & FLEXIBLE PAVEMENT

Rigid pavements refer to a pavement type consisting of concrete slabs or layers constructed on a granular or cement treated base layer over the subgrade soil. The base layer serves to increase the effective stiffness of the slab foundation. Flexible pavements in contrast, are composed of an asphaltic concrete surfacing, a granular base either bound or unbound and subgrade. In some cases, the subbase is included and is mostly a local aggregate material. The series of layers is arranged such that the highest quality materials are at or near the surface.

The load transmission mechanisms by which rigid and flexible pavements achieve load distributions are very different. Whereas the flexible pavement is designed to provide

sufficient thickness to distribute the applied load with depth, the rigid pavement relies on concrete slab or layer action to spread the load over a large area (Figure 2-2). Flexible pavements are designed to bend and rebound with the subgrade. The design criteria involve placing sufficient layers of the base so as to limit the strains in the subgrade so that no permanent deflections result. This necessitates placing quality high strength materials at or near the surface.

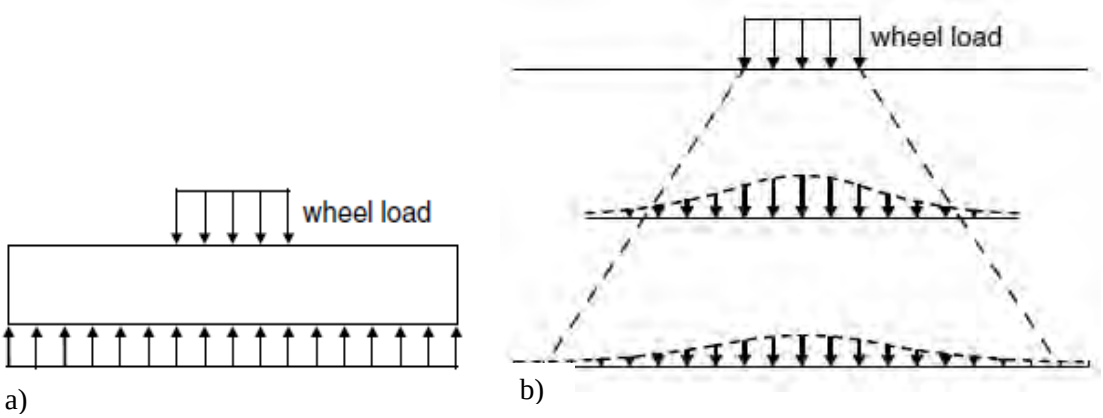

Figure 2-2 Load transmission in a) Rigid pavement b) Flexible pavement (Fwa, 2005)

The strength of flexible pavement is as a result of thick layers that distribute the load over the subgrade rather than the bending action of a slab as in rigid pavements. The design is related to performance parameters that predict the traffic loadings that the pavement can sustain over its design life.

2.3 CHARACTERISTICS OF FLEXIBLE PAVEMENTS

The distribution of load in flexible pavements is what makes them unique; as the depth increases, the same load is distributed over a large area. This depicts that a pavement structure works in unison. High quality materials form the upper surface and the material quality decreases with depth. Some of the flexible pavement properties are as discussed below (Yoder, 1959).

2.3.1 Multilayered system

The pavement consists of layers with different materials and properties that are built over a subgrade. The distribution of stresses and strains within the layers depends on the

thickness and material properties of these layers. The pavement layers are the subgrade, subbase and base, and the surfacing (Figure 2-3).

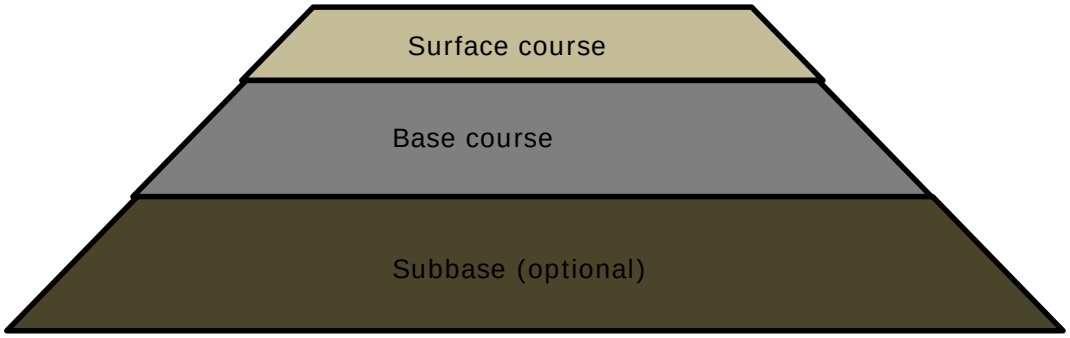

Figure 2-3 Flexible pavement cross section

The surfacing is the uppermost layer in paved flexible pavements that provides the riding surface for vehicles. It normally consists of surface dressing or asphalt concrete or both. Asphalt less than 50 mm provides little structural strength to the pavement. Hence, methodologies currently used for thin surfaced pavements are mainly for structural design of bases and subbase of aggregate surfaced roads with thin wearing course (Geoffroy, 1998).

The use of the base and subbase in flexible pavements is to provide a stress distribution medium which will spread the load applied to the surface, hence protecting the subgrade from shear and consolidation deformations. The subgrade is the material beneath the base/subbase and may include in situ material, fill and improved subgrade.

2.3.2 Nature of traffic loading

When a vehicle is moving on the pavement, the surface experiences both static and dynamic effects. Static load is imparted through vertical (axle, wheel and tyre) loads on the pavement; because of the force of gravity, these are constant.

Due to unevenness of the road pavement, the vehicle will move up and down causing a dynamic variation of the loads on the pavement, above and below their static values. The

magnitude of this dynamic variation depends on various factors such as static loading, the spring and damper characteristics of the vehicle and the road roughness (i.e. the unevenness of the road surface in the longitudinal direction) and the vehicle speed (Hjort, Haraldsson, & Jansen, 2008). Generally, the dynamic variation increases with both speed and road unevenness. The dynamic loads get propagated down the pavement layers to the subgrade through reflections and refractions at the layer interfaces (Yoder & Witczcak, 1975).

The wheel load P (kN), is the load applied by one of the wheels in the case of single wheel axle loads and is the load for two wheels in the case of dual wheel axles. The wheel load P is considered to be half of the axle load. The relationship between wheel load and tyre contact pressure in equation 2-1 (Mallik & El-Korchi, 2013).

$$P = pA \qquad \text{Equation 2-1}$$

Where, A = Tyre contact area in m^2; p = Tyre contact pressure in kPa. For practical reasons, tyre contact pressure p is normally taken as equal to the tire inflation pressure.

The tyre contact area is represented as a circular area called the equivalent tyre contact area, with radius r. Replacement of the circular area formula into Equation 2-1 and making the radius (r) subject of the formulas yields;

$$r = \sqrt{\frac{P}{p\pi}} \qquad \text{Equation 2-2}$$

For instance, considering a standard axle of 80kN, Wheel load P of 40 kN and a tyre inflation p of 550 kPa as used in AASHO road test, the radius (r) of an equivalent contact area as r = 152 mm is obtained.

2.3.2.1 Dynamic wheel loads concept

Dynamic loading increases pavement wear because of the fourth power law dependency of pavement distress on axle loads. Therefore, the loads above the static load increase the pavement wear more than the loads below the static load. Apart from the load magnitude, frequency content is also important for pavement wear.

The mass of the vehicle can be broken down into a "sprung mass" and "unsprung mass" (Figure 2-5). The sprung mass includes the body frame, payload and drive. The unsprung mass includes axles, spindles, brakes, wheels and tyres.

Each vehicle can be represented as a mass spring system as schematised in Figure 2-4. The tyre (schematised as a spring) can be seen as well as the carriage work, the axle and the spring-damper system in between the carriage work and the axle. When a vehicle is subjected to vibrations with a certain frequency, the vehicle reacts strongly on specific frequencies than on other ones depending on the vehicle characteristics.

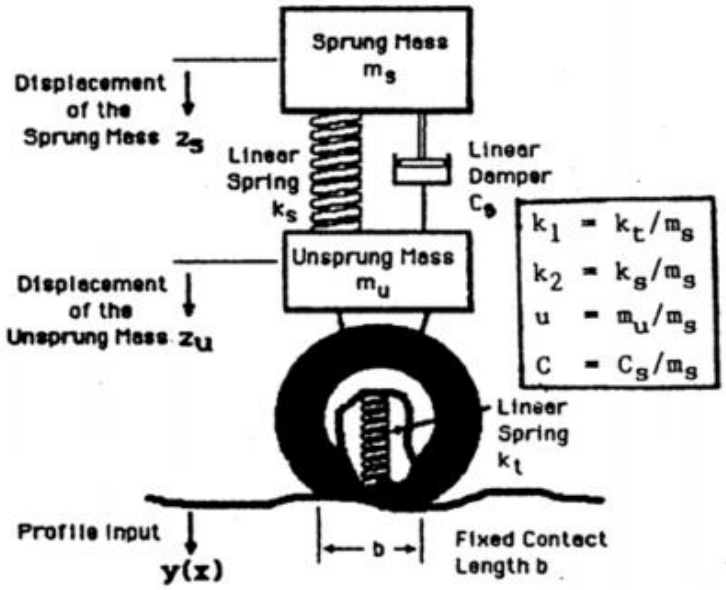

Figure 2-4 Model for a quarter of a vehicle (Delft Technical University, 1989)

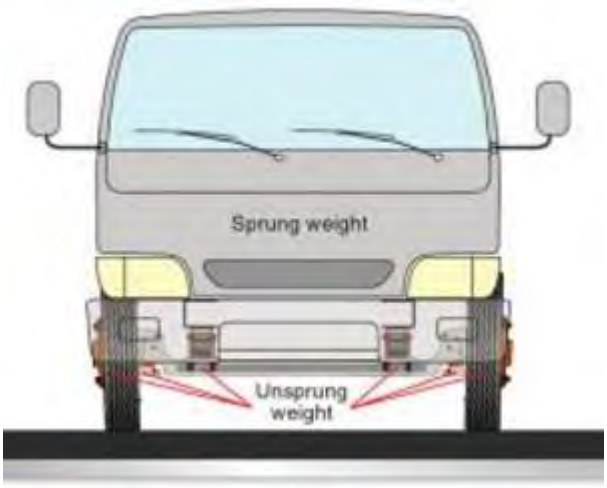

Figure 2-5 Unsprung mass versus sprung mass (Duffy & Wright, 2016)

The dynamic load induced by a road vehicle is concentrated at two frequencies, the first corresponding to the vertical vibration of the sprung mass (weight of the carriage work e.g. chassis frame and vehicle body) of the vehicle while the second reflects the vertical vibration of the unsprung mass (i.e. the vertical hop of the axle, rims, tyres, etc.). The majority of the dynamic loading results from the vibration of the sprung mass and for commercial vehicles, it ranges from 1.5-3.5 Hz. In comparison, the unsprung mass frequency has been reported in the range of 8-15 Hz (Hjort, Haraldsson, & Jansen, 2008). The frequency of the unsprung mass is usually much higher than vibration due to the sprung mass because the sprung mass is larger than the unsprung mass. Hence, Al-Hunaidi et al. (1996) from his experiments has concluded that even though the unsprung mass is not the dominant of the dynamic load, it is the main cause of ground vibrations and the reason for annoying traffic vibrations.

2.3.3 Axle load configuration

Loading to a pavement occurs through an axle that distributes the load to the wheels. Different vehicles have different axle configurations and with a different number of wheels at each axle. The axles can be single, tandem, tridem, or multiple, while the wheels can be either single or dual (Figure 2-6). Passenger cars can have single axles and single wheels while trucks can take different combinations of axle and wheel configurations.

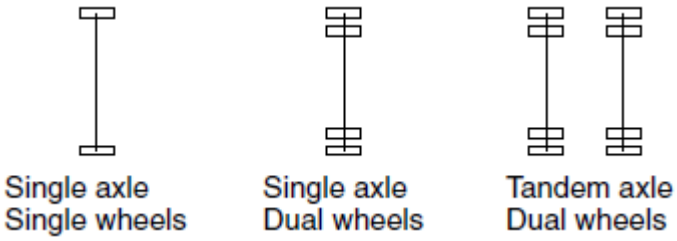

Figure 2-6 Schematic of common axle and wheel configurations. (Fwa, 2005)

The effects of the tandem, tridem and other axle configurations on the Load Equivalence Factor (LEF) is not considered in South Africa. The standard axle adopted is an 80kN single axle load with a dual wheel configuration. The single axle load consideration overestimates the number of equivalent axles by 15% when the effect of the multi-axles is not considered. This overestimation is not considered significant, taking into account the wide limits of design traffic classes, especially at the higher end of the load spectrum (SAPEM, 2013).

Hjort, Haraldsson, & Jansen (2008) in contrast stated that the load spreading characteristics of tandem and triaxle groups can carry more weight due to the primary response fields of nearby axles to overlap, such that there may be a substantial increase in the responses under the axle considered. Such increased responses will lead to much more pavement wear than the summed responses of individual axles. In spite of the possible adverse effects from tandem and triaxle groups, pavement design procedures still adopt the conversion or tandem and triaxles to an equivalent standard axles load.

2.3.4 Fast deterioration with time

Each traffic load application to some extent contributes to pavement distresses. Different types of stresses ensue, for instance, rutting, fatigue cracking, material disintegration roughness and bleeding. When one of these stresses exceeds some acceptable level, the pavement is considered to have failed.

Due to the fast deterioration and short service lives, pavements are not designed on the criteria of maximum possible load like other structures but rather its design incorporates a design life that gives an indication of the expected lifeline of the pavement before failure.

2.4 STRESSES AND STRAINS IN FLEXIBLE PAVEMENTS

An important criterion to the structural design of pavements is how it responds under traffic motion. This response is reflected in the changes in stress, strain and vertical deflection in each of the pavement layers. Although stress, strain and vertical deflection are distributed throughout the pavement structure, there are critical values that occur at specific locations within the structure. These impact the pavement, significantly affecting its performance (Ntirenganya, 2014).

The effect of a moving load on the pavement is a resultant development of vertical, shear and bending stresses and strains in each layer of the pavement. For flexible pavements, especially when unsurfaced or thinly surfaced, the ability to withstand such stresses within the granular layers is key to the overall performance of the pavement structure.

Lekarp et al. (2000) highlighted the complexity in understanding the stress patterns induced from moving wheel loads on the pavement as shown in figure 2-7. The pavement in the field is usually loaded by moving wheel loads, which at any time impose varying magnitudes of vertical, horizontal, and shear stresses in the pavement. The principal stresses are shown to act vertically and horizontally only when the shear stresses are zero, i.e. directly beneath the centre of the wheel load. Such is an attempt to simplify the resulting response to loading; however, the true nature of the deformation mechanism of aggregates in granular layers is not yet fully understood.

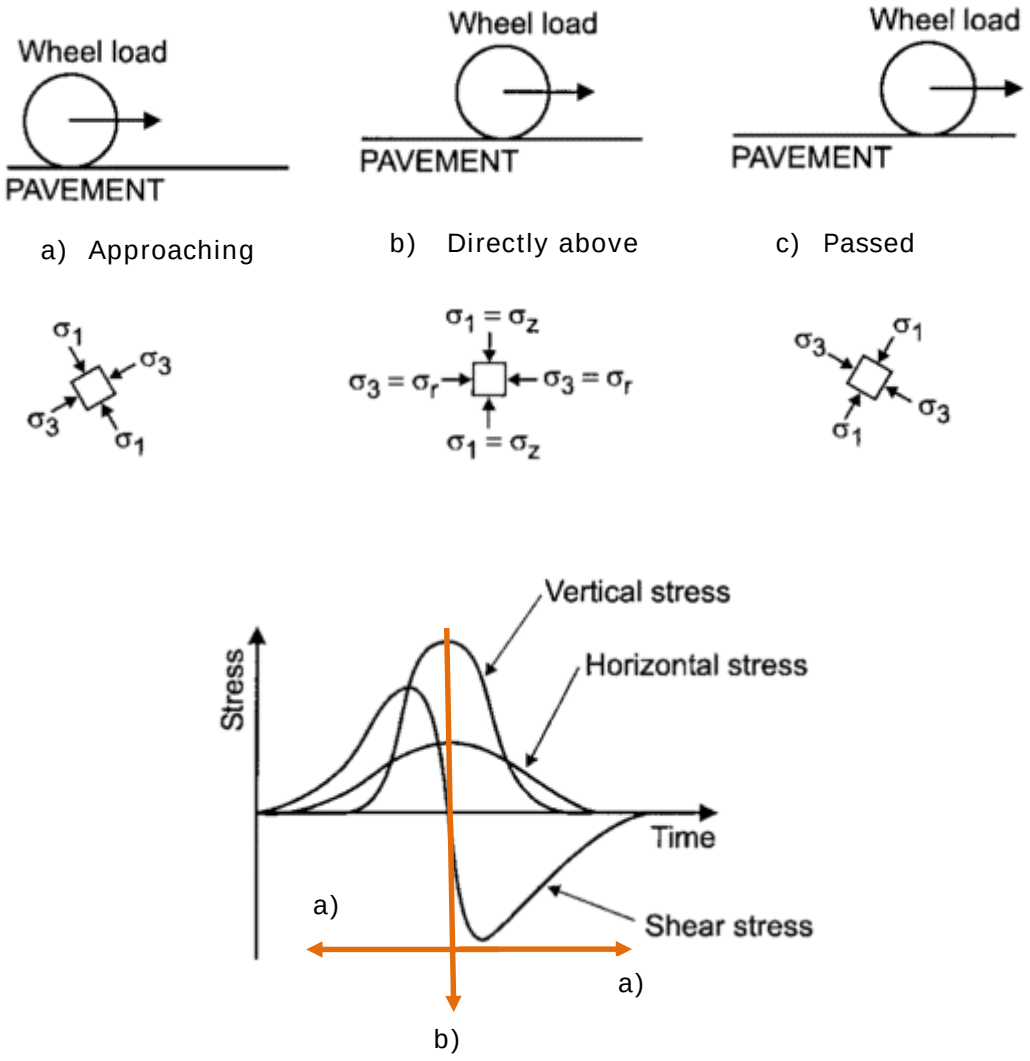

Figure 2-7 Stresses beneath a rolling wheel load (after Lekarp, Isacsson, & Dawson, 2000)

i. Vertical stress and strain

Vertical loading is the standard loading used in pavement design and it arises due to the vehicular loading on pavement. The vertical loading that is dissipated through the wheel of the moving vehicles cause compressive stress in the pavement structure. Beyond a certain point, the stresses lead to permanent deformation and hence rutting on the pavement surface. The rate of deformation is dependent on the strength characteristics of the pavement materials.

ii. Horizontal and Shear stress and strain

In unbound layers, horizontal and vertical stresses are usually positive, whereas the shear stresses are reversed as the load passes, thus causing a rotation of the principal stress axes (Figure 2-7). The horizontal stresses are the main cause of pavement interlayer shear stresses that occur as the vehicle accelerates, decelerates, brakes or turns. This can lead to interlayer slipping due to the effect of the horizontal shear stress. Figure 2-8 illustrates the conceptual distribution of shear movement within the pavement structure.

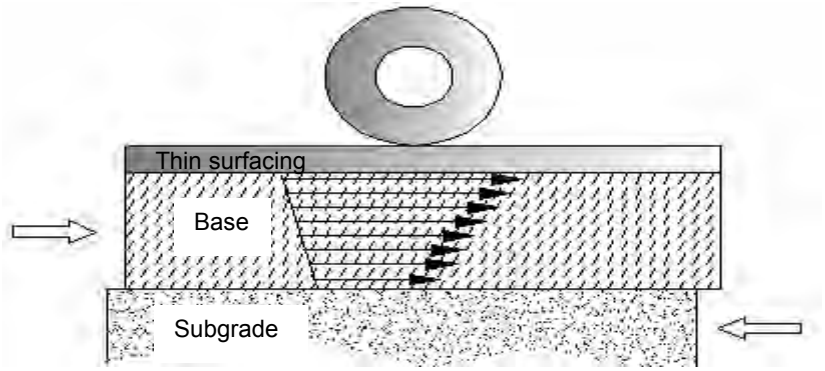

Figure 2-8 Conceptual representation of shear flow at the interface (Ntirenganya, 2014)

2.4.1 Flexible pavement response to loading

Flexible Road pavements comprise of various layers: Subgrade, Subbase/Base and an Asphalt surfacing. Layered systems offer a set of complexities due to their many variables such as properties and thickness of layers, the effect of environmental conditions on each layer, layer response to loading and interactions between layers.

Understanding the material's behaviour is key to the estimation of pavement structure response and consequently the accurate prediction of pavement performance. There are three fundamental theories established that are key to understanding the behaviour of pavement materials, namely: elasticity, plasticity and viscosity. However, very few materials can follow precisely one material mode of behaviour. The most practical prediction of behaviour involves combining the behavioural types to model the material behaviour accurately as shown in Table 2-1.

Table 2-1 Behaviour of different pavement materials (Jenkins, 2013)

Pavement materials	Material behaviour
Cement/ Concrete	Elasticity
Granular materials	Elasto-plasticity
Bituminous materials	Visco-elasticity
Asphalt	Visco-elastoplasticity

For this study, the selected pavement comprised of a granular base overlying a soft subgrade material since such subgrade soils are encountered in road construction in South Africa. Hence, the controlling behaviour is the base, which is expected to provide adequate support for the loading. Moreover, all granular materials exhibit the elasto-plastic behaviour which is further discussed.

2.4.1.1 Elasto-Plastic behaviour of granular materials

The granular material in pavements behaves as a combination of the elastic and plastic deformation through the cycles of loading. This behaviour is referred to as elasto-plastic behaviour as shown in Figure 2-9. When the loading extends beyond the elastic limit into the plastic behaviour, it results in accumulation of non-recoverable or plastic strain. With each cycle of loading, plastic strain occurs resulting in permanent deformation after each loading cycle.

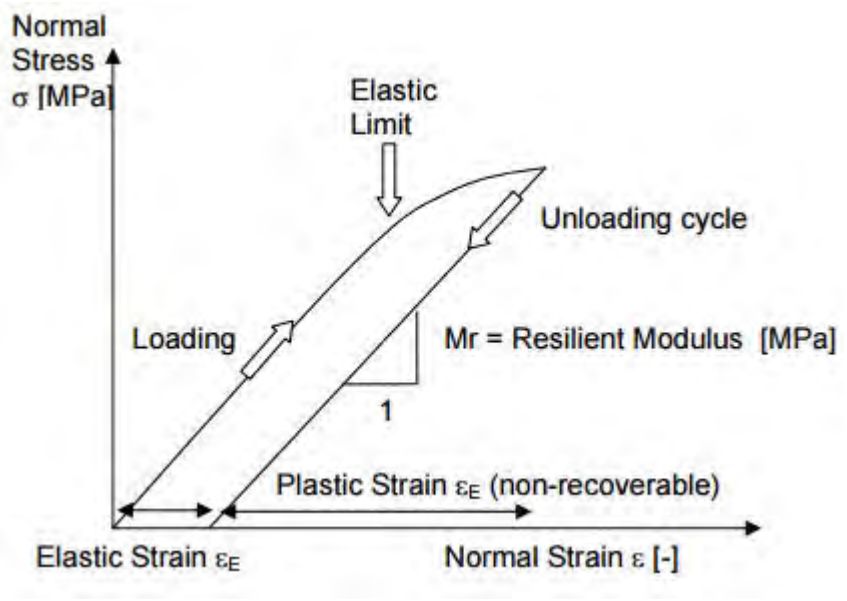

Figure 2-9 Elasto-plastic behaviour of granular material (Jenkins 2013)

2.4.2 Effect of tyre pressure and total load to pavement stress

The magnitude of the total stress at a point due to a load at the surface of the pavement is dependent upon the applied pressure as well as the magnitude of the total load. Higher tyre pressures have the most impact on the upper layers of the pavement. Therefore, high tyre pressures call for high quality materials in the upper pavement layers, but the total depth of pavement is not appreciably affected by tyre pressures. On the other hand, for a constant tyre pressure, an increase in total load increases the vertical stress for all depths as shown in Figure 2-10. For instance, an increase in tyre inflation pressure from 689 kPa to 1379 kPa, results in higher compressive strains at the surface (Figure 2-10). However, higher tyre pressure results in very little change in the surface deflection or compressive strain in the subgrade. Therefore, the surface layers are sensitive to changes in the tyre pressures but the deeper layers are more sensitive to changes in load (Pavement interactive, 2015).

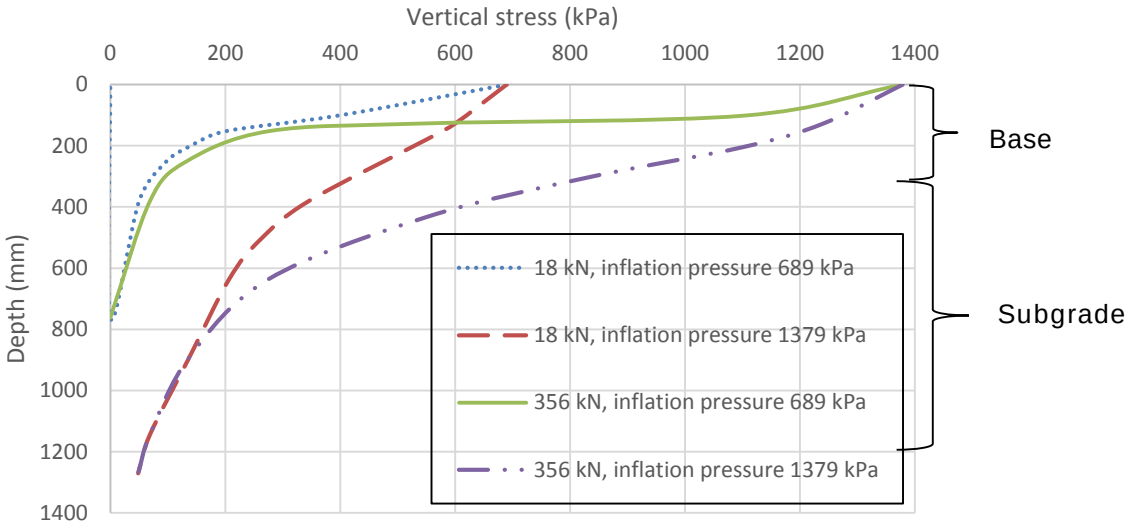

Figure 2-10 Variation of vertical stress with depth (after Yoder & Witczcak, 1975)

Earlier studies conducted by CSIR, (1997) and Morton et al., (2004) showed that there has been a significant increase of tyre pressures over the allowable level by up to 30% in South Africa. This has resulted in increase in stresses on the surfacing and base, which has consequently led to premature failure of South African road pavements.

2.4.3 Pressure distribution in flexible pavements

The pressure distribution of a wheel load takes the form of a bell-shaped surface. Maximum stresses are felt at the vertical plane passing through the point of load application. The pressure is at its maximum at shallow depths and theoretically assumed to approach zero at infinity.

The load on a tyre is considered to be distributed over a circular area. However, this is not strictly correct since the tyre imprint will take the shape of an ellipse (Figure 2-10 above). For design purposes, the application of loading through flexible pavements is considered as a circular area, while for rigid pavement the distribution is considered to be elliptical (Yoder & Witczcak, 1975).

a) b)

Figure 2-11 a) Approximate tyre contact area b) Tyre contact area commonly used in flexible pavements

For circular tyre imprints, the radius of contact is considered as follows:

$$r = \sqrt{P/\rho\pi}$$ Equation 2-3

Where: r =the radius of contact, P =total load on the tyre, ρ =tyre pressure (assumed to be equal to contact pressure

2.4.4 Concept of significant depth

The pressure from vehicular loads is significant up to a certain depth. The depth of the stressed zone within the depths of the pavement is called the significant depth. Terzaghi recommended that a stress contour equal to 0.2q (q-foundation contact pressure) be taken as the significant depth. The direct stresses are considered negligible when they are 20% less than the intensity of the applied stress. It is postulated that 80% of the settlement under load takes place at a depth less than the significant depth. The significant depth is equal to 1.5 times the width of the square or circular footing (Murthy, 2002).

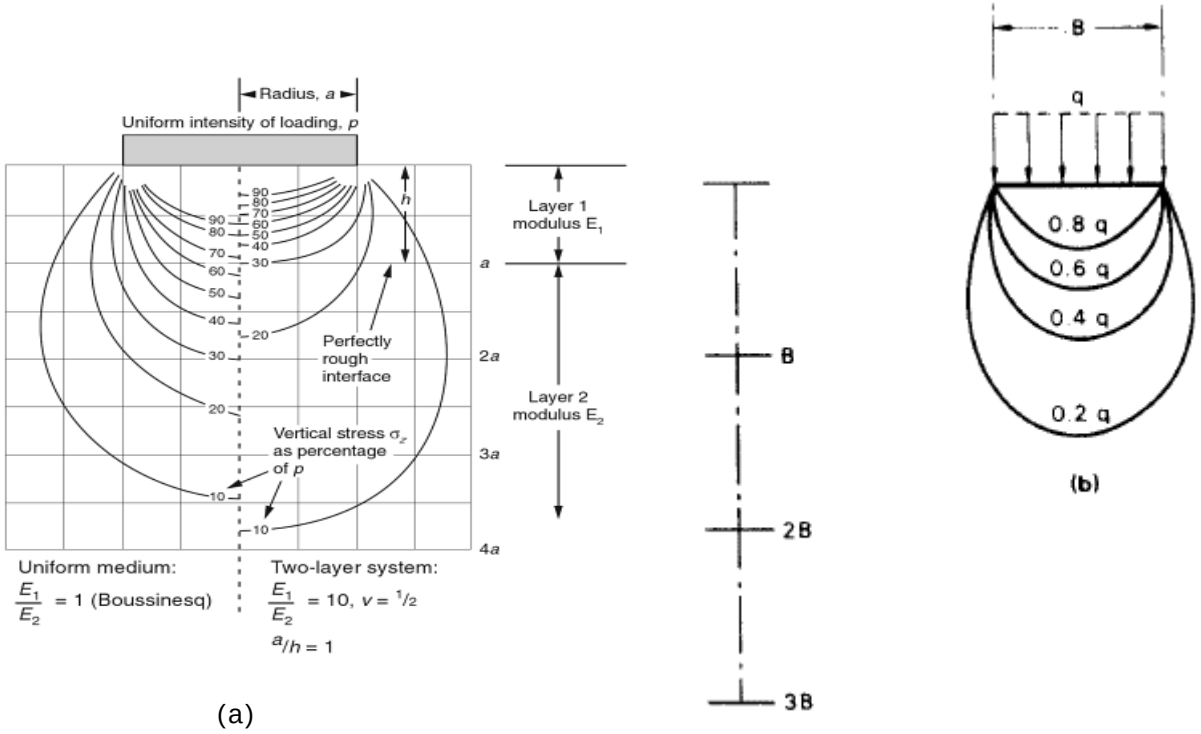

Figure 2-12 a) Westergaard stress distribution for a two-layer system (Munfakh et al. 2001), and zone of influence for: b) circular footings (Craig, 2004)

2.4.5 The shakedown concept

The shakedown concept is applicable to a pavement structure to determine if the progressive accumulation of permanent strain will lead to a state of incremental collapse or if the increase in permanent strain will cease resulting in a stable response. The understanding of shakedown material behaviour is important as it typically determines the load bearing capacity of the structure if it is not to reach excessive permanent strain (Siripun, Jitsangiam, & Nikraz, 2011). The permanent deformation is usually a fraction of the total deformation produced by repeated loading since the large accumulation of these small plastic deformations eventually leads to failure from a maintenance view point (Jung, Choi, & Nsabimana, 2012).

There are three responses that can occur when an elastic-plastic structure is subjected to cyclic loads, namely; purely elastic, elastic shakedown, plastic shakedown and ratchetting (Figure 2-13 below). It is desirable for pavement materials to function below the plastic shakedown, which presents reversible strain under additional cyclic loading.

i. Purely Elastic

The applied repeated stress is sufficiently small that no element of the material achieves any yield condition. At this stage, all deformations are fully recovered and the response is elastic. Therefore, the road behaves elastically if the load magnitude is so low that the structure does not reach the point where it is responding plastically.

ii.) Elastic shakedown

If the load is larger than the elastic limit so that the structure is deforming plastically but below than the critical limit, the structure behaves plastically within a range of load cycles after which it responds elastically for the remaining load cycles. At this point the structure is said to have "shakedown", and the maximum stress level at which this condition is achievable is termed the "elastic shakedown limit".

iii.) Plastic Shakedown

It occurs when the applied stress is slightly less than that required to produce collapse after the incremental accumulation of plastic strain. The material attains a long-term steady state response, i.e. no further accumulation of plastic strain and each response is hysteretic. Intrinsically, this means that a finite amount of energy is being absorbed by the material on each application of stress. This long term steady response is referred to as "shaken down" and the maximum stress level at which this condition is achievable is termed the "plastic shakedown limit".

This was consistent with the findings of Tafreshi & Dawson (2010) where a steady state achieved as seen from the hysteresis loop was obtained for the footing settlement under repeated loading. As the load cycles increased, the repeated loading and unloading became symmetric, thus indicating that less energy loss is in the system.

Iv.) Incremental collapse or ratchetting

The repeated loading is relatively large such that the plastic strains accumulate rapidly, with failure occurring in a small number of load cycles and within a relatively short time. The applied stresses cause the material to reach and exceed the yield condition.

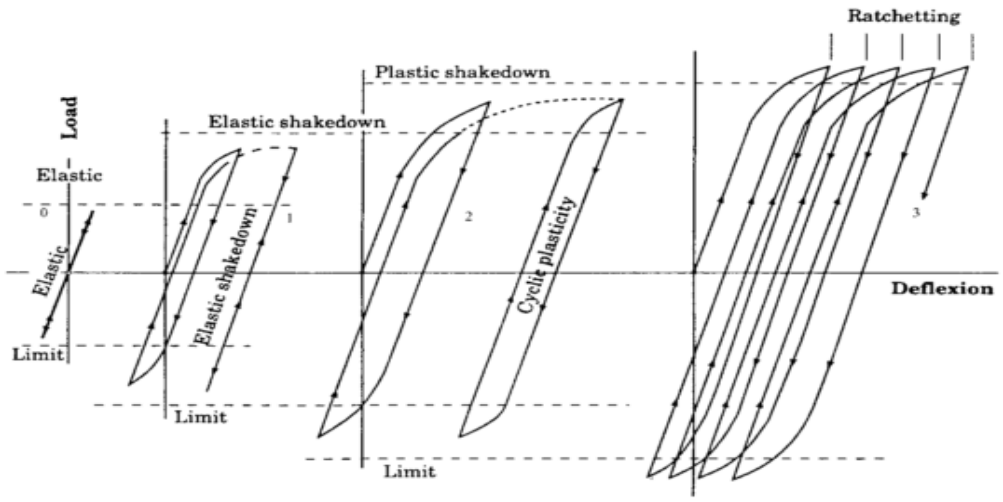

Figure 2-13 Elastic/Plastic behaviour under cyclic pressure and tensile load (Werkmeister, Dawson, & Wellner, 2005)

2.5 PAVEMENT DISTRESSES

Distress refers to conditions that reduce the serviceability or indicate structural deterioration of a pavement, while failure denotes a pavement section that has experienced excessive rutting or cracking, greater than what has been anticipated within the time period. Failure of a pavement may or may not be accompanied by lateral shoving and pushing of the underlying layers and by the upheaval of the surface outside the loaded area forming ruts. Yoder and Witczak (1975) have defined pavement distress or failure in two ways.

Structural failure: whereby there is collapse of the entire structure or breakdown of one or more pavement components, hence making the pavement incapable of sustaining loads imposed on its surface.

Functional failure: the pavement in this instance, due to its roughness, is unable to fully carry out its intended purpose. Therefore, it results in a low serviceability; the drivers or passengers experience discomfort and high stresses are imposed on the vehicles. Functional failure leads to and accelerates structural failures.

Some of the causes of functional and structural failures include excessive loads, excessive repetition of loads, higher tyre pressures, poor drainage conditions, disintegration of the component materials and unanticipated loss of base materials due to subgrade intrusion.

Table 2-2 below shows factors that influence various pavement distresses leading to either structural or functional failure.

From Table 2-2, concerning geotechnical influences on distresses in flexible pavements, it is observed that the leading reasons for flexible pavement failures are: insufficient base stiffness/strength; moisture/drainage problems; insufficient subgrade stiffness/strength and contamination.

Table 2-2 Geotechnical influences on major distresses in flexible pavements (Christopher et al. 2006)

Distress	Insufficient Base stiffness/ strength	Insufficient subgrade stiffness/ strength	Moisture/ Drainage problems	Swelling	Contamination
Fatigue Cracking	X	X	X		X
Rutting	X	X	X		X
Corrugations	X				
Bumps				X	
Depressions	X		X		X
Potholes			X		
Roughness	X	X	X	X	X

2.6 TYPES OF PAVEMENT DISTRESSES

There are four predominant modes of distress in flexible pavements, namely (Fwa, 2005; Yoder & Witczcak, 1975):

- Permanent Deformations
- Fatigue Cracking
- Potholes
- Roughness

These distresses at the initial stages result in functional failure where there is a reduction of serviceability with time up to a point when there is a complete breakdown of the

pavement structure. The pavement is then considered to have experienced structural failure, and it is not able to sustain loads imposed on its surface. It is also noteworthy that rutting failure, which is one of the permanent deformations, is the most experienced type of failure in roads. Hence, the rut depth failure criterion will be discussed in Section 2.7 as used in different design methods.

2.6.1 Permanent deformations

Deformation refers to a change of the road structure, which leaves the road surface in a shape different from the one intended. Examples of permanent deformations are Rutting, Bumps, Corrugations, and Depressions. It can be load associated (traffic) or non-load associated (environmental) influences. Deformations affect the serviceability of the pavement, reflect its structural inadequacy and have a significant impact on vehicle operating costs.

Surface rutting, also referred to as deformation (Figure 2-14a) is often the controlling stress mode in flexible pavements. Rutting refers to the permanent deformation in the wheel path. Any rutting observed at the surface is partly due to permanent deformations in the asphalt layer and primarily due to accumulated permanent deformations in the underlying unbound layers and the subgrade. It has been determined that two-thirds (2/3) of the rutting observed on the surface is due to accumulated permanent deformations in the geomaterials within the pavement structure (Christopher, Schwartz, & Boudreau, 2006)

Corrugations (Figure 2-14b) are transverse waves in the pavement profile and are found mostly at stop signs, at stop lights and on hills. It is typified by ripples or abrupt waves across the pavement surface. They are found in the wheel track and they are caused by acceleration and deceleration of heavy trucks in a regular pattern on the roadway surface (Brokenbrough & BoedeckerKenneth, 2004).

Depressions (bird baths) (Figure 2-14c) are localised pavement surface areas where the pavement surface is lower than the surrounding surface, but the transition is not abrupt enough to be considered a distortion. They are noticeable after rain when they fill with water.

Some causes of permanent deformation in the geomaterials (soils) of the pavement are:

- Inadequate inherent strength and stiffness of the material,
- Degradation of strength and stiffness due to excessive moisture
- Contamination of base and subbase materials by subgrade fines (i.e., inadequate Separation of layer materials).

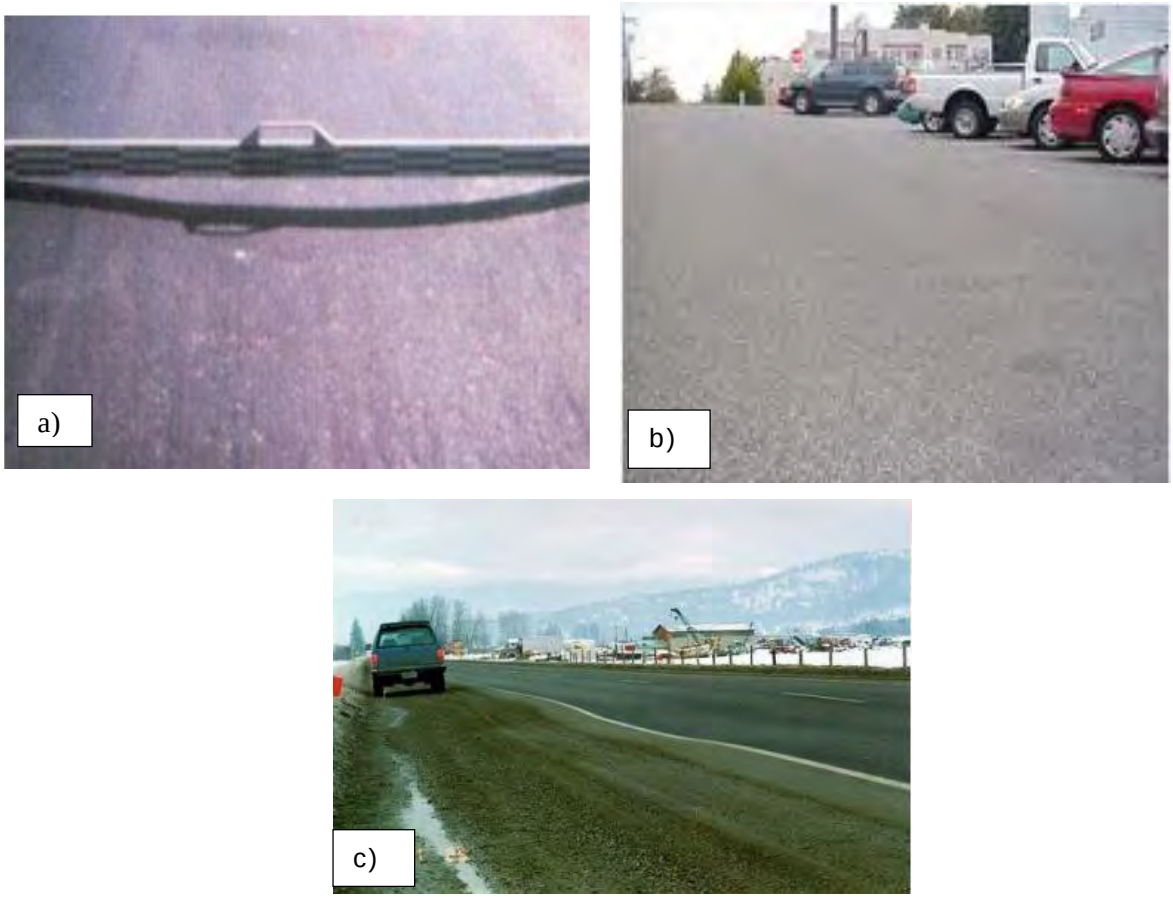

Figure 2-14 a) Rutting (Sapem, 2013) b) Corrugations (Pavement Interactive, 2006) c) Depressions (Erlingsson, 2013)

2.6.2 Fatigue cracking

This form of distress is caused by repetitive wheel loads; the cracks that ensue are a series of longitudinal and interconnected cracks (Figure 2-15). It manifests first as short longitudinal cracks in the wheel path and progresses to an alligator cracking pattern (interconnected cracks).

This type of cracking occurs because of the repeated bending action on the asphalt layer when the load is applied; this generates tensile stresses that eventually create cracks at the bottom of the asphalt layer. The cracks then propagate to the top of the layer.

Figure 2-15 Alligator Cracking (Redlight-Gbarnga-Guinea Border, 2012)

Low stiffness of the base, subbase or subgrade materials, whether due to poor material quality, insufficient thickness and moisture influences contribute to the increase in the tensile strains at the bottom of the asphalt layer, thereby increasing the potential for fatigue cracking. In addition, localised fatigue is possible when there are non-uniformities in the base/subbase along the pavement alignment e.g. local zones of low stiffness material.

2.6.3 Potholes

Potholes are small, bowl shaped depressions in the pavement surface that penetrate through the asphalt layer to the base course (Figure 2-16 below). They are formed due to a localised loss of support of the traffic loads through either failure in the subgrade or base/subbase. As alligator cracks become severe, the interconnected cracks create small chunks of pavement, which can be dislodged as vehicles drive over them.

Figure 2-16 Potholes (Redlight-Gbarnga-Guinea Border, 2012)

2.6.4 Roughness

This refers to irregularities in the pavement profile which causes uncomfortable, unsafe, and uneconomical riding. Surface roughness is caused by the non-uniform permanent deformations and cracking along the wheel path. All permanent deformations and cracking also impact roughness. Non-uniformity of the stiffness/strength of geomaterials along the pavement is a major cause of roughness.

2.7 RUT DEPTH FAILURE CRITERION

Rutting is the most commonly observed pavement distress in pavements, and for this reason, it has been considered in the design of unpaved roads. Rutting of between 50-100mm is usually considered as a measure of failure in unpaved roads (Giroud & Han, 2004). At higher rut depths, there is contamination of the base material with the subgrade material, causing failure. Giroud & Han (2004) have explained the different causes that might lead to the formation of ruts as follows:

- Repeated traffic loading that causes compaction of the base course aggregate and/or the subgrade soil.
- Bearing capacity failure due to the initial traffic loads on the pavement.
- Bearing capacity failure resulting from progressive deterioration of the base course material due to the base layer contamination by the subgrade soils which interferes with the pavement's structural integrity.
- Lateral displacement of the base course material due to the accumulation of plastic strains with each load cycle.

A failure criterion widely used for unpaved roads is 75 mm. This has been adopted by the Army Corps of Engineers, for instance in Hammitt (1970). Also, the AASHTO design guidelines (AASHTO 1993) consider allowable rut depths of 13mm − 75mm. In unpaved roads, overall subsidence in excess of 100 mm is considered failure (Hammitt, 1970; Giroud & Han, 2004).

In this study, failure of roads is observed from the point of shear failure or excessive deformation of the subgrade. It is assumed that the base course material quality is sufficient to impede failure within the base course. Furthermore, the allowable rut depth is from a serviceability perspective; it does not necessarily translate to the actual failure of the base and subgrade soil.

2.8 IMPORTANT FLEXIBLE PAVEMENT DESIGN PARAMETERS

The design of road pavements is influenced by the level of serviceability that is acceptable, the traffic loading that the pavement will carry and the roadbed soil resilient modulus that is an indication of the strength of the soil materials. These important parameters are as discussed below.

2.8.1 Serviceability

Present serviceability relates to the ability of a pavement to serve traffic. It is measured on a scale of 0-5, with 0 for impassable and 5 for perfect. The pavement distress measurements were taken (i.e. rut depth, cracking, etc.) concurrently with the subjective ride assessment to provide a correlation between distress and ride quality (AASHTO, 1993).

To avoid riding and rating every pavement, a relationship was established between the present serviceability rating (PSR) and the measurable pavement attributes. The value determined by this relationship is called the Present serviceability index (PSI). The relationship between the pavement thickness and the serviceability index is defined by the AASHTO pavement design Equation 5-11.

2.8.2 Traffic loading

This is the most important element in pavement design. The traffic loading is normally assumed to be channelised, which is represented by the number of traffic passes (N) of a

given axle during the design life of a structure. This is because unrestricted traffic is more difficult to characterise and depends on the judgement of the designer (Giroud & Han, 2004). Overestimation of the design traffic results in a thicker pavement than is necessary, resulting in higher costs. Similarly, underestimation of traffic results in thin pavements that will fail prematurely, hence requiring higher maintenance costs.

For design purposes, all traffic equates to an equivalent 80 kN single axle load or Equivalent Standard Axle (ESAL). Each vehicle in the expected traffic design volume is converted to ESAL by an equivalency factor which is a function of the axle loading, pavement thickness, axle configuration and terminal serviceability.

Most design procedures are dependent on the static load test used to determine the resistance of the road to movement and deflection. However, road pavements experience the repeated loads from traffic which lead to either plastic and/or elastic deformation. The relative magnitudes are dependent on the number of load applications.

Even though the load applications might be small, accumulation of such plastic deformations may be of such magnitude as to cause pavement failure. Laboratory studies (Perkins, 1999; Leng, 2002; Qian et al., 2011) have indicated that structural failure of the pavements under repeated loading is in some cases the primary factor which limits the life of pavements.

Soils under repeated loadings tend to deform much more than identical specimens subjected to sustained loads of equal magnitude (Yoder & Witczcak, 1975). In some instances, just one or two load applications are sufficient to cause failure. It is therefore important to have a pavement that can withstand the repeated traffic loads and the heavy traffic loads.

2.8.3 Relative effects of different axle loads

A commonly used design approach in many countries is to design flexible pavements for resistance to failure by fatigue and rutting. Elastic or viscoelastic layer theory is used to calculate strains and stresses in the pavement due to a static standard axle wheel load. The load damaging effect, also called the fourth power Law, is used to estimate the expected number of standard wheel loads (in mixed traffic) during the service life. This load sensitivity is referred to as the Load Equivalence Factor (LEF) and its unit is Equivalent Standard Axles (ESA). It is measured in MESA, an abbreviation for Million Equivalent Axle.

$$LEF = \left(\frac{p}{80}\right)^n$$ Equation 2-4

Where:

LEF = Load Equivalence factor (LEF)

P = Any axle load for which the load equivalency is required (kN)

80 = Reference axle load, typically 80 kN (standard axle)

n = Damage exponent, a value of 4 normally adopted

Cebon (1999) connoted that the validity of the fourth power rule is questionable since the current axle loads and axle group configurations, tyre sizes and pressures and road construction technique and traffic volumes are all different from the conditions adopted in the AASHO road test for the fourth rule derivation. Furthermore, the fourth rule may not be adaptable in all situations unless there is a similarity between the prevailing environment, traffic, pavement type and construction as in that of the AASHO road test. The fourth power rule was derived from measurements of heavy vehicles in the AASHO test; hence, it is more suited for evaluating the damaging effect of heavy vehicles. Thus, its application to light vehicles such as passenger cars results in a vast extrapolation outside the range of vehicle loads used in the AASHO test (Hjort, Haraldsson, & Jansen, 2008). One of the limitations of the fourth power rule is that it was developed on the basis of static axle weights of the vehicle. It also refers to the global rather than the local deterioration, thus it cannot be used to evaluate the road damaging effect from dynamic forces that build up locally. Despite these shortcomings, the fourth power rule still remains an acceptable criterion for assessing the axle load damaging effect.

2.8.4 Roadbed soil resilient modulus

Resilient modulus is the ability of a soil or granular base to resist permanent deformation under repeated loading. It is known that pavement materials are not elastic, but experience some deformation after each load application. However, if the load is small compared to the strength of the material, the deformation is completely recoverable after each load application and the material is considered elastic.

Resilient modulus has been used to duplicate the dynamic loading that the pavement experiences and the confining pressures that the road is subjected to due to the effects of the heavy vehicles (Lee et al., 2003).

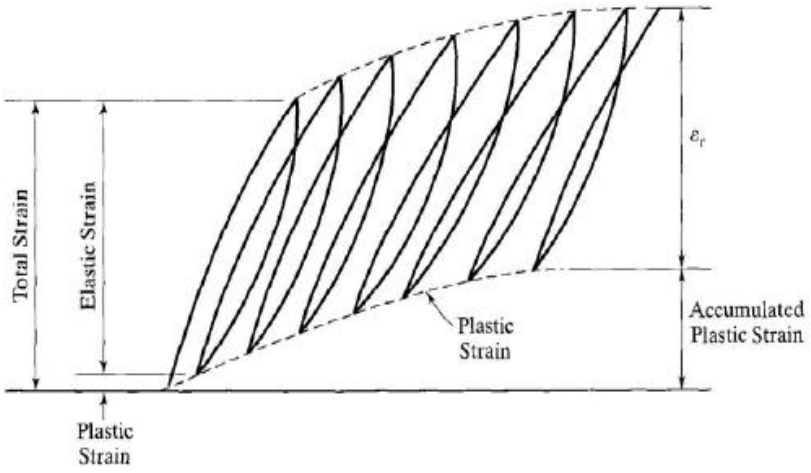

Figure 2-17 Strains under repeated loads (Yang, 2004)

The straining of a soil under repeated loading is as shown in Figure 2-17 above. The initial stage of load application is marked by considerable permanent deformation as indicated by the plastic strain. As the number of load repetitions increases, the plastic strain due to each load repetition decreases. After about 100-200 repetitions as in Figure 2-17, all the strain is practically recoverable as indicated by ε_r (Malla and Joshi, 2006). Therefore, the elastic modulus based on the recoverable strain under repeated loading is referred to as the resilient modulus (MR) and is defined as in Equation 2-5. The determination of the resilient modulus in the laboratory is obtained through repeated load triaxial test as illustrated in Figure 2-18 below.

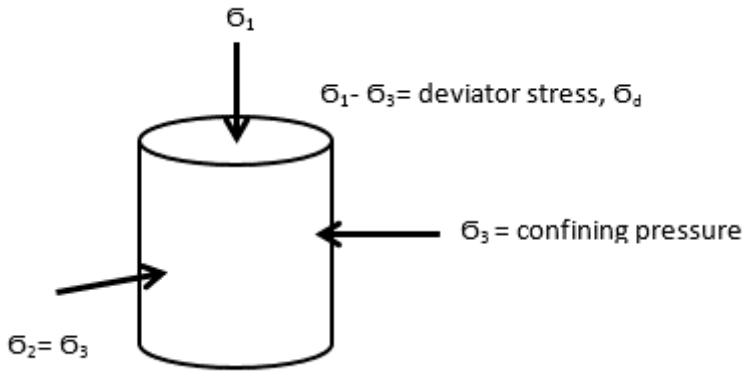

Figure 2-18 Triaxial determination of the resilient modulus

$$M_R = \frac{\sigma_d}{\epsilon_r}$$ Equation 2-5

Where:

σ_d -the deviator stress, which is the axial stress in repeated load triaxial test.

ε_r- Elastic strain

Since laboratory determination of resilient modulus is time consuming (Figure 2-18), equations have been determined relating resilient modulus to soil properties that are more easily determined.

Table 2-3 Different equations used to determine the soil resilient modulus (Erdem, 2007)

Institution	**Formulae**
South African Council on Scientific and Industrial Research (CSIR)	MR (psi) = 3,000 CBR $^{0.65}$
Transportation and Road Research Laboratory (TRRL)	MR (psi) = 2,555 CBR $^{0.64}$
AASHTO Design guide	M_R (psi) = 1500.CBR
U.S. Army Corps of Engineers	MR (psi) = 5,409 CBR $^{0.71}$

3.0 PROBLEMATIC SOILS

3.1 INTRODUCTION

Problematic soils can be naturally occurring or man-made soils. Such soils can give rise to many geotechnical difficulties including inadequate bearing capacity and the potential for unacceptable settlements (Slocombe, 2001). Damage to structures in South Africa is commonly related to soil characteristics that form the foundations. There are many types of problem soils, but some of the most noteworthy are expansive soils, collapsible soils, soft clays and dispersive soils (Diop et al, 2011).

Road pavements have had to be constructed on such problematic soils forming the subgrade. This, however, does not suit the roadbed requirements for stability and does not provide a suitable platform for construction. To curb this difficulty, proper considerations are normally instituted to alter and improve the undesirable characteristics of these soils that form the roadbed, thereby mitigating premature failure of the constructed roads. The occurrence of this failure may render the road pavement untrafficable and translate to monetary losses due to excessive maintenance.

This chapter discusses the different types of problematic soils, their behaviour and effect on infrastructure. Further study centres on the behaviour of soft soils and its implications in construction. Currently adopted methods used to solve the difficulty in constructing on the problematic soils are discussed, including their merits and demerits.

3.2 COLLAPSIBLE SOILS

Collapsible soils are characterised by poor gradation with respect to particle size with a porous texture and generally exhibit low in-situ density (Figure 3-1). These soils can be partially saturated and can withstand relatively large imposed stresses with small settlements. However, if wetting occurs, the soils exhibit a decrease in volume and an associated additional settlement with no increase in the applied loads (Figure 3-2). A collapsible grain structure is usually associated with silty or sandy soils containing low clay content. The collapse is sudden and non-reversible and can be in excess of 20% of the original soil volume.

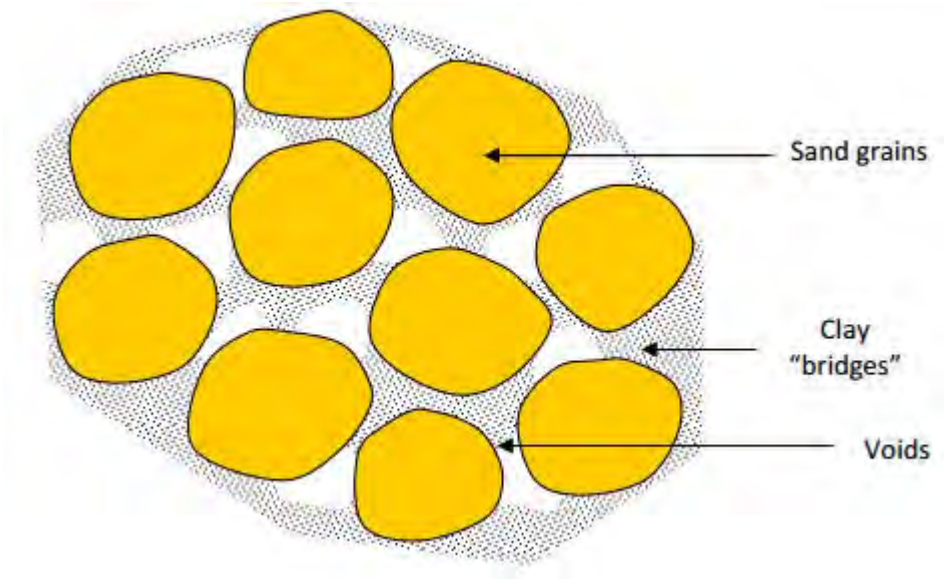

Figure 3-1 Schematic image of a collapsing structure (Diop et al., 2011).

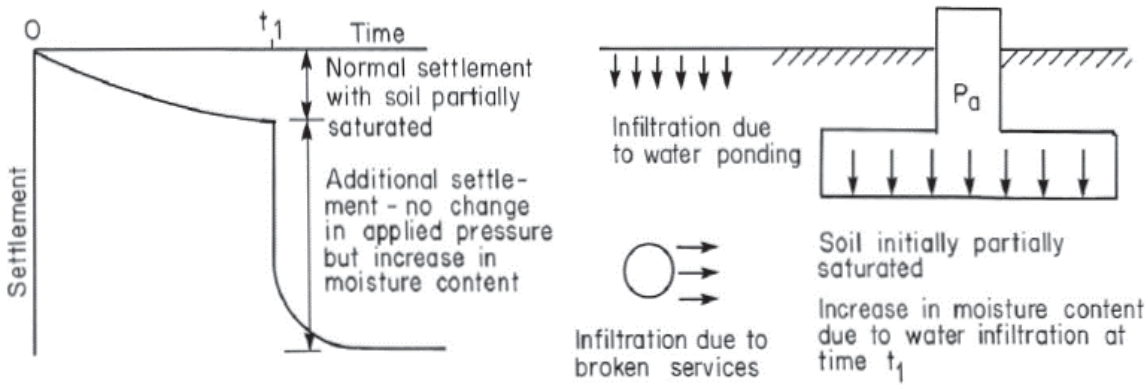

Figure 3-2 Mechanism of collapse settlement (Franki Book, 2008)

A collapsible soil fabric can be found in wind deposited sands (loess); old, highly weathered and leached granite soils; or residually weathered, so-called "dirty" sandstones, but in some instances also in soils which have been deposited by sheet-wash, gulley wash, wave action, or termite activity. The collapse occurs in localised zones that exhibit collapse conditions that are "favourable", thus leading to a pattern of localised damage to structures. If collapsible soils are identified prior to construction, the preventive measures become simplistic, centring on proper densification or compaction of the founding horizons (Diop et al., 2011).

3.3 EXPANSIVE SOILS

This refers to soils that experience volumetric change i.e. swell or shrinkage of the soil skeleton with variations in the moisture content. On wetting, the clay minerals absorb water molecules and expand; conversely, as they dry, they tend to shrink, leaving large voids in the soil.

According to Diop et al. (2011), expansive soils, depending on the geographical location, can be referred to as either a swell clay, active clay, shrinkable clay or heaving clay. Since South Africa has a predominantly dry climate, this soil type is referred to as a swelling clay, while in countries such as Great Brittan, with its wetter climate, it is more often referred to as shrinkable clay (Figure 3-3).

a) b)

Figure 3-3 Expansive clays showing a) Shrinkage cracks and b) Saturated wet expansive soils (Diop et al., 2011).

Expansive soils are mainly comprised of the smectite mineral, which is a 2:1 layer silicate. Smectites have two tetrahedral sheets joined to a central octahedral sheet. The most common mineral in the smectite group is the montmorillonite. Smectites have permanent negative charges because of the isomorphous substitution that occurs in either the octahedral sheet or the tetrahedral sheet. The interlayer is hydrated and cations are present within the interlayer to balance the negative charges on the sheets themselves. Smectites have a high cation exchange capacity (CEC) in the order of 60-100 mEq/100 g of clay. Soils having Smectites can undergo as much as 30% volume change due to wetting and drying or these soils have a high shrink/swell potential and upon drying will form deep cracks (Suppes, McConnell, Dennehy, Abel, & McConnell 2013).

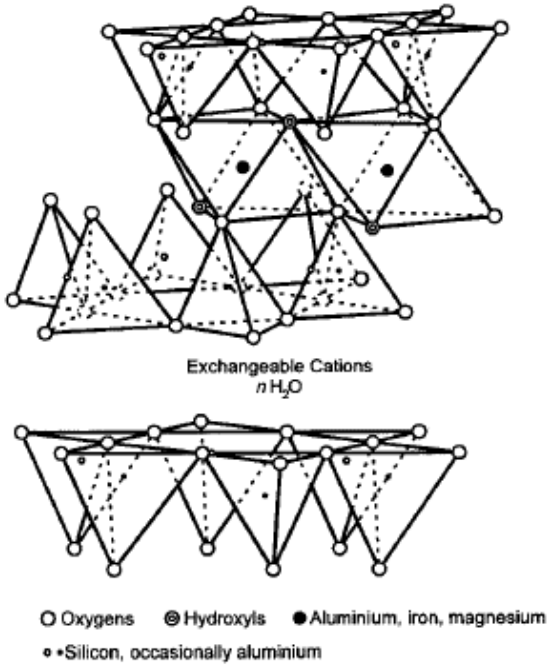

Figure 3-4 Smectite Structure (Murray 1999)

Expansive soils are the more commonly occurring problematic soil in Southern Africa. The swelling of the clays underlying the foundations causes cracking of existing structures, fissures in the ground surface and a myriad of problems in roads and other services. This causes a reduction in the passenger serviceability index (PSI) due to driving discomfort on roads affected by the movement caused by underlying expansive clays as evidenced by the many problems experienced on the N1 where it crosses the Springbok Flats north of Pretoria and the northern Free State (Public Works South Africa, 2007).

The challenge with expansive soils is that the magnitude of soil movement is not often recognised in a timely manner. This is because structural damage can occur even when as little as 2 to 3 % of soil expansion or contraction occurs. To better understand their effect or influence on structures, extensive studies have been conducted to identify expansive soils. Hence, countermeasures and additional construction costs to prevent structural damage are now well understood. Therefore, a proactive approach has been achieved that allows for extra design and construction pre-emptive measures once the potential problem has been identified (Diop et al., 2011).

3.4 DISPERSIVE SOILS

Dispersion occurs in any given soil that has a high percentage of Exchangeable Sodium Percentage (ESP), causing internal erosion and eventual piping through embankments. The tendency for the dispersive erosion in a given soil is subject to variables such as mineralogy and chemistry of the clay and the dissolved salts in the soil water and the eroding water. Extra care should be taken when designing earth dams, drainage channels and lateral support where the soil structure is dispersive because the soils are susceptible to erosion and piping. Dispersive soils do not affect roads except for serious erosion problems on the slopes of cuttings and fill embankments side slopes.

Dispersive clays can be identified visually through features such as gully erosion and field tunnelling (piping and jugging) together with excessive turbidity in any storage water. It also softens rapidly and has a greasy feel on contact with water (Franki Book, 2008).

3.5 SOFT CLAYS

There is no standard definition that exists for soft clays in terms of conventional parameters, mineralogy or geological origin. They are clays that are partially or fully saturated, frequently have high organic content and are highly compressible. Thus, they are associated with low shear strength, compressibility and severe time related settlement problems. These soils are mostly common in the coastal areas in South Africa, with the most significant deposits in Durban, Richards Bay, the Natal North and South Coasts, and Cape East and Southern coast (Jones & Davies, 1985).

South African soft clays are relatively small in lateral extent and are generally highly variable; they have undrained shear strength of between 10 kPa to 40 kPa. The soft clays cause stability failures, construction problems and long-term settlement in road embankments (Ministry of Public works, 2007; Paige-Green, 2004).

The construction of roads in the coastal areas has embraced the use of high fills across these estuarine deposits with the concomitant settlement and low subgrade bearing strengths. Furthermore, rigorous site investigations requiring delineation of the soil profile, identifying drainage paths, high quality undisturbed soil sampling and good laboratory testing become key. Inevitably, stage construction has been used to permit stepwise loading of the subgrade, leading to dissipation of the excess pore water pressures. Overall,

this bumps up the construction costs in time delays and extra man hour costs (Paige-Green, 2004).

3.5.1 Classification system for soft clays

Fine grained soils are divided into silt and clay according to the Unified Soil Classification System (USCS) as shown in the plasticity chart Figure 3-5 below. In addition, based on the organic content, the clay can be classified as either an inorganic clay or organic clay.

When silt plasticity and the liquid limit is plotted on the plasticity chart, the plots are located below the A-line, while for clays the plots are located above the A-line.

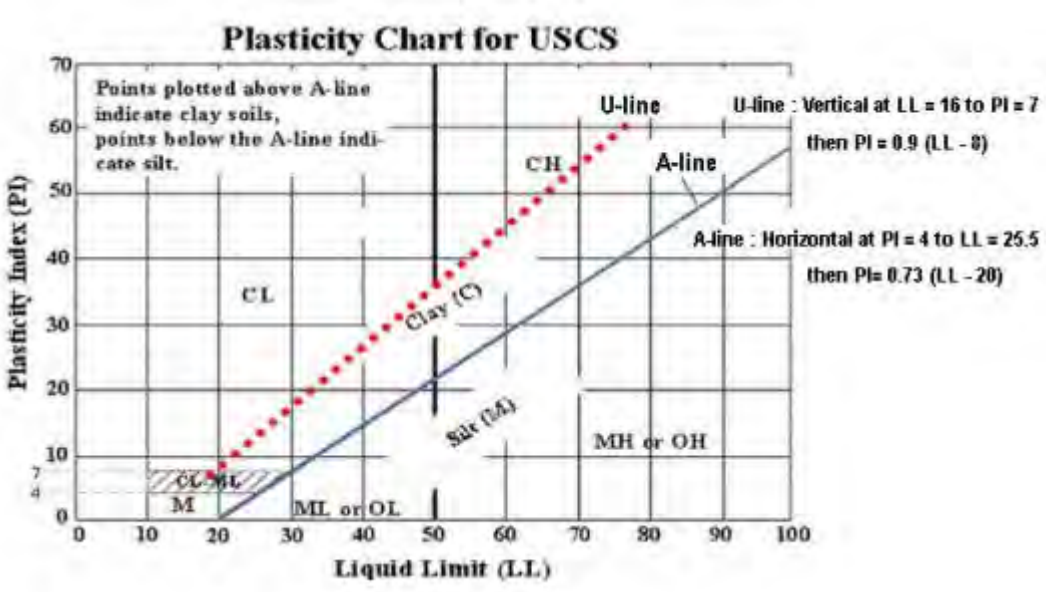

Figure 3-5 Atterberg limit for organic and inorganic soils (Widodo, 2013)

As outlined in ASTM D2487, the USCS classifies silts and clays as organic based on the difference in the liquid limit (LL) measured before and after oven-drying the soil. For soils of ratio $LL_{oven\ dried}/LL_{pre\text{-}oven} < 0.75$ (liquid limit of the sample after oven drying to the pre-oven drying liquid less than 0.75) are termed as organic. The engineering properties of such a soil are significantly influenced by the organic matter. Hence, clays and silts in this category are referred to as organic, with terms OL and OH depending on whether the LL is smaller or greater than 50.

Construction of foundations in the presence of soils with organic matter presents difficulties due to their high compressibility, unsatisfactory strength characteristics and low unit weight. Thus, strict restrictions are required to be instituted on the minimum percentage of organic matter in the soil. Many departments of transportation in the United States of America have adopted requirements for organic matter of the soil to be below 2-7%. Huang et al. (2009) in addition has indicated that a 5% addition of organic matter to an inorganic clay led to an increase of liquid limit from 49% to 72%.

3.5.2 Undrained shear strength of soft clays

Soft clay has clay minerals and a high moisture content causing low shear strength and high compressibility. Additionally, under loading, soft clays respond in a different manner depending on the type of foundation over it, as in rigid and flexible pavements in Boussinesq's theory in Section 5.2.1. The high compressibility of the soft clay also has been associated with construction difficulties whereby the base material gets contaminated with the subgrade, leading to a failure of the road pavement. The spectrum undrained shear strength (Cu) for the clay soil is as indicated in Table 3-1.

Table 3-1 consistency of clay (Look, 2014)

Consistency	**Cu (kPa)**
Very soft	0−12 kPa
Soft	12−25 kPa
Medium	25−50 kPa
Stiff	50−100 kPa
Very stiff	100−200 kPa
Hard	>200 kPa

In South Africa, soft clays are classified with undrained shear strengths of between 10kPa to 40kPa (Jones & Davies, 1985). In the field, the soils can be identified in the following manner as in Table 3-2 below.

Table 3-2 Field indicator of undrained shear strength of soft clays (Jones & Davies, 1985)

Consistency	**Field indication**
Very soft	Exudes between fingers when squeezed
Soft	Easily moulded in fingers

Additionally, soft clays when subjected to loading respond in different ways depending on the type of foundation. A rigid foundation resting on a soft clay which is loaded with a uniformly distributed load (q/unit area) undergoes a uniform settlement. The contact stress distribution is as shown in Figure 3-6b, with maximum stress along the centre. In contrast, a flexible foundation on an elastic material such as saturated clay will experience a sagging profile with a uniform contact pressure (Figure 3-6a).

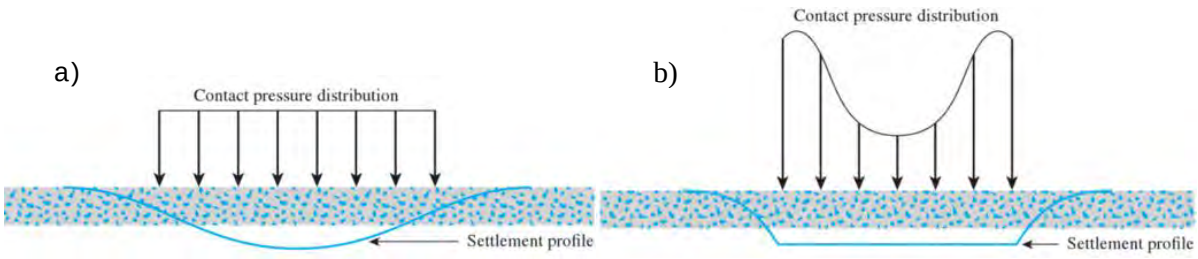

Figure 3-6 settlement profile and pressure distribution over a) flexible foundation, b) flexible foundation in clays (Das & Sobhan, 2013)

3.6 FACTORS AFFECTING THE BEHAVIOUR OF SOFT SOILS

3.6.1 Organic content

Organic content of about 27% by weight or about 55% of the volume has been shown by Hobbs, (1987) to have a great influence on the properties of clay. The presence of organic matter influences the behaviour of soil leading to increased liquid limit, high compressibility and low permeability.

3.6.2 Loading rate

The most direct method of examining the influence of strain rate on the undrained strength is to perform tests on identically prepared samples at different controlled strain rates. Data shown by Graham et al. (1983) indicate that changes in strain rate can result in major changes in the undrained strengths of samples which have been anisotropically consolidated to their in-situ vertical stress. They showed a change in undrained stress over tenfold change of strain rates of about 12-14°.

Under cyclic loading, cyclic simple shear tests conducted by Mukabi & Tatsuoka (1999) showed that there was not much variation in equivalent shear modulus (G_{equiv}) at lower

strains. However, at larger strain rates, the effect of loading rate on the shear modulus became pronounced.

Therefore, the rate of strain is important in determining the behaviour and strength of clays as the use of the strength parameters informs engineering designs.

3.6.3 Weathering

Clays and clay minerals are formed through weathering of rocks and soil. The weathering involves physical disaggregation and chemical decomposition that change original minerals to clay minerals. The types of clay minerals in the weathered rock determine how the eventual soil behaves under the various climatic conditions.

Kaolinite is found in most weathering zones and soil profiles, whereas montmorillonites, which are more reactive than kaolinites, can be found nearer to the rock where chemistry exerts a strong control on mineralogy (US Geological survey, 1999). Leaching, which is connected to chemical weathering, has been shown by Bjerrum (1967) to cause a reduction in undrained shear strength and an increase in compressibility of clays.

3.7 METHODS OF IMPROVEMENT OF SUBGRADE SOILS

The strength of problematic soils forming the subgrade is often unsatisfactory in its natural state. It calls for altering of its mineral and grain composition by using methods such as the addition of admixtures, aggregates and proper compaction in order to make it possible for subgrade construction.

In road construction, soil stabilisation is a method that has been used to improve the bearing characteristics, hence creating a stable working platform and reducing settlement. Soil stabilisation technique is classified into mechanical and chemical.

Mechanical stabilisation can be achieved through compaction, addition of granular material and compaction and the use of reinforcement such as geotextiles or geogrids. On the other hand, chemical stabilisation is done using additives such as lime, Portland cement and asphalt.

3.7.1 Densification (compaction)

Compaction refers to the artificial increase of the density, thereby decreasing the void ratio of, the soil mass. The mechanism involves a reorientation of soil particles, fracture of soil particles, breaking of bonds between them and distortion of soil particles.

The primary mechanism in fine grained soils is reorientation and distortion. The compactive energy must be high enough to subdue the cohesive forces. Increased water content in this instance decreases cohesion; therefore, more controls are required in dealing with fine grained soils. In comparison, the primary mechanism in coarse grained soils is the reorientation with some fracture. This requires compactive energy, which is high enough to overcome the friction between particles so as to reorient them. Water assists in the compaction by lubrication of the contacts.

Also, in cohesionless soil, the contribution of compaction is in terms of increase in strength and stiffness and decrease in compressibility and permeability. The density that is to be achieved with a specific compactive energy affects the soil properties. In comparison, cohesive soils when subjected to a given compactive energy offer a difference in properties even at the same dry density. This is attributed to the difference in soil structure that results, which can be either flocculated or dispersed (Mallik & El-Korchi, 2013).

3.7.2 Soil-cement stabilisation

This consists of adding cement to a pulverised soil and allowing the mixture to harden. The benefits resulting from the mixture greatly depend upon the degree of compaction. The soil cement mixture is then left for about seven or eight days for it to cure, thus hardening. During curing, the mixture is kept moist and evaporation minimised.

Cement stabilised soils are classified into three groups (Mallik & El-Korchi, 2013):

- A mix of a natural soil of low or marginal quality and cement. This finds its use in subgrade soils and the feasibility of this mixture becomes an issue where the demand of cement exceeds 20%.
- A mixture of granular soils of high quality, normally meeting the base course specification and cement forming a Cement Treated Base (CTB). It results in a stiff base of high quality and is applicable for heavily trafficked roads. The cement content is kept lower than 4% in order to prevent reflective cracking in pavements.

- Econocrete, which is a mix of low quality aggregates (not meeting required specifications) and cement. It is used as a subbase in airport pavements.

The soil cement base behaves as a semi-rigid slab and will potentially develop cracks due to shrinkage, especially if the mix is rich. The cracks can permit ingress of surface water which reduces the base durability. Also, if the mixing requires an excessive amount of time, less durable mixtures result. Typically, construction must be completed in five to six hours after the cement is mixed with soil. Cement stabilised soil will not function as a proper wearing surface since it may become dusty and ravel under the action of heavy traffic. A light surface treatment of the bituminous material is thus applied to withstand the abrasive action (Yoder & Witczcak, 1975).

The merits of soil-cement stabilisation include a reduction in plasticity, a decrease in volume change capacity as well as increased strength and stiffness. Cement treatment is limited to unique and very special soil types and project conditions. It also becomes difficult to attain the correct mix proportions and achieve a uniform mixture. Several tests are also required to be done in the laboratory before the initiation of the treatment in the field.

3.7.3 Soil-Lime stabilisation

The use of lime for stabilisation is limited to warm or moderate climates since lime is susceptible to breakup under freezing and thawing. The rule of thumb is that lime stabilisation should not commence unless the temperature is 4° C - 7° C and rising. Low temperatures interfere with the hydration or modification reaction of lime (Tencate, 2010b; Mallik & El-Korchi, 2013).

The action of lime in soil is explained in three basic reactions:

- Modification process that happens through cation exchange. Ca^{++} is substituted for absorbed cations in the clay soil water system. This process is more effective if the absorbed cations are sodium, Na^{+}, which ends up being replaced by Ca^{++}.
- The second process is coagulation and agglomeration process which makes the soil particles behave like larger particles.
- The last process is the cementing of soil particles due to carbonation of lime. The two main components of soil, alumina and silica, react with lime forming cementitious compounds through a process called a pozzolanic reaction. It occurs

only when there is excess lime and after completion of the cation process. The amount of lime used in construction generally ranges from 3%-5% of hydrated lime by weight of soil that results in a concentration of calcium ion greater than what is actually needed. However, adding more than 10% lime is not economically viable.

An important advantage of using lime is that it changes the soil's plasticity significantly. For soils that have plasticity index (PI) of less than 15, lime increases both the liquid and the plastic limit which in turn increases the plasticity index. For more plastic soils, lime decreases the liquid limit and increases the plastic limit, which in turn decreases the plasticity index (Yoder & Witczcak, 1975).

The application of lime in subgrade soils is used to reduce the potential change in volume while in the base and subbase material it is mainly to improve their quality. The main benefit of lime is the reduction in plasticity, hence reducing the effect of water. This improves the constructability and performance of the pavement. The resulting effect is strength gain but less than what could be achieved by the addition of Portland cement. A drawback is that soils with Ca^{++} are not affected by lime treatment.

Curing of the lime should be done by spraying an asphalt binder which prevents moisture loss, erosion and damage from traffic. Safety considerations are key in the use of quicklime, which is dangerous for the skin and causes dust problems in urban areas. Moreover, lime possesses the same disadvantages as cement stabilisation, such as it being suitable for specific soils, wasting time in curing and difficulty in attaining the correct mix.

3.7.4 Bitumen stabilised materials

This involves mixing bituminous materials with soil to serve as a stabilising agent. The viscosity of asphalt has to be reduced for it to be mixed with soil through a hot or cold process. In the hot process, the asphalt can be heated then mixed with the heated aggregates to produce Hot Mix Asphalt (HMA). In the cold process, asphalt emulsion is mixed with soil to produce a low quality material.

There are two concepts involved with asphalt treatment of soil (Yoder & Witczcak, 1975; Mallik & El-Korchi, 2013):

- Waterproofing: The soil particles are coated with asphalt and water does not get in contact with the particles, hence making the soil less sensitive to water and

lowering the water absorption. This maintains the inherent strength of the material under all conditions of weathering.

- Cementation: The asphalt increases the cohesion of the mix.

The advantage of the concept of cementation is that it obtains maximum stability for continued traffic. It is in most cases effective but has a disadvantage of the relatively high cost of stabilisation. The first concept deals with low quantities of bituminous materials that waterproof the fines. The water absorption of the mix is the critical factor rather than the initial stability of the mix. The main advantage behind waterproofing is the low cost of stabilisation. Bituminous mixtures result in compacted densities that are slightly different from that of the natural soil. Therefore, density as a result of the admixture should not be used as a criterion for stability.

Stabilisation with bitumen is, however, suited to specific types of soil. A rule of thumb is that soils that can be pulverised by mix in place equipment are satisfactory for bitumen stabilisation. Soils having more than 30% passing the number 200 sieve, or with a plasticity more than 10% are not suitable for bitumen stabilisation (US. Army, 1974).

3.7.5 Use of geosynthetic reinforcement inclusions

Geogrids and geotextiles have been primarily used to reinforce road sections. The inclusion of a reinforcement geosynthetic in soft soils has the advantage of tensile reinforcement, confinement, lateral spreading reduction, separation, construction uniformity and reduction in strain. Sufficient stiffness and interlock with the materials are fundamental to the performance of the geosynthetic. The contributions of geosynthetic reinforcements are discussed in detail in Chapter 4.

Installation of a geotextile or geogrid at the interface prior to the aggregate enables construction in soft soils. The separation role comes in handy and the losses of the material become minimal. Therefore, the use of geosynthetics eases the construction on very soft soils.

Geocells have also been used in the construction of roads. Geocell, a honeycomb three-dimensional cell structure, which provides containment of compacted fill soils, thus preventing the lateral spreading of the infill material. The confinement characteristic increases the stiffness and load deformation behaviour of the granular base. However, the majority of research in the past has concentrated on the use of planar reinforcements and

design methods have been developed for them (Giroud, Ah-Line, & Bonaparte, 1985; Tencate, 2014). For geocell reinforcement, the use is still limited due to lack of established design methods.

Geosynthetics can be installed with available equipment on site and do not require a contractor with special skills to lay them. This is unlike the cement and lime treatment process that requires speciality equipment and an experienced specialised contractor. Moreover, cement and lime treatment is stepwise, with each step requiring a waiting period; should a step need to be repeated, it results in much delay in the work schedule. For geosynthetics, they are installed on the go with no delays like the curing period or the uncertainty of the materials having not properly mixed.

4.0 GEOSYNTHETICS

4.1 INTRODUCTION

ASTM D4439 (2015) defines geosynthetics as planar products manufactured from polymeric material, which are used with soil, rock or other geotechnical engineering related material as an integral part of a man-made project, structure or system. There are many types of geosynthetic products with various structures, different polymeric materials, and design functions. The most common ones are geotextiles, geogrids, geocells, geonets, geomembranes, geofoams and geocomposites (Figure 4-1).

Geotextiles are permeable, polymeric textile products in the form of flexible sheets. Among the different geosynthetic types, geotextiles are the ones that present the widest range of properties. They are classified into woven geotextiles, non-woven geotextiles and knitted geotextiles depending on the manufacturing process. They are commonly used to provide separation, reinforcement and filtration in soil and rock (Koerner, 2012).

A Geogrid is a polymeric mesh-like planar product formed by intersecting elements, called ribs, joined at the junctions. The key feature of geogrids is the apertures, which are openings between adjacent transverse and longitudinal ribs. The ribs of geogrids are normally stiffer in comparison to the fibres of geotextiles. The ribs are linked by extrusion, bonding or interlacing, and the resulting geogrids are called extruded geogrid, bonded geogrid and woven geogrid respectively. Within the groups, the geogrids can either be uniaxial, biaxial or triaxial depending on the direction of stretch during manufacturing. They are mainly used for reinforcement purposes in soil applications (Holtz, Christopher, & Berg, 2008).

Geonets are planar polymeric products consisting of a regular dense network of integrally connected parallel sets of ribs overlying similar sets at various angles. At first glance, geonets appear similar to geogrids; however, they are different from each other in function. They are used for their in-plane drainage capability, and they have diamond-shaped apertures with the resulting angles between a set of ribs being of the order 70-110° (Sanjay, 2012).

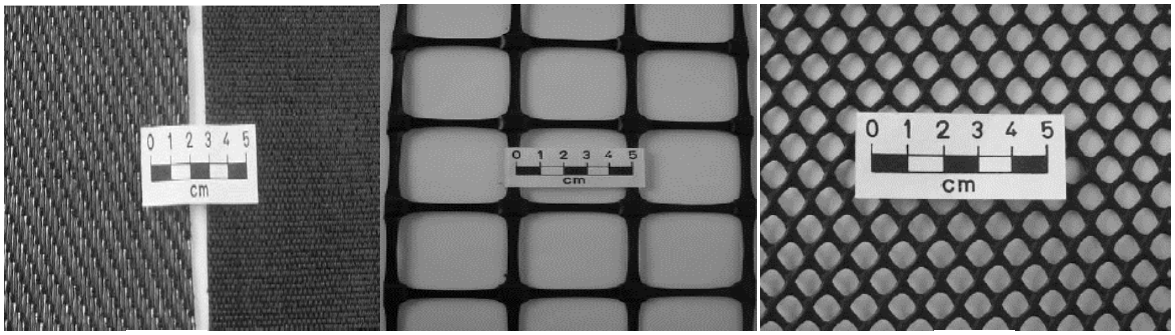

a) b) c)

d) e) f)

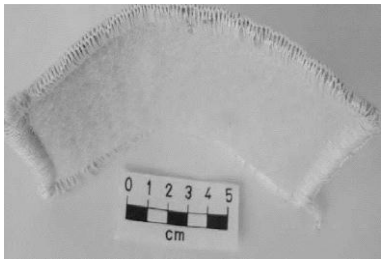

g)

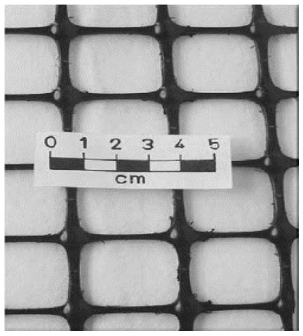

h)

Figure 4-1 a) Geotextile, b) Geogrid, c) Geonet d) Geocell e) Geomembrane f) geofoam g) Geocomposite h) Geocomposite (Figures a,b,c,g,h: Shukla & Yin, 2006) (Figure d: Pokharel, 1997) (Figure e: Wikipedia) (Figure f: Federal Highway Administration, 2006)

Geocells are three dimensional, permeable, polymeric, interconnected honey comb cells or web structure, which are ideal for soil and rock confinement. They are mainly used for basal reinforcement and any other civil engineering works requiring confinement (Pokharel, 1997).

Geomembrane is a continuous membrane-type barrier/liner composed of materials of low permeability to control fluid migration. The materials may be asphaltic or polymeric, or a combination of both, making them impervious. They are referred to as barriers when

used inside a soil mass and are liners when the geomembrane is used at the interface or a surface revetment. They are commonly used in landfill applications for base and cover liner systems and barriers for liquid and solid wastes containment (Holtz et al., 2008).

Geofoam is a light weight product in slab or block form with a high void content and is used primarily as a lightweight fill, thermal insulators and drainage channels. They are used within embankments built over soft soils under the road and airfield pavements subject to freeze and thaw, and beneath on grade storage tanks containing cold liquids (ASTM D4439).

Table 4-1 Geosynthetics and their functions (Koerner, 2012)

Function(s) to be served by geosynthetic	Category	Geosynthetics that can be used
Separation	Primary	Geotextile, geocomposites, geofoams
	Secondary	Geotextiles, geogrids, geonets, geomembranes, geocomposites, geofoams
Reinforcement	Primary	Geotextile, geogrids, geocell, geocomposites
	Secondary	Geotextile, geocomposites
Filtration	Primary	Geotextile, geocomposites
	Secondary	Geotextile, geocomposites
Drainage	Primary	Geotextiles, geonets, geocomposites
	Secondary	Geotextiles, geofoams, geocomposites
Fluid Barrier	Primary	Geomembranes, geocomposites
	Secondary	Geocomposites

Geocomposites are products that are manufactured in laminated or composite form from two or more geosynthetic material (geotextiles, geogrids, geonets, geomembranes etc.) such that in combination they perform specific functions more effectively than when used separately. Various combinations can result such as geotextile-geonet, geotextile-geomembrane, geomembrane-clay etc., which are used in different civil engineering applications (Sarsby, 2007).

Upon installation, geosynthetics perform by serving more than one function which has been categorised as either primary or secondary depending on the dominant function. Table 4-1 shows such a classification of the different geosynthetics. However, of all the geosynthetics discussed, this study focuses on geotextiles and geogrids primarily serving the reinforcement and separation functions in road pavements.

4.2 GEOTEXTILES

Geotextiles are classified into woven geotextiles, non-woven geotextiles and knitted geotextiles depending on the manufacturing process (Figure 4-2). They are characterised by pore size distribution, which is referred to as the apparent opening size (AOS), designated as O_{95}. For instance, if a geotextile has O_{95} value of 0.3 mm, this means that 95% of the geotextile pores are 0.3 mm or smaller.

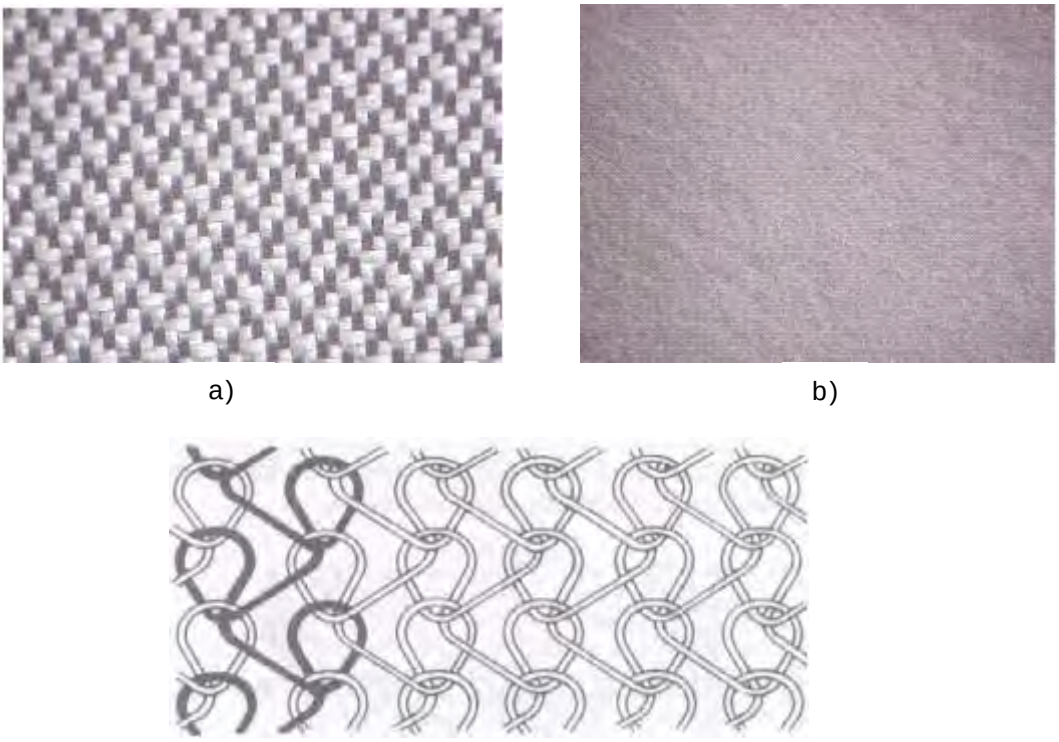

a) b)

c)

Figure 4-2 a) Woven geotextile b) Non-woven geotextile c) Knitted geotextile (Kiron, 2016)

Woven Geotextiles are obtained by the conventional weaving process. The yarn warps and wefts at right angles, forming a weave. The pattern is usually tight enough to filter some sand particles and is characterised by a comparatively regular distribution of pore or mesh

openings. The resulting structures are usually 1-2 mm with a regular distribution of pore or mesh openings (Sanjay, 2012).

Non-woven geotextiles are obtained by processes other than weaving. They are manufactured from either short staple fibre or continuous filament yarn. The type of fibre (staple or continuous) used has very little effect on the properties of the non-woven geotextile. Non-woven geotextiles are usually relatively thick. The filaments or fibres are then laid onto a moving conveyor belt to form a loose web slightly wider than the finished product. This passes along the conveyor to be bonded mechanically, thermally or chemically. The result is the three types of geotextiles: mechanically bonded non-woven geotextile, thermally bonded non-woven geotextile and chemically bonded non-woven geotextile. Thermally bonded non-woven geotextiles have a typical thickness of about 0.5-1 mm; chemically bonded types have a thickness of about 3 mm and the mechanically bonded non-woven type have a thickness in the range of 2-5 mm and are comparatively heavy because of the large quantity of polymer filament required for bonding (Kiron, 2016).

Knitted geotextiles are manufactured through the knitting process which involves interlocking of yarns together to form a planar structure. However, the use of these geotextiles is in very limited quantities.

Woven geotextiles are commonly used in applications that require increased support and stabilisation in comparison to non-woven geotextiles. Furthermore, woven geotextiles display generally the lowest extensibility and the highest strengths of all geotextiles, as shown in Figure 4-3 below. Woven geotextiles are also able to provide high tensile strength at low strains and are considered better reinforcement materials in contradistinction to non-woven geotextiles that provide high strength at high strains. For this reason, a woven geotextile was chosen for use in this study on road pavements.

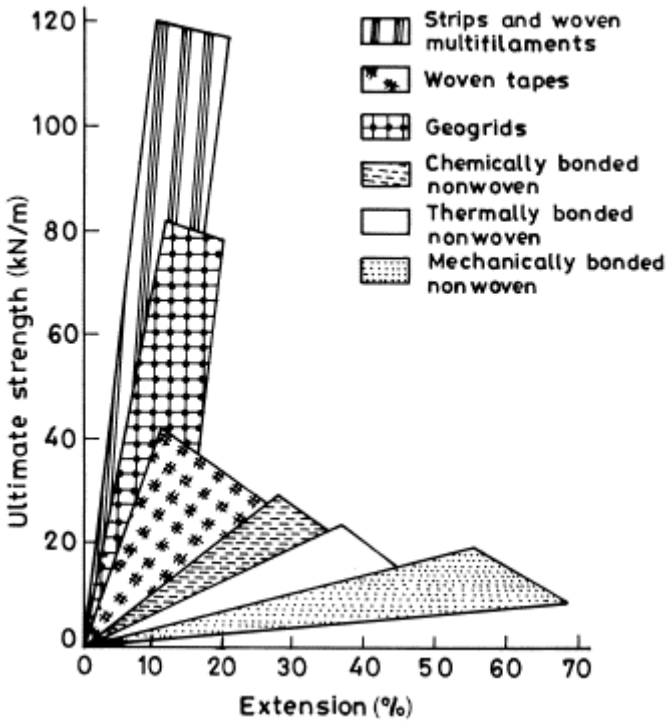

Figure 4-3 Typical strength properties of some geosynthetics (Shukla & Yin, 2006)

4.3 GEOGRIDS

Geogrids are manufactured by weaving, knitting, extrusion or by bonding the mutually perpendicular strips together at their cross points ultrasonically or thermally forming woven geogrids, knitted geogrids, extruded geogrids and bonded geogrids respectively. A woven geogrid is produced by interlacing, usually at right angles, two or more yarns or filaments. A bonded geogrid involves two or more sets of strands which are bonded together perpendicular to each other. Knitted geogrids are yarns knitted together perpendicular to each other, and an extruded geogrid is made of a sheet that is fed into a punching machine to form the geogrid.

In addition, the extruded geogrids can be stretched in one, two or multidirectional ways to form three main categories of geogrids, namely uniaxial, biaxial or triaxial, formed depending on the direction of stretch during manufacturing. After feeding the sheet in the punching machine, the punched sheet is then heated and stretched or drawn in the machine direction (MD-longitudinal direction, unrolled roll length); the overall effect is an enhancement of tensile strength and stiffness in the machine direction. At this stage the product is a uniaxially oriented grid; the grid can then be warm drawn in the transverse

direction (cross machine direction XD, corresponds to the shorter direction) to form a biaxially oriented grid (Maxwell, Kim, Edil, & Benson, 2005). The sheet can also be drawn in three directions forming the triaxial geogrid, where the strength is balanced in the three axes.

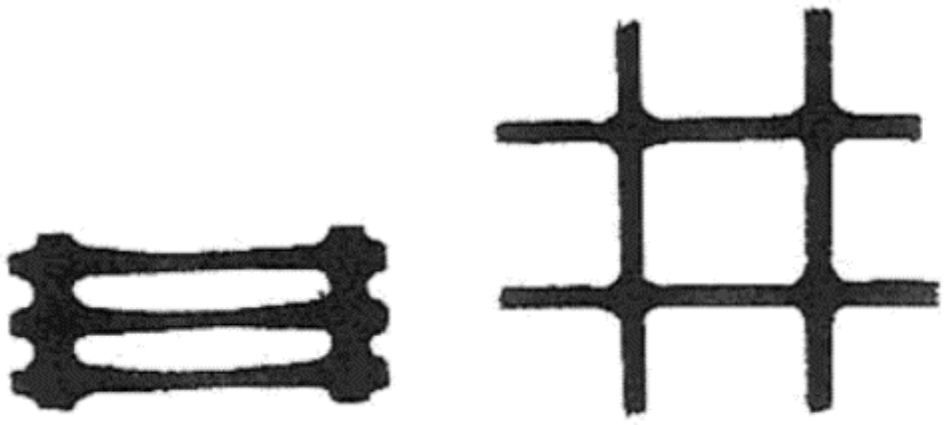

a) b)

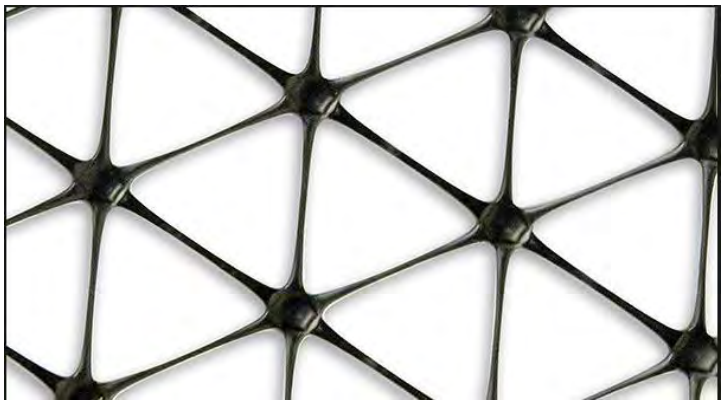

c)

Figure 4-4 Geogrid: (a) uniaxial; (b) biaxial; (c) Triaxial (Yu, McDowell, Dawson, & Thom, 2008)

Uniaxial geogrids usually exhibit a high stiffness in the machine direction [MD] with low to negligible stiffness in cross-machine direction [XMD]. However, it should be noted that there are products which have their maximum properties in the XMD. Uniaxial geogrids are intended for use in plane strain conditions where the secondary direction has a minimal loading. They are used to reinforce retaining walls, steepened slopes, dams, levees, landslide repairs, and roadway embankments. In comparison, biaxial geogrids have strength in both the longitudinal and transverse direction. By having tensile strength in two directions, they can distribute load forces, making them ideal for basal reinforcement and subgrade improvement (Kupec & McGown, 2004). Triaxial geogrids, which are a recent

development in the industry, have strength in multiple directions. They have a triangular structure with three principal directions of stiffness (Figure 4-4).

Overall, geogrids are often quite stiff as compared to the fibres of geotextiles (Figure 4-3). They have a mass per unit area which varies widely between 200-1000 g/m^2 and a percent open area of between 40-95%, suggesting that almost all soils can be able to interlock within the grid (Koerner, 2012). Owing to the two orthogonal directions of stresses, the biaxial geogrid was selected to be used for in this study as reinforcement inclusions within the pavement.

4.4 FUNCTIONS OF GEOGRIDS AND GEOTEXTILES

The most common use of geotextiles and geogrids as inclusions in road pavements primarily serve the function of reinforcement, separation and filtration, which is mostly associated with geotextiles. The performance of these geosynthetic reinforcements depends on the tensile stiffness mobilised with the limiting factor being the soil-geosynthetic interaction. Geotextiles and geogrids interact with the base soil in different ways, as will be discussed in Section 4.7.

The benefits of using geotextiles and geogrids are most significant in weak subgrades of California Bearing Ratio (CBR)<3% as shown by Montanelli et al. (1997). A prerequisite to the mobilisation of the strength was that the geosynthetic had to be deformed. They further advanced that the influence of the reinforcement tensile stiffness decreases if the subgrade has a high bearing capacity. From this point of view, it is clear that only an elongated reinforcement can develop strength and that is why the reinforcing effect in unpaved roads on soft subgrade does not develop until trafficking and deformations occur (Ashmawy & Bourdeau, 1995). However, long term benefits have also been realised over the course of time with pavements overlying competent subgrades of CBR > 3% with geotextiles serving the separation function. Road pavements have been exhumed after 30 years of service and the inspection has shown that they maintained their full structural section since they were built over a geotextile (Propex, 2011).

4.4.1 Reinforcement

The reinforcement function of geosynthetics develops through the shear interaction between the base course layer and the geosynthetic. Vehicular loads cause a spreading effect on the base aggregates; inclusion of the geosynthetic allows for shear interaction to

develop, thus inhibiting the lateral spread. This shear interaction occurs in different ways for the geotextile and geogrid.

Reinforcement in road pavements is provided by geogrids through friction or interlock developed between the aggregate and the geosynthetic, whereas geotextiles provide tensile reinforcement through frictional interaction with the base course materials. This reduces the applied stresses on the subgrade, thus preventing rutting due to subgrade overstress.

4.4.2 Separation

Koerner (2005) defines separation as the placement of a flexible porous textile between dissimilar materials so that the integrity of and functioning of both materials can remain intact or be improved. The geosynthetic is then able to provide physical separation of subgrade and base materials during the construction and operating life of the pavement.

In road pavements where a granular aggregate is placed on fine-grained soils, two detrimental mechanisms occur over time without use of geosynthetic separators:

- Fines from the subgrade can migrate to the base course of the pavement during trafficking hence contaminating the base layer. The aggregate loses the rock to rock contact thus diminishing the strength of the aggregate base leading to an acceleration of pavement failure.
- Also, mechanical action due to traffic causes the aggregate to be pushed/punched down into the fine grained aggregate; this reduces the effective thickness of the aggregate layer.

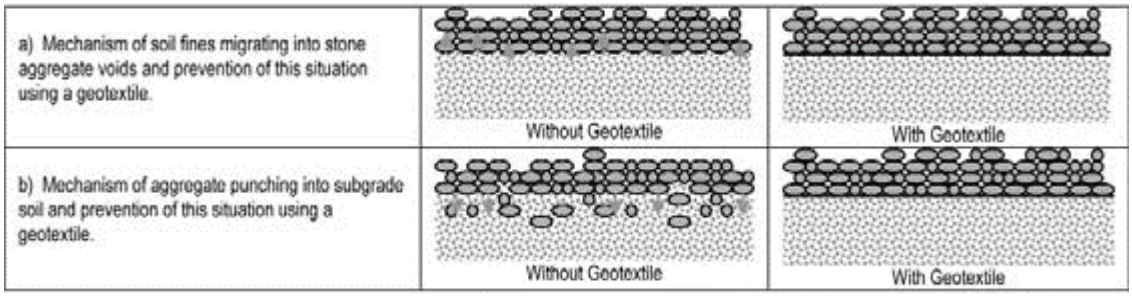

Figure 4-5 Separation function by geotextiles (Koerner, 2012)

In both cases in Figure 4-5, the base course is contaminated. The base course in such a state is not able to offer its intended structural support to vehicular loads. Thus, there is a reduction in strength, stiffness and drainage characteristics, promoting distress and pavement failure accordingly. The primary function of geotextiles is separation, bolstered by their very nature of being flexible sheets with relatively small pores. In distinction to geotextiles, geogrids can serve the separation function, but as a secondary characteristic. Geogrids, as shown by Fannin & Sigurdsson (1996) limit the amount of fines contamination in comparison to similar pavement sections without a geosynthetic. The ability of a geogrid to act as a separator is related to its functioning as a reinforcement. The geogrid as a reinforcement at the interface of base-subgrade limits the shear and vertical stress in the subgrade, as a result limiting the potential for mechanical mixing (Sanjay, 2012).

4.4.2.1 Relationship between separation and reinforcement function

The separation function of the reinforcement can supersede the reinforcement function if the ratio of the applied stress on the subgrade soil to the shear strength has a low value (less than 8). This is considered independent of the settlement of the reinforced soil system, as shown in Figure 4-6 (Shukla & Yin, 2006).

However, it is important to note that separation depends on the grain sizes of the soils involved. Typically, the low strength foundation soils have small grains and they are overlain with a layer of coarser materials as in road pavements, shallow foundations and railway tracks. In such an instance, separation takes priority regardless of the ratio of the applied stress on the subgrade to the shear strength of the subgrade soil.

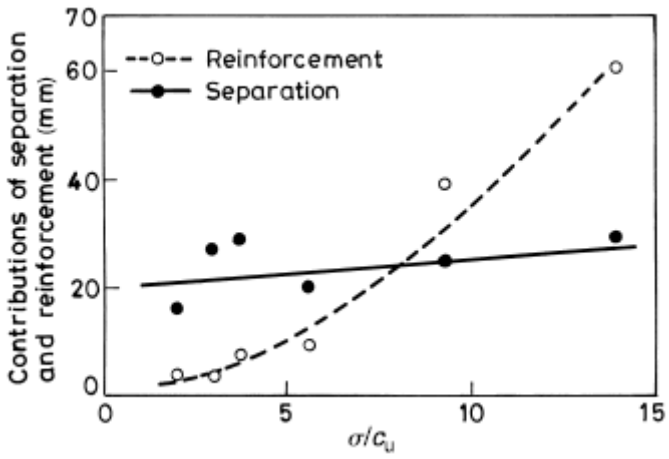

Figure 4-6 Relationship between the separation and the reinforcement functions (after Nishida and Nishigata, 1994) (Shukla & Yin 2006)

Separation and reinforcement functions of a geosynthetic complement each other. For instance, the reinforcement function is directly responsible for the reduction of deformation and in doing so it reduces the mixing of particles and thereby indirectly serves the separation function. The separation function prevents mixing, thus preventing progressive loss of the strength of the subsequent layers.

4.4.3 Filtration

Filtration refers to the ability of the geosynthetic to filter out fines contained in pore water as the water flows from the subgrade to the base. Traffic loading generates pore pressures in the subgrade and the fines may become suspended in the pore water and can be carried into the base in the absence of a proper filter. The migration of the fines into the base layer causes deterioration of the structural capability of the base, leading to failure of the pavement.

Therefore, a geotextile is needed to filter fines without getting clogged. The amount of fines pumped through a geotextile is dependent on the opening size of the material. Geotextiles with a high permeability have more pore water dissipation and allow more pumping than geotextiles with a greater thickness, which reduces the hydraulic gradient (Sanjay, 2012).

4.5 GEOSYNTHETIC REINFORCED PAVEMENTS

Roadway construction represents the initial application of geosynthetic materials with the applications of geogrids and geotextiles in unpaved and paved roads being widely adopted. It is of essence to note also that prior to paving, all paved roads undergo a period of being unpaved where they are subjected to the traffic of construction equipment.

The determinant as to the need of reinforcement geosynthetics (geotextile and geogrid) within a pavement is normally the subgrade, it being the foundation upon which the road pavement structure is supported.

4.6 SUBGRADE CONDITIONS FOR GEOSYNTHETIC REINFORCEMENT

Based on experience and several case histories, the following subgrade conditions have been found to be most appropriate for geosynthetic use in roadway construction as determined by Holtz, Christopher, & Berg, (1998):

- Poor soils
    - Unified soil classification system: SC, CL, CH, ML, MH, OL, OH and PT.
- Low undrained shear strength soils
    - $\tau_f = Cu < 60\ KPa$
    - CBR < 3
    - Resilient modulus M_R =30

Under these conditions, separation is the primary function of the geosynthetics and the subgrade is improved through stabilisation hence allowing for long term strength improvements. However, if large ruts develop upon the application of the load, then some reinforcing effect gets mobilised. Also, AASHTO M288-96 infers that when the subgrade soil has a CBR of 1-3 or undrained shear strength of 30 to 90 Kpa, reinforcement of the subgrade is needed.

Reinforcement benefits have been observed for subgrade strengths up to a CBR of 8 (M_R of 80 MPa) as shown in Table 4-2. In addition, there appears to be a relationship between decreasing reinforcement benefits with increasing subgrade strength as shown in Table 4-2.

Table 4-2 Reinforcement benefits for paved permanent roads (Berg, Christopher, & Perkins, 2000)

BENEFIT	PERMANENT PAVED ROADS SUBGRADE CONDITIONs		
	Low CBR < 3 (MR < 30 MPa)	Moderate 3 < CBR < 8 (30 < MR < 80 MPa)	Firmer CBR > 8 (MR> 80 MPa)
Reducing undercut	✓	O	◇
Reducing disturbance of the subgrade during construction	✓	O	◇
Reinforcement of the base aggregate in a roadway to reduce the section	O	✓	O
Reinforcement of the base aggregate in a roadway to increase the design life of the pavement	✓	✓	O
KEYS ✓ - usually a benefit, O - a known benefit in certain (various) conditions , ◇ - usually not a benefit			

4.7 MECHANISMS OF SOIL REINFORCEMENT

Different studies (Giroud & Bonaparte, 1984; Perkins & Ismeik, 1997; Gupta, 2010) have identified the three modes of geosynthetic reinforcement in roadways, namely: lateral confinement, increased bearing capacity, and tension membrane effect. The reinforcement function is produced when the geosynthetic is placed either within the base or at the interface of the base and subgrade. The mechanisms were initially based on observations from static loading. Similar reinforcement mechanisms were also observed by studies done under cyclic loading (Webster, 1992)

4.7.1 Lateral restraint/confinement

The main function of the base of a road is to reduce the loads induced by traffic to such an extent that the underlying subgrade is protected from deformation. A vertical load will induce lateral loads that spread the aggregates, leading to local deformations of the base. However, as a result of the frictional interaction and the interlocking between the geotextile-soil and geogrid-soil respectively, the aggregates are restrained between the

interface of the subgrade and fill. The geosynthetic is then able to take the additional shear stresses between the subgrade and fill that would have otherwise been applied to the subgrade, hence acting as a buffer. This eventually leads to an improvement in load distribution of the subgrade and reduction of the fill thickness (Figure 4-7) (Hufenus et al., 2006).

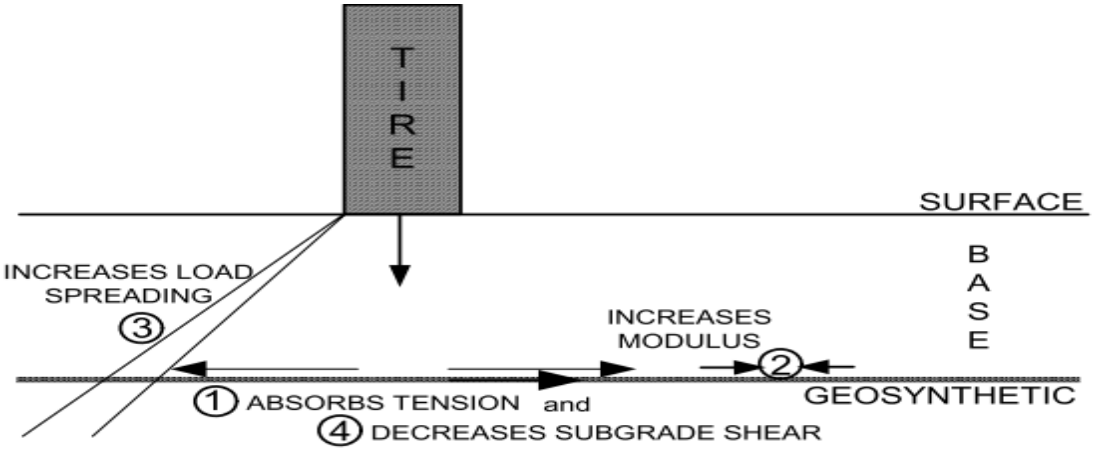

Figure 4-7 Lateral restraint (Maxwell et al. 2005)

Also, in the case of subgrades, when the vertical stresses on the subgrade exceed the elastic limit in an unreinforced unpaved road, local shear and large deformations ensue. These deformations cause accelerated deformation of the base layer which furthers fatigue of the subgrade soil due to the increased stress levels (i.e. an increased ratio between applied and allowable stress). After a relatively small number of vehicle passages, the plastic limit (ultimate bearing capacity) is exceeded and general shear failure occurs. From experience, if the subgrade is confined, the local shear failure does not become large and the subgrade soil can support a vertical stress close to its elastic limit (J. P. Giroud et al., 1985).

Confinement requires a geosynthetic with small apertures or grid as in geotextiles which have small openings. Geogrids provide confinement if the quantity of the subgrade soil escaping through geogrid openings is not sufficient to cause heave of the base layer. The effectiveness of a reinforcement geosynthetic does not only rely on its ability to adequately transmit loads to the fill material through interlocking and friction, but it is also improved by the stiffness of the geosynthetic.

4.7.2 Improved load distribution

Load distribution is a function of the mechanical properties and thickness of the base. The presence of a geosynthetic layer in the base generally leads to a change in the stress and strain relationship in the subgrade. For a layered system with a weak subgrade underlying a base, the increase in the modulus of the base layer results in a more improved, broadly distributed vertical stress on the subgrade (Figure 4-7 above). This means that the surface deformation will be less and more uniform as well (Perkins, 1999). Therefore, a confined base layer is able to provide better applied load distribution than is possible with unreinforced base layers. A better performance is expected for a geogrid than geotextile reinforced base owing to the different nature of their interactions with the granular base (Giroud et al. 1985).

4.7.3 Increase of bearing capacity

The inclusion of reinforcement geosynthetics shifts the failure envelope of the pavement system, from the relatively weak subgrade to relatively strong base by forcing the potential bearing surface plane to develop at an alternate higher shear strength surface (Figure 4-8). This tends to increase the bearing capacity of the roadway.

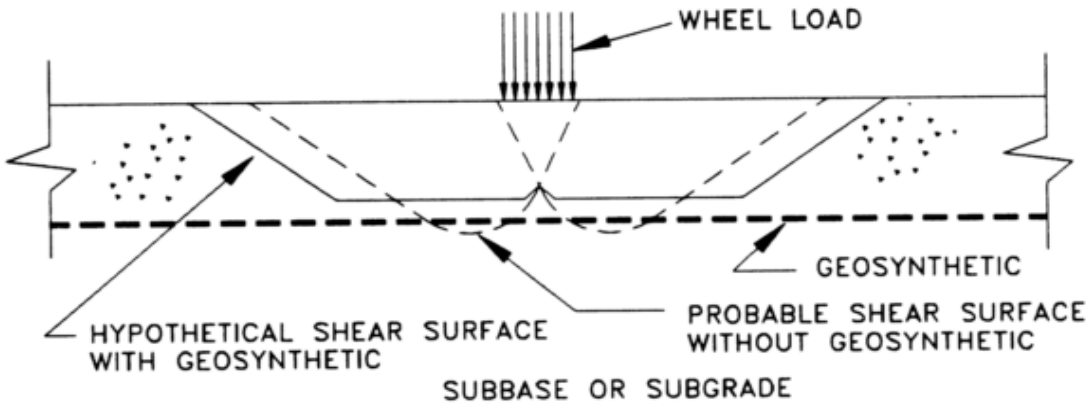

Figure 4-8 Improved bearing Capacity (Holtz et al. 1998)

In Figure 4-8, the reinforcement action of the geosynthetic decreases the shear stresses transferred to the subgrade, thus providing vertical confinement on the subgrade outside the loaded area where the heave occurs. This decreases shear strain at the top of the subgrade and minimises subgrade deformation and upheaval. The bearing failure model

may change from punching failure without reinforcement to general failure with an ideal reinforcement as established by Binquet and Lee (1975) (Gupta 2010).

The increase in bearing capacity additionally results in the effect of reduction of settlement as in Figure 4-9.

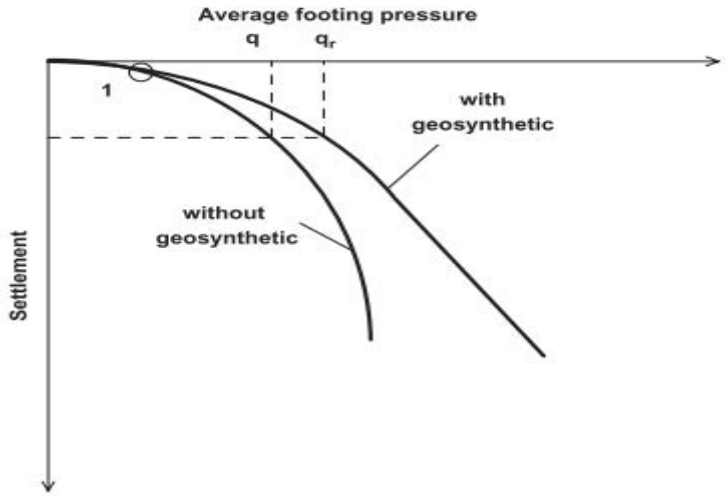

Figure 4-9 General nature of the load–displacement curves for unreinforced and reinforced subgrade. (Kazimierowicz-Frankowska 2007)

4.7.3.1 Mechanics of increased bearing capacity

The improvement in bearing capacity due to the use of geosynthetic has been demonstrated using triaxial tests. Two phenomena have been established and demonstrated using the Mohr circle: 1) Concept of apparent cohesion, 2) concept of increase of apparent confining pressure.

1) Concept of apparent cohesion

Reinforcement assists in the introduction of an apparent cohesion to a granular soil which initially had no cohesion (Figure 4-10). The reinforcement in the soil increases the major principle stress at failure from σ_1 to σ_{1R} (with an apparent cohesion C'_R) as shown in the Mohr stress Figure 4-10 (Pham, 2009). When reinforcement is provided in the direction of σ_1, interaction between the reinforcement and the soil generates frictional forces at the interface. Tensile stresses will be generated by the reinforcement and a corresponding compression as long as there is no slippage between the soil and reinforcement.

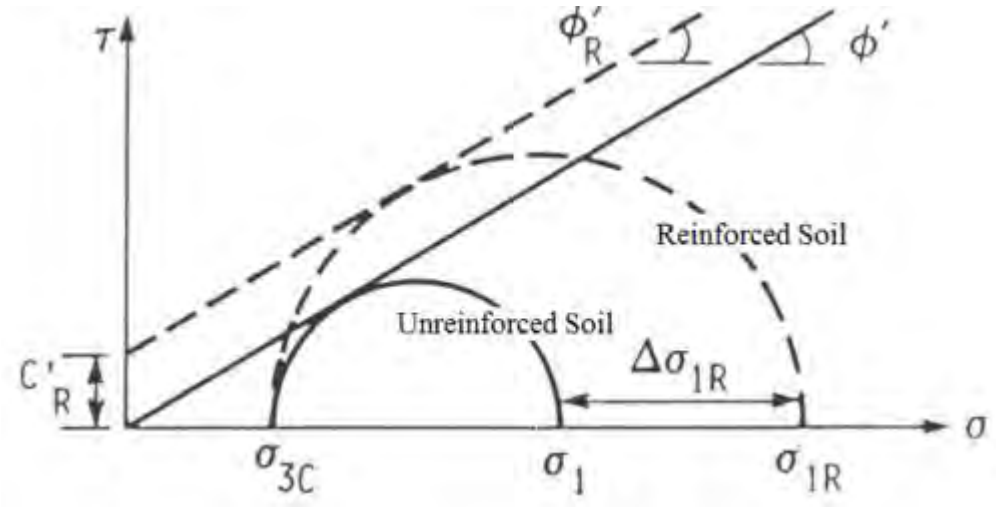

Figure 4-10 Concept of Apparent Cohesion due to the Presence of Reinforcement (Scholosser & Long, 1972; Pham 2009)

2) Concept of apparent confining pressure

The inclusion of a tension member increases the axial strength from σ1 to σ_{1R} with an increase of confining pressure of $\Delta\sigma_{3R}$ (Figure 4-11). Therefore, the increase in strength due to reinforcement can be equated by a change in the stress state of the soil that resulted in an enhancement of the confining stress $\Delta\sigma_{3R}$ (Ruiken & Ziegler, 2008).

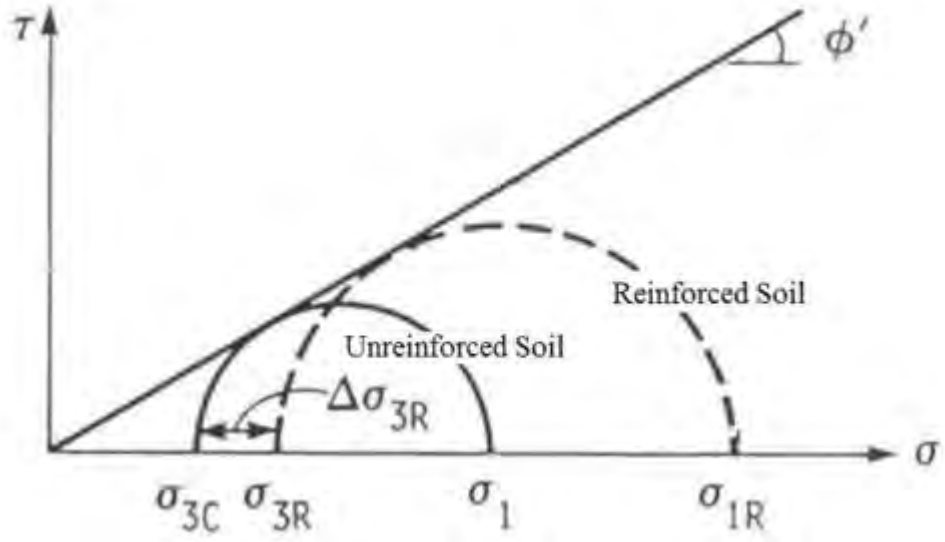

Figure 4-11 Concept of apparent confining pressures due to presence of reinforcement (Yang 1972; Pham 2009)

4.7.4 Tension membrane effect

For tensioned membrane to be triggered, the wheel loads should cause plastic deformation and ruts in the subgrade. The geosynthetic should have a sufficient high tensile modulus for the tensile stresses to develop within the reinforcement. The action of the load leads the geosynthetic to exhibit a wavy shape that causes it to stretch (Figure 4-12 below). When a stretched flexible material has a wavy structure, the normal stress against its concave face is higher than the normal stress against its convex shape. In a practical sense, the pressure on the soft subgrade ends up being smaller than the pressure applied to the fill on the upper concave side. This is known as the tensioned membrane effect.

The membrane effect counteracts the traffic load, hence limiting the vertical component of the load, and the reinforcement in tension distributes the load over a larger area leading to a reduction in settlement (Bloise & Ucciardo 2000). Therefore, the mobilisation of the membrane effect requires that the geogrid and geotextile be deformed and tensioned through the development of ruts. This indicates that the tensioned membrane effect mostly finds its application in unpaved roads where large rutting is allowable.

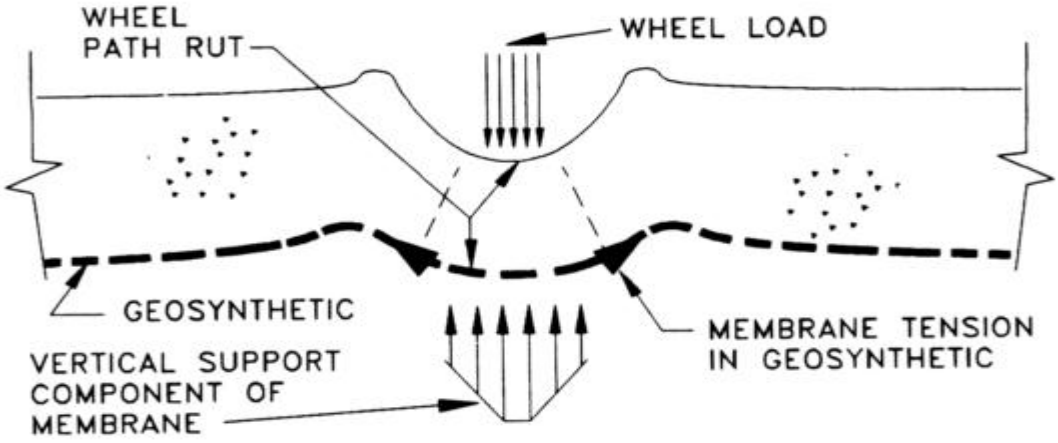

Figure 4-12 Tensioned membrane effect (Holtz et al. 1998)

4.8 REINFORCING MECHANISM ASSOCIATED WITH DYNAMIC LOADING

Over and above the membrane action, lateral restraint and the passive anchorage, there are three main mechanisms associated with the cyclic loading conditions, namely, the

additional compaction of the aggregate base course, the dynamic interlock and improvement of the soil elastic modulus.

4.8.1 Additional base aggregate compaction

The repeated traffic loads lead to additional compaction of the aggregate base course as it triggers the lateral restraint and membrane action which increases the stiffness and resistance of the granular material. This has been shown by tests in the laboratory on a reinforced soil; after application of cyclic loading, monotonic loading was then applied and a significant improvement in performance was noted, better than monotonic load application prior to the cyclic load application. This was attributed to the additional compaction that results from the cyclic loading. This compaction phenomenon due to the presence of reinforcement prevents the occurrence of bearing failure during the early cycles of loading (Ashmawy & Bourdeau, 1995).

4.8.2 Dynamic interlock

This mechanism applies only for geogrids because of their grid sizes. Upon loading, aggregate particles become locked in the grid apertures, and on unloading, the locked soil particles in the apertures prevent complete recovery of the elastic and viscous components of the reinforcement tensile strain, hence locking in stresses within the reinforcement. As a result, the geogrid remains stressed, hence improving its mechanical performance and the lateral confining pressure in the surrounding soil is enhanced (Ashmawy & Bourdeau, 1995).

4.8.3 Improvement of the soil elastic modulus

Geosynthetics exhibit an elastic plastic stress-strain response when subjected to loading. A nonlinear response is observed during loading, and a stiffer response is seen during the unloading phase which is approximated by a linear response representative of the elastic behaviour of the material, as shown in Figure 4-13 below (Perkins, 2000).

The geosynthetic quickly responds to the applied loads with an increase in the elastic modulus which enables the mobilisation of the geosynthetic's tensile resistance. Moreover, the geosynthetic increases the dynamic damping characteristic of the reinforced soil compared with the unreinforced soil. This occurs through the absorption of energy by the geogrid or geotextile, and also due to the friction generated in the dynamic loading (Carotti & Rimoldi, 1998; Moayedi et al., 2009).

Figure 4-13 Elastic plastic geosynthetic behaviour

4.9 SUMMARY OF GEOSYNTHETIC REINFORCING EFFECTS

Vehicular loading in reinforced pavements mobilises the positive effects was discussed broadly in Sections 4.7 and 4.8. The resulting advantages include separation, increased load distribution that prevents overstressing of the subgrade soils and increased load bearing capacity; both have an effect of reduced settlement and heaving. On the contrary, unreinforced pavements experience the adverse effects of loading such as contamination of the layers and limited load distribution, hence excess stresses act on the subgrade (Figure 4-14 below). All these causes high rutting and heaving, resulting in premature failure of the road pavement.

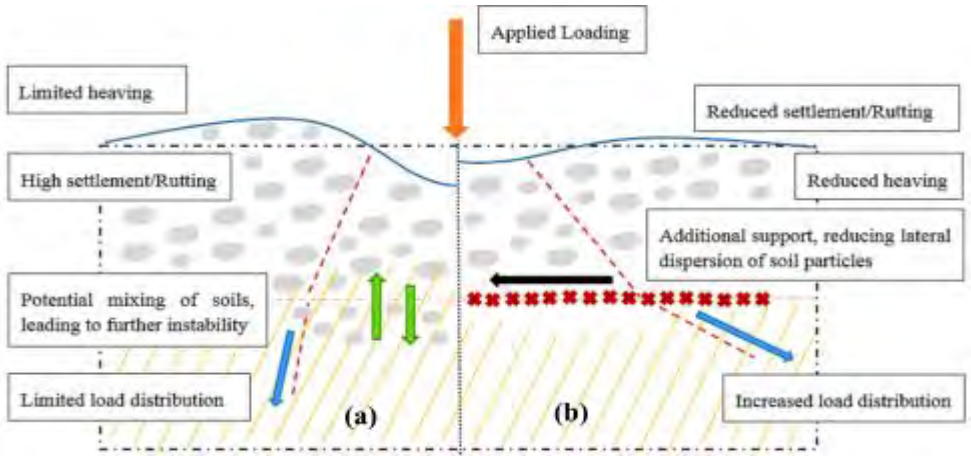

Figure 4-14 Comparison between a) unreinforced and b) geosynthetic reinforced pavement (Oriokot, 2014)

4.10 BEARING CAPACITY

Bearing capacity is the ability of a soil to support imposed load without undergoing shear failure or excessive settlement. The ultimate bearing capacity is the theoretical maximum pressure the soil can support without failure. In considering the ultimate bearing capacity, the pavement structure is assumed to fail under shear when subjected to sufficiently high traffic stresses.

The ultimate strength of a pavement remains a complex parameter to determine since deformations prior to pavement collapse cannot easily be quantified. Deformation of the pavement through its service life therefore determines its serviceability and must be controlled (Oloo, Fredlund, & Gan, 1997). Plate load tests have been conducted to try and understand the load bearing capacity of soils. Experimentally, the loading due to traffic has been simulated through static plate load tests and cyclic plate load tests. This is discussed in Section 4.11.

The inclusion of geosynthetic results in improvement of the road pavement's bearing capacity. The geosynthetic reduces the outward shear stress transmitted from the overlying soil/fill to the underlying foundation soil. This improvement leads to an increase in shear strength in the reinforced soil mass due to the geosynthetic inclusion, which results in a general shear failure rather than a local shear failure. The reduction in shear stresses and the change in failure mode is the key benefit of a geosynthetic layer at small deformations (Figure 4-15).

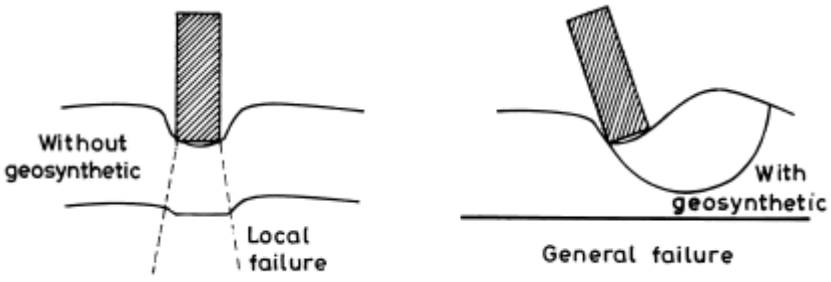

Figure 4-15 Change in failure mode resulting from geotextile inclusion in two layered soil (Shukla & Yin, 2006)

4.11 PLATE LOAD TESTS

Plate load test is used to obtain a load-settlement curve of a soil at a particular depth in order to obtain the bearing capacity of a soil and evaluate the strength of flexible pavements. Static plate load and cyclic plate load tests have been used experimentally to understand the response of road pavements under vehicular loading. Different loading regimes and box sizes used by different researchers in dynamic loading will be discussed in Section 4.11.6. Additionally, Section 4.11.7 discusses the concept of vehicular wander against the cyclic plate load test. The test involves loading a steel plate and recording the measurements corresponding to the load increment. In reinforced systems, it is recommended to observe settlement as a failure criterion since the peak load may be difficult to determine, as will be explained in Section 4.11.5. The load at any settlement is divided by the area of the plate to give the value of bearing capacity at a particular depth.

The bearing capacity of soils from plate load tests are representative of soils within a depth of influence, which is approximately 1.5B-2.0B (B- Width or diameter of footing). This connotes that the increment of loading results in stress predominant in the region of 0 to 1.5B-2B. Stress versus settlement behaviour from plate load tests differs with changes in plate sizes since different plate sizes result in different levels of stress bulbs and mean stresses in soils. This phenomenon is conventionally referred to as 'scale effect' (Oh & Vanapalli, 2013). Additionally, the density of the soil affects the results from plate load tests, especially laboratory simulations, since the packing of the soil has an implication on its strength.

4.11.1 Influence of scale

Siddique et al., (1999) describe scale effect as the variation in the bearing capacity characteristics with the variation in the footing size. Small scale laboratory models encounter the scale effect primarily due to boundary effects from the small sample size, scale effect arising from the limited ratio of the footing size to grain size as highlighted by Ovesen (1975) and scale effect from the limited footing width (Cerato & Lutenegger, 2007).

The bearing capacity equation 4-1 from Terzaghi (1943) has three bearing capacity terms, namely the surcharge term (N_q), the weight term (N_γ) and the cohesion term (N_c) that are dependent on the internal angle of friction of the soil. For surface footings, the surcharge term is not considered.

$$q_u = C.N_c + q.N_q + 0.5\,\gamma' B.N_\gamma$$ Equation 4-1

The weight factor (N_γ) in Terzaghi's equation decreases with an increase in the width of the footings. Attempts by different researchers (Cerato, 2005; Lau & Bolton, 2011; Toyosawa, Itoh, Kikkawa, Yang, & Liu, 2013) have resulted in three explanations that are generally accepted:

I. There is a reduction in the internal friction angle ϕ′ with increasing footing size. The scale effect observed between N_γ and the footing size is directly related to the mean stress underneath the footing, with larger footings resulting in higher mean stresses and lower friction angles (Mohr-coulomb when tested over a large stress range). Whereas small footings experience low mean stresses but high N_γ values which indicate high friction angles, Cerato & Lutenegger, 2007 have shown that a small footing (small mean stress) behaves as if it were in a dense state of soil than a larger footing even at the same void ratio. The stress dependency has been related to a curved Mohr-coulomb envelope which has helped to explain why small footings have larger N_γ values. However, model scale footings test results cannot be used to observe the behaviour of full scale foundations; as model scale footings produced higher N_γ values, a reduction should be applied for a full scale foundation.

II. The effect of the particle size occurs due to the shear band thickness, since the shear band thickness is proportional to the particle size, d_{50} (grain size corresponding to 50% passing in grain size distribution). Coarse grained soils have an absolute scale that is relative to the foundation element. In comparison, fine grained soils by virtue of their small size are oblivious of dimensions of a foundation element. As much as both coarse and fine grained soils exhibit scale dependence, scale effect on footings on coarse grained (i.e. sands) soils is much projected. Hence, when the particle size is not so small in comparison with the footing model, there can be formation of a shear band, a phenomenon called "particle size effect" (Toyosawa et al., 2013). Ovesen (1975) has showed that the particle size effect becomes negligible for B/d_{50} greater than 30 for foundations.

III. Progressive failure mechanism results in a different mobilised angle of friction ϕ′ along the slip surfaces beneath the footing, resulting in progressive mobilisation of strength in different regions. The non-uniformity of strength is

anisotropy which leads to reduced angle of friction ϕ′ values on the slip surface (Lau & Bolton, 2011; Toyosawa et al., 2013).

4.11.2 Effect of size of the plate

The increase in the width of the plate results in an increase in loading. Therefore, bearing capacity of footings increases with increasing dimensions of the footing and for this reason, settlement decreases with increasing the width of the footing.

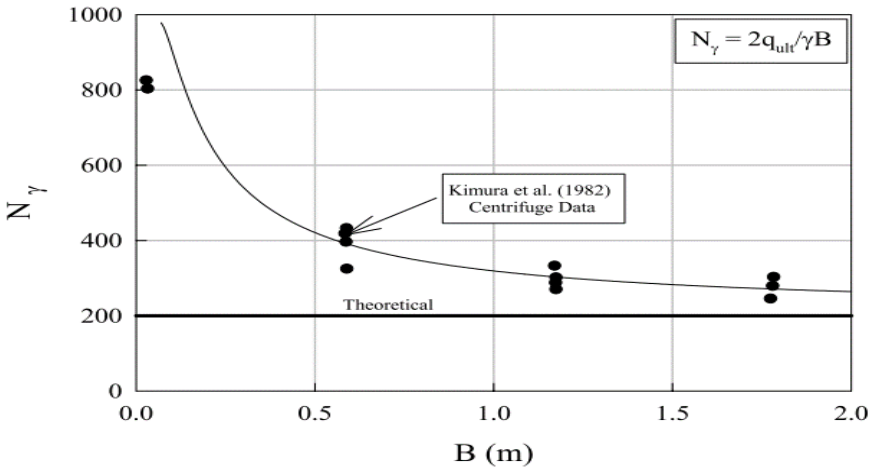

Figure 4-16 Theoretical versus Experimental Results of N_γ and Footing Width, B (Cerato, 2005).

This phenomenon has also been shown by Kimura et al. (1982) and Berry (1935), that bearing capacity increases disproportionately with increasing footing size. This means that the bearing capacity factor, N_γ , decreases with increasing footing size, if N_γ is back calculated from Terzaghi's bearing capacity equation 4-1 for a dense sand, cohesion (c) = 0. It has been shown experimentally that the value of N_γ varies with increasing footing width (Figure 4-16) which contradicts the N_γ obtained theoretically for bearing capacity equations.

4.11.3 Effect of shape of footing

The shape of the footing influences the bearing capacity; Terzaghi incorporated a correction factor for shapes other than strip footings based on their experimental findings. Strip footing and rectangular footings experience plane strain (2 dimensional) conditions,

whereas square and circular footings are axisymmetric. Therefore, much pressure is required to displace the soil due to the 3-D effect.

4.11.4 Effect of density

The degree of compaction of a soil is characterised by its dry density which is dependent on the degree of compaction or the moisture content. The change in moisture content or compactive effort brings about a change in density.

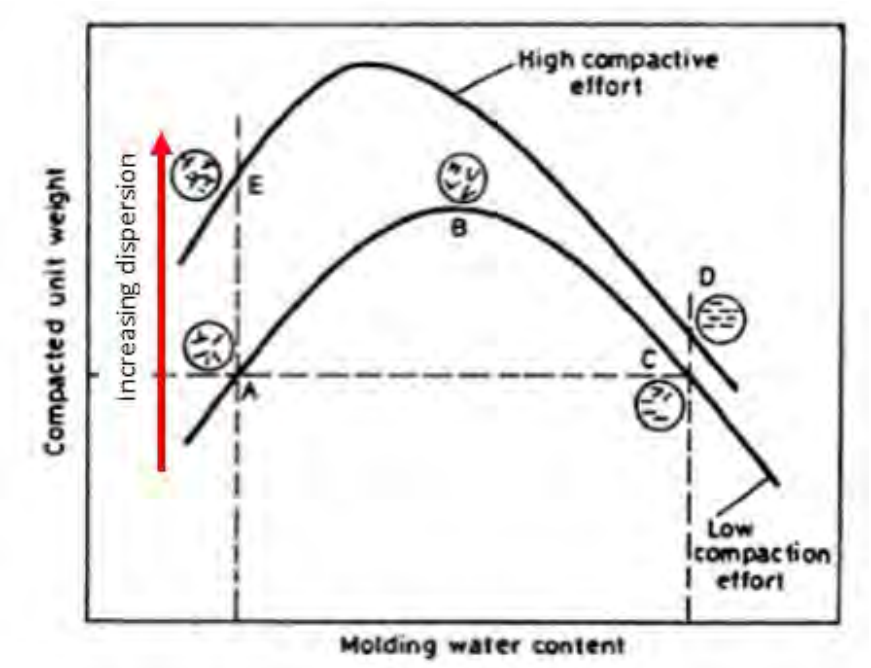

Figure 4-17 Effect of compaction on structure (after Lambe, 1958)

The higher the density of the base soil, the closer the packing of the soil particles and the higher the friction, hence a higher strength. Furthermore, the soils become less compressible with an increase of density. As the compactive energy increases, the soil becomes more orientated (dispersed) (Figure 4-17). For this reason, geosynthetic reinforced bases are able to perform more effectively if the soil particles are closely packed. This increases the frictional interaction between the geosynthetic and the soil, and the soil particles are able to more adequately interlock within the geogrid.

The effect of density is represented by the third term in Terzaghi's bearing capacity Equation 4-2.

$0.5\,\gamma' B.N_\gamma$ Equation 4-2

From the equation, it can be theoretically determined that the higher the density of soil, the higher will be the bearing capacity.

4.11.5 Experimental measurement of failure

Plate load tests are conducted using circular footings which replicate a wheel footprint on a pavement. For reinforced systems in a plate load test, it is recommended that the footing settlement, rather than the footing pressure, be used as an indicator of failure. This is because the settlement data for the reinforced soil layer indicates that the average footing pressure increases continuously with an increase in footing settlement, revealing no definite failure point as in Figure 4.18 below. This makes it hard to define a failure point (Som & Sahu, 1999).

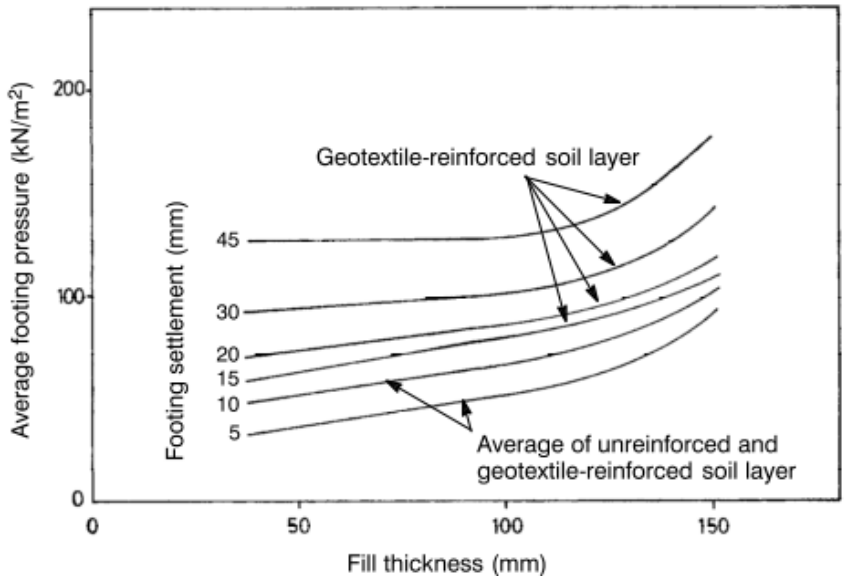

Figure 4-18 Variation of the average footing pressure values for different fill thicknesses carrying (Som & Sahu, 1999)

4.11.6 Vehicular wheel wander

Experimental testing conducted to simulate wheel loads have been through the cyclic application of load, as in the plate load test. This applies to vertical concentrated loads whilst the real traffic load is typified by wheel loads moving with lateral wander. Hence, it

is expected that the performance of model pavements from cyclic simulations will be different from a rolling wheel with wander.

When subjected to a rolling wheel, the pavement experiences vertical, horizontal and shear stresses with an extension–compression–extension multiple stress path and continuous rotation of the principal stress. These cause the recurring movement and rearrangement of the particles and results in a dramatic degradation of the unbound aggregate layer, which reduces the strength of the unbound materials. The degradation with each cycle pass results in permanent deformation of the wheel track.

Existing studies (Brown and Brodrick, 1999; Hornych, Kazai, and Quibel, 2000; Abu-farsakh & Chen 2012) have shown that the rolling wheel load has a much more damaging effect than the cyclic plate load. Therefore, in a field test it is anticipated that the benefit of including a geosynthetic reinforcement in the pavement could be more significant than in laboratory cyclic plate load tests. However, research carried out by Chen and Abu-Farsakh (2010) on various pavement sections using both cyclic plate load test and rolling wheel tests showed the performance of the sections to be similar under both types of loading. Hence, the cyclic plate load test can be a good indicator of determining the potential benefits of including a geosynthetic reinforcement within the pavement (Abu-Farsakh & Chen, 2011)

4.12 LITERATURE REVIEW OF PREVIOUS STUDIES

Since the commencement of the use of geosynthetics in civil engineering, research has been undertaken to investigate their benefits when used in pavements overlying soft subgrades. Different variations of laboratory and field tests have been conducted in order to understand their benefits and how they can be appropriately considered in design. Different parameters have been varied such as the size of the box, size of footing (Section 4.11.2), depth of placement of geosynthetic and type and stiffness of reinforcement.

4.12.1 Effect of size of the box

Different box sizes have been used by different researchers (Mandal & Das, 1993; Leng, 2002; Patra, Das, & Atalar, 2005; Latha & Somwanshi, 2009) in investigating the potential improvements arising from the use of reinforcement geosynthetics. However, the size of the box is affected by the plate size and shape, as discussed earlier in Section 4.11.2. Furthermore, the pressure bulbs of the plate determine the lateral and vertical extent of

the loading, such that energy is not absorbed by the wall of the box but is concentrated within the soil.

Oh & Vanapalli, (2013) have shown that in plate load tests the stress due to loading on a footing is predominant in the range of 0 to 1.5B, where B represents the width or diameter of the plate. Similar findings have been obtained by Yetimoglu et al., (1994) and Chen, (2007), who have shown that the increase in the Bearing Capacity Ratio (BCR) became insignificant beyond the depth of 1.5B.

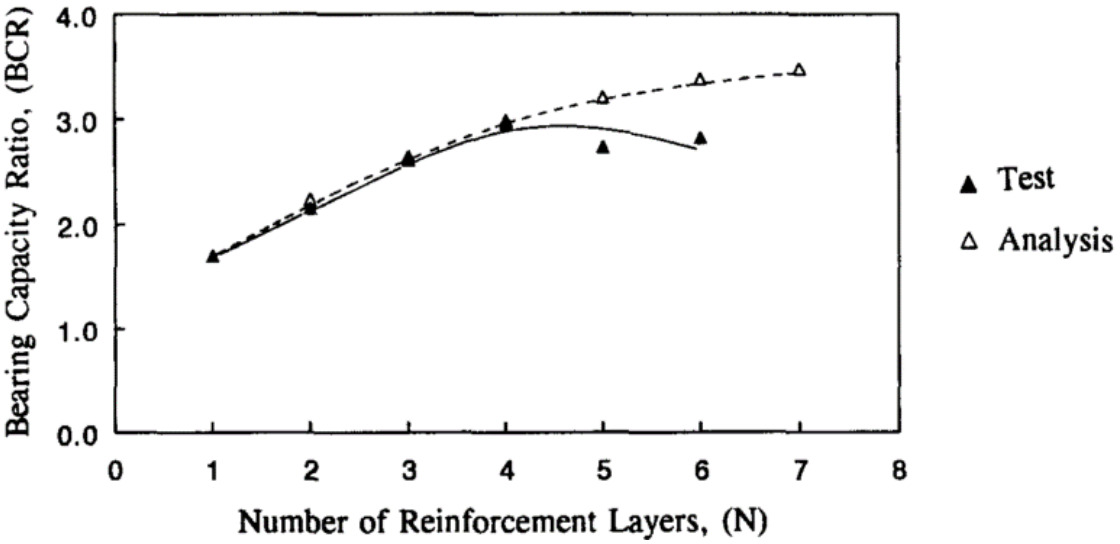

Figure 4-19 Variation of BCR with number of reinforcement layers (Yetimoglu et al., 1994)

From Figure 4.19, as the number of reinforcements increased, so did the BCR up to N=4. Beyond N=4, the increase of BCR proceeded but at a decreased rate; this represented the point at which the depth was 1.5B, as stated by Yetimoglu et al., (1994).

4.12.2 Effect of number of reinforcements

Studies have been conducted by Murad Abu-Farsakh, Chen, & Sharma, (2013), Haeri, Noorzad, & Oskoorouchi, (2000) and Latha & Somwanshi, (2009) to determine the implications of geosynthetic reinforcements within the soil whilst varying the number of reinforcements (N) within the soil. The results showed that the bearing capacity increased as the number of reinforcement layers increased. However, the significance of additional reinforcement decreased after N=4 as reported by Chen, (2007), Latha & Somwanshi,

(2009) and Yetimoglu et al., (1994), and N=3 as investigated by Murad Abu-Farsakh et al., (2013) and Mawer, (2013).

In road pavements, different authors (Moayed & Nazari, 2011; Oriokot, 2014; Tencate mirafi, 2010a) have employed the use of reinforcement layers (N) up to two in the pavement for laboratory and field tests. Furthermore, there is an optimum depth at which the reinforcement function of the reinforcement geosynthetic is felt most. The bearing capacity was seen to reach its maximum value at 51 mm (Chen, 2007; Oriokot, 2014) or between 0.1-0.2B (Latha & Somwanshi, 2009). However, this depth is not practical in field situations since placement at such a shallow depth might result in installation related damages of the geosynthetic. Additionally, Coleman, (1990) stated that for pavements on weak subgrades, the optimum benefit is achieved by placing the first layer of geogrid at the bottom of the base (interface) and the second layer at the midpoint of the base.

4.12.3 Effect of tensile strength and type of reinforcement

The performance of a geosynthetic reinforced pavement is dependent on the tensile strength of the fibre. Test results have shown that the performance improvement is different for different types of geosynthetics. This difference has been attributed to the tensile stiffness of the geosynthetic material, which is expressed in terms of the secant modulus. The secant modulus is obtained from the slope of the geosynthetic stress-strain curve which is determined from the wide-width tensile tests (Kim, Edil, & Benson, 2006).

Table 4-3 Geosynthetic properties (Chen, 2007)

Reinforcement	**T^a, kN/m**		**J^b, kN/m**		**Aperture Size, mm**
	MD	**CMD**	**MD**	**CMD**	
Mirafi BasXgrid11 geogrid	7.3	7.3	365	365	25x25
Tensar BX6100 geogrid	3.6	5.1	182	255	33x33
Tensar BX6200 geogrid	5.5	7.4	272	372	33x33
Mirafi HP570 geotextile	14	19.3	700	965	≈ 0

T^a-Tensile strength at 2% strain, J^b- Tensile modulus at 2% strain,

MD=Machine Direction CMD=Cross Machine Direction

Results from different authors (Kim et al., 2006; Latha & Somwanshi, 2009; Oriokot, 2014) have shown that tensile stiffness is not governing the strength improvement but the tensile modulus. This has also been demonstrated by Chen, (2007) as shown in Table 4-3 above.

From Table 4-3, it was seen that BX6100 and BX6200 geogrids was made of the same material and had similar aperture size, but BX6200 had higher tensile strength/modulus than BX6100. As seen in Figure 4-20, the performance of the BX6200 geogrid was better than BX6100. Furthermore, the behaviour of these two geogrids was very similar until a settlement of about 3 mm was reached. It is hence hypothesised that deformation is required to mobilise the geosynthetic strength. BasXgrid 11 geogrid with the highest stiffness/modulus in geogrids presented the best performance of all the geosynthetics. At relatively low settlements, the increase in bearing capacity of the geogrids was more significant than the HP570 geotextile which is of a higher tensile modulus; while after a certain amount of settlement, the geotextile reinforced soil became stiffer than the BX6100 & 6200 reinforced soil (Figure 4-20 below). This was attributed to the tensioned membrane effect, in that at higher deformations the geotextile was stretched such that its reinforcing effect was appreciably mobilised in comparison to the geogrids BX6100 & 6200.

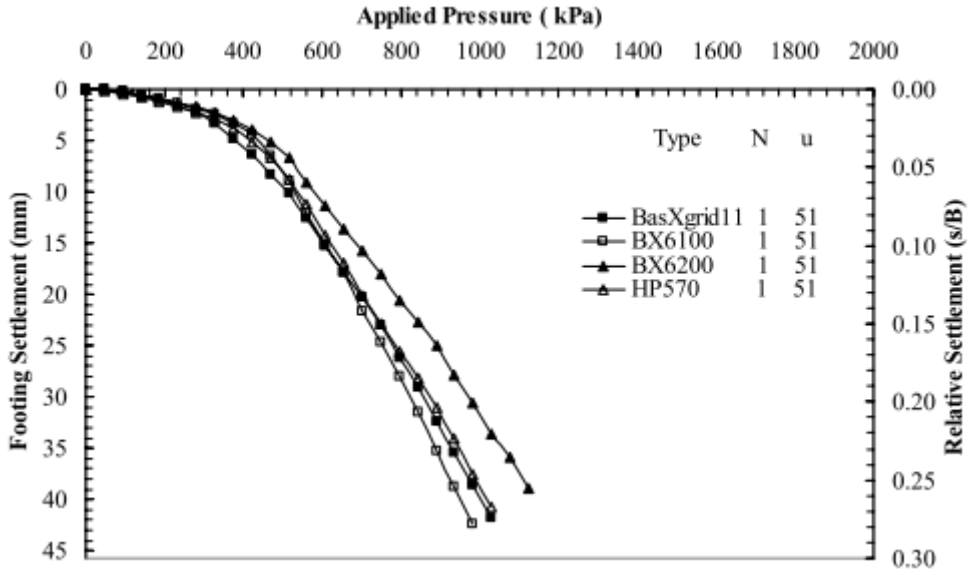

Figure 4-20 Pressure-settlement curves for model footing tests with one layer of different types of reinforcements (B×L: 152 mm×152mm) (Chen 2007)

4.12.4 Effect of anchorage

The triggering of tensioned membrane effect of reinforcement geosynthetics is an important phenomenon to the effectiveness of the reinforcement function of the geosynthetics. Giroud & Noiray, (1981) in their design assumed that for tensioned membrane to develop, there has to be sufficient anchorage of the geotextile to prevent slippage at the interface. Furthermore, they recommended a distance of at least 2B to 4B between the edge of the wheel and shoulder of the road for a sufficient anchorage. This has been further analytically confirmed by Zhan & Yin, (2001).

Studies conducted on unpaved roads, as discussed by Weng, (2003), have shown that adequate anchorage lengths are required for a better rutting resistance. However, for other laboratory and field tests, the evaluation of the effects of anchorage has shown conflicting findings on the benefits. Studies by Bourdeau, Chapuis & Holtz, (1988) and Palmeira & Cunha, (1993) indicated that anchorage is key to the functioning of reinforcement geosynthetics, whereas Bearden & Labuz, (1999) and Asha & Madhavi, (2010) reported no significant difference in anchored and unanchored reinforcement models.

In understanding the conflicting findings, Weng, (2003) has attributed the disparities to the interpretation of test results and variations in the test configurations and conditions.

The lack of proper slippage measurement and strain measurement made it difficult for the authors to substantiate their conclusions on the implications of anchoring. The slippage is fundamental to the mobilising of strength in the geosynthetic as the fibre is stretched. Weng, (2003) argues that if internal anchorage is adequate within the loading range, additional anchorage by increasing the length of the geosynthetic or an external anchorage method would therefore result in no additional benefit. Pretensioning prior to loading was recommended as a way of mobilising the reinforcement potential without incurring large deformations at the subgrade. However, excessive pretensioning could also lead to premature failure during loading, hence diminishing the benefits of pretensioning.

4.12.5 Improvements due to the use of reinforcement geosynthetics

As discussed in Section 4.6, the reinforcement function of geosynthetics is felt most with a soft subgrade of CBR of 3 or less. The two main benefits obtained are the reduction in the thickness of the pavement and extended pavement life. The tests conducted to investigate the improvements in the laboratory are dynamic tests (Figures 4.21 & 4.22 below) and static tests (Figure 4.23) which are further highlighted in Table 4-4. Field tests have also been undertaken by different authors (Collin, Kinney, & FU, 1996; Hufenus et al., 2006) to explore the performance of geosynthetic reinforced pavements.

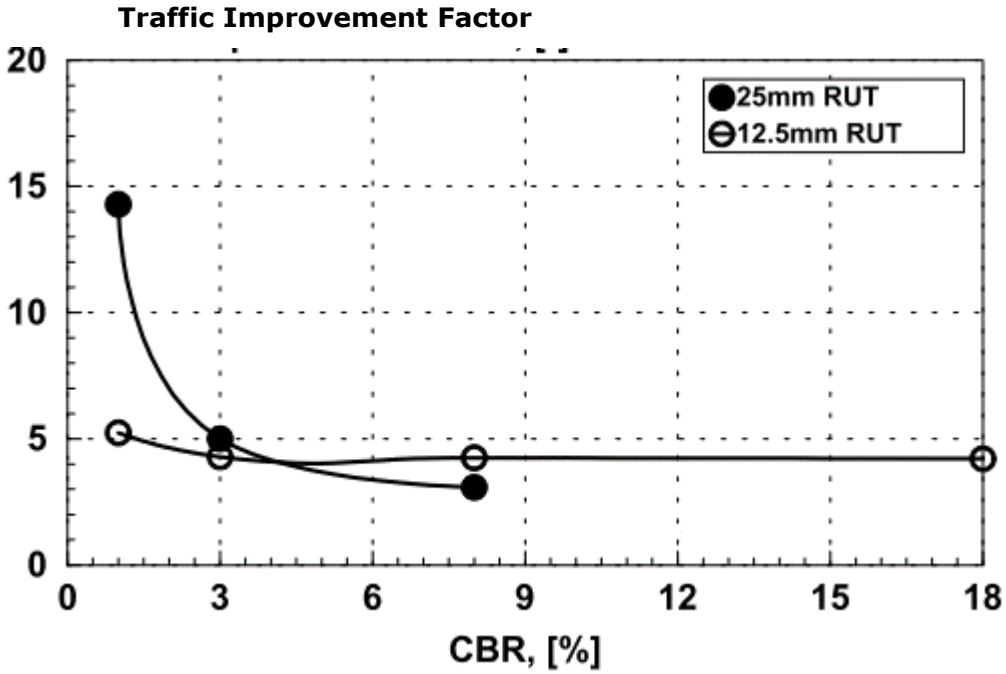

Figure 4-21 Traffic improvement factor vs. CBR for two rut depth (Montanelli et al., 1997)

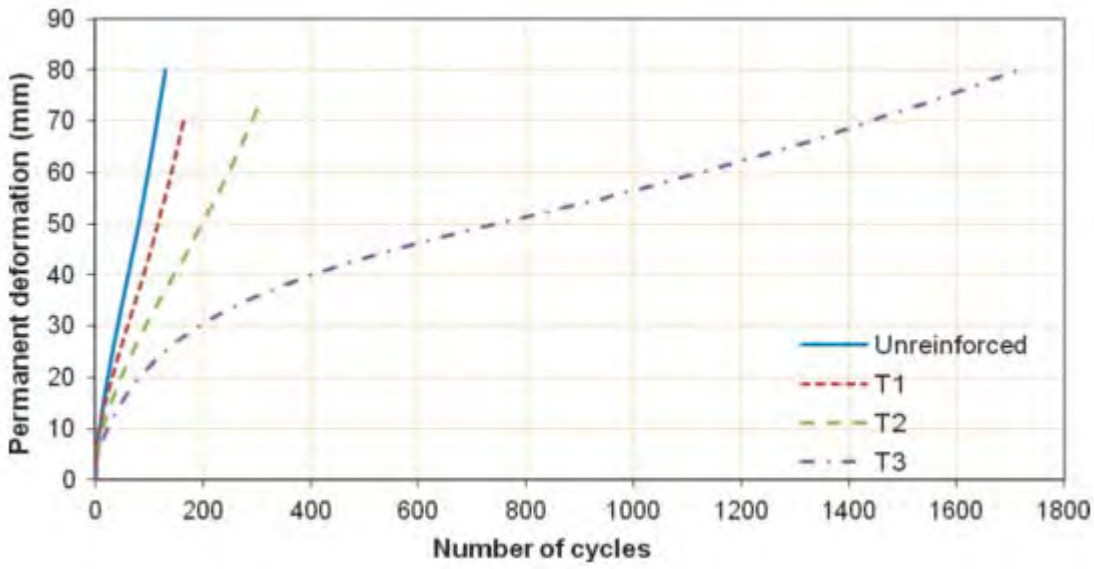

Figure 4-22 Permanent deformations of loading plate versus the number of cycles (Qian, Han, Pokharel, & Parsons, 2011)

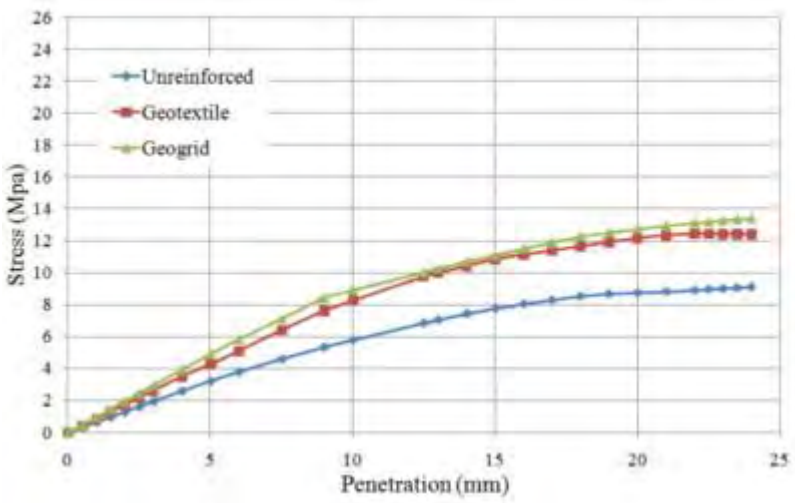

Figure 4-23 Stress-penetration curves of a subbase (Moayed & Nazari, 2011)

It was observed that there were outlying advantages from the use of geosynthetics as was indicated by the percentage reduction in deformation, Bearing Capacity Ratio (BCR) and Traffic Benefit Ratio (TBR). The magnitudes and extents of the benefits varied depending on the type and tensile strength of reinforcement geosynthetic used, depth of placement and strength of the subgrade and base (Table 4-4).

4.12.6 Summary of review of previous literature

From this review, it is evident that the use of reinforcement geosynthetics as inclusions within the road results in desirable benefits whose extent varies from author to author. Furthermore, most of the research has concentrated on the loading application in either static or dynamic loading as shown in Table 4-4 below. Additionally, the number of reinforcements (N) within a soil that is able to give optimum benefits has been determined to be N = 3 or 4, beyond which the significance of improvement reduces. However, in road pavements, the use of reinforcement geosynthetics is usually limited to two. It has also been identified that 51 mm or 0.1-0.2B is a minimum depth of placement of geosynthetics at which the reinforcement function is most mobilised. However, this depth is not adequate to prevent installation damage. There are contrasting views on the effect of anchorage to the performance of reinforced roads. It is, however, apparent in laboratory tests that the influence on performance is not significant in anchored and unanchored geosynthetics for as the long internal anchorage is adequate within the loading range.

There is a general consensus by previous authors (Table 4-4) that the incorporation of reinforcement geosynthetics has resulted in an increase in the load-bearing capacity, a reduction in settlement and base thickness and an extended life of the pavement. This study, however, maintained the same properties of the base, subgrade and geosynthetics and varied the type of loading to draw a comparison in the level of the benefits under static and dynamic load.

Table 4-4 Summary of previous literature

Source	Geosynthetic type	Subgrade	Base & Surfacing	Size of the box (m)	Loading type	Distress mode	Range of improvement	Major findings
Dynamic loading								
Perkins, (1999)	Geogrid (Tensar BX 1100 & 1200) Geotextile (Amoco 2006)	Clay CH (USCS) A-7-6 (AASHTO) CBR= 1.5 % & 15%	Crushed stone GW (USCS) A-1-a (AASHTO) **Surfacing**: Asphalt concrete=75 mm	2.0 x 2.0 x 1.5	Cyclic loading load of 40KN at Frequency 0.67Hz	Rut depth 5-25 mm	TBR from 8 to 56.	Geogrid provided improvement superior to geotextile. Substantial improvement measured with soft clay subgrade of CBR = 1.5%
Leng, (2002)	Geogrid	Kaolinite-Sand mixture CBR =3 %	Aggregate GW-USCS	1.5x1.5x1.35	Cyclic loading: 10KN seating load, cyclic load with amplitude 40kN at Frequency 0.67Hz	deformation	Reduction of surface deformation by 15%-30%	An unpaved road design model
M. Abu-Farsakh & Chen, (2011)	Geogrid	Silty clay CL (USCS) A-6 (AASHTO)	Limestone Aggregate: GW (USCS) A-1-a (AASHTO) **Surfacing**: HMA =51 mm	2.0x2.0x1.7m 0.305, plate diameter	Cyclic loading A 9-kip(40KN) load at a frequency of 0.77 Hz.	Rut depth 19.1 mm	TBR between 5.5 to 15.3	Construction method associated with placing the geogrid within the base for better strength mobilisation.

Source	Geosynthetic type	Subgrade	Base & Surfacing	Size of the box (m)	Loading type	Distress mode	Range of improvement	Major findings
Qian et al., (2011)	Geogrid	Aggregate CBR=20%	Mixture of sand and Kaolin CBR=2% **No surfacing.**	2.0x2.2x2.0 0.3, plate diameter	cyclic loading peak load of 40 kN at frequency of 0.77Hz	Deformation at 25, 50, 75 mm	TBR between 1.4 to 8.7	Reduction in maximum vertical stress on the subgrade. Better stress distribution Thicker & higher mechanical property geogrid had the best performance.
Tingle & Jersey, (2005)t	Geogrid Geotextile	Clay CH (USCS) CBR=1%	Crushed limestone SW-SM (USCS) **No surfacing.**	1.83×1.83 ×1.37	sinusoidal load pulse of 40 kN with loading of 0.1 sec load time, 0.9 sec rest time	Deformation between 12-50 mm	TBR between 1.3 to 36	Weaker pavement could not sustain the loading. Separation is primary function of geotextiles. Reinforcement is the core function of geogrids

Source	Geosynthetic type	Subgrade	Base & Surfacing	Size of the box (m)	Loading type	Distress mode	Range of improvement	Major findings
Static loading								
Oriokot, (2014)	Geogrid Geotextile	Kaolin CL (USCS) CBR < 3%	Aggregate GW (USCS) **No surfacing.**	0.95x0.14x0.5m	Static loading at 1.2 mm/sec	Deformation at 25mm	Improvement in load bearing capacity of between 35%-60% Reduction in settlement in the range of 35%-60%.	Optimal depth of placement was 0.67B. Optimum range of fill thickness obtained was 1.0B – 1.5B.
Patra, Das, & Atalar, (2005)	Geogrid	None	Sand	0.8x0.365x0.7m 0.36x0.8m rectangular plate	Static load applied in small increments	Deformation at ultimate bearing capacity	BCR of between 2.7 and 3.2.	Ultimate bearing capacity and BCR increases with increase in depth of placement
Chen, (2007)	Geogrid Geotextile	None	Sand SP (USCS) A-1-b (AASHTO)	3.658x3.658x1.829m Square footing 0.457x0.457m	Static load	Deformation	Maximum BCR at 0.34B	A new bearing capacity formulae incorporating geosynthetics benefits

Source	Geosynthetic type	Subgrade	Base & Surfacing	Size of the box (m)	Loading type	Distress mode	Range of improvement	Major findings
Abu-farsakh et al., (2008)	Geogrid	None	Silty clay CL (USCS) A-6 (AASHTO)	3.658x3.658x1.829m Square footing 0.457x0.457m	Static load	Deformation at 0.03B, 0.05B & 0.1B	BCR of between 1.14 and 1.48	Bearing capacity increases with increase in number of reinforcements. Geogrid beyond 4B results in insignificant mobilised strength

5.0 FLEXIBLE PAVEMENT DESIGN

5.1 INTRODUCTION

This chapter focuses is in the different methodologies that have been used in pavement design. Methods available for the design of flexible pavements can be grouped as (Yang, 2004):

- Theoretical methods
- Empirical methods
- Mechanistic-Empirical methods.

These methods and their extent of applicability are discussed broadly. In addition, with the introduction of geosynthetics as reinforcement inclusions within the pavement, different methods have been developed that would reflect their positive contributions as will be discussed in Section 5.5.

5.2 THEORETICAL METHODS

The behaviour of pavements subjected to wheel load applications can be studied using either full scale experiments or by formulation of theoretical models. The advantage of theoretical analysis over full scale experiments is the flexibility and convenience of being able to vary different parameters without the expense of full scale experiments. However, full scale experiments are required to validate the applicability of the model selected for the problem being considered. The models selected should be tested to ensure they are relevant and capable of predicting the behaviour of the pavement structure under the repetitive loading which simulates traffic loading.

The pavement structure experiences the transient traffic load on the surface. The subgrade and aggregate layers both exhibit non-linear stress strain relationships, which are influenced by factors such as soil properties and loading conditions. The low frequency cyclic loading from traffic makes it difficult to analyse the cyclic stresses and strains in the aggregate and subgrade. Therefore, simplification is done in order to simulate loading conditions, stress distribution and deformation computation.

Viscoelastic models have been developed to predict the pavement behaviour under different loading and environmental conditions. However, elastic theories still remain as the best alternative for theoretical analysis of flexible pavements. The theoretical approach is also known as the analytical, rational or structural design approach. Some examples are Boussinesq's Theory, Burmister's theory, multilayer system analysis, among others. In pavement design analysis, a single loading is usually represented by a uniformly distributed pressure over a circular area. The base and subgrade are assumed to be elastic materials.

5.2.1 Boussinesq's theory

Boussinesq's theory is ideal for material which is perfectly elastic, homogenous, isotropic and obeys Hooke's law. The Boussinesq's equation has been primarily developed for one layered system under a point load on the surface. The behaviour of a flexible pavement under wheel loads is considered as a homogenous elastic half space.

The distribution of vertical stresses below a concentrated load on any horizontal plane is in the form of a bell shaped surface. Maximum stress is felt at the point of load application and gradually decreases to zero at a finite depth.

For a uniformly distributed circular load on a homogenous layer of infinite depth, Boussinesq's theory defines the stress at a given depth as follows:

$$\sigma_z = \left\{1 - \frac{z^3}{(a^2+z^2)^{\frac{3}{2}}}\right\} \qquad \text{Equation 5-1}$$

$$\sigma_x = \frac{P}{2}\left\{(1+2\mu) - \frac{2(1+\mu)z}{(a^2+z^2)^{\frac{1}{2}}} + \frac{z^3}{(a^2+z^2)^{\frac{3}{2}}}\right\} \qquad \text{Equation 5-2}$$

Where: P = applied surface pressure, $б_z$ = vertical stress along the vertical axis of loading, $б_x$ = horizontal stress on the vertical axis of loading, a = radius of applied circle of loading, z = distance of the point from the surface and μ = Poisson's ratio

The Poisson ratio is the ratio of the strain normal to the applied stress to the strain parallel to the applied stress. For soils, it is generally around 0.5. The modulus of elasticity, E, of soil is the ratio of unit stress to the unit strain in the region of elastic behaviour.

The vertical displacement at the surface (z = 0) under the centre of the applied load is given by:

$$\Delta = \frac{2pa}{E}(1 - \mu^2) \qquad \text{Equation 5-3}$$

$\mu = 0.5$

For a flexible pavement, the deformation Δ can be computed as:

$$\Delta = 1.5\ \frac{pa}{E} \qquad \text{Equation 5-4}$$

For a Rigid pavement:

$$\Delta = 1.18\ \frac{pa}{E} \qquad \text{Equation 5-5}$$

This equation can be used for the design of a pavement by limiting the value of Δ, the deformation of the pavement, to a desired value.

In comparison to full scale experiments, Boussinesq's equation results in stresses and deflections that are larger than the actual values. The drawbacks of Boussinesq's approach are (Murthy, 2002):

- The assumption that soil is perfectly elastic and homogeneous is not true. Soil is layered and non-linear in behaviour.
- The pavement consists of a number of layers, each with its own modulus of elasticity. Hence, the assumption of one constant property for the entire mass is not justified
- The assumption that the load is uniformly distributed may not be correct

In spite of the drawbacks, Boussinesq's theory formed the initial attempt at analytical pavement design.

5.2.2 Burmister's theory

Flexible pavements consist of layers in which the modulus of elasticity decreases with depth. This in retrospect leads to a reduction of stresses and deflections in the subgrade from those obtained from the ideal homogenous case. Flexible pavements have differing

stiffness of the various pavement components from that of the subgrade. Practically, soils are neither homogeneous nor isotropic, and therefore the true stresses and strains depart from results given by the theoretical Boussinesq equations (Yang, 2004).

However, for a two layered soil, the materials in the layers are assumed to be homogenous, isotropic and elastic. The surface layer is assumed to be of infinite length in the lateral direction and of a finite depth. The underlying layer is assumed to be both of an infinite depth and length. Stress and deflection values are dependent on the strength ratio of the layers, E_1/E_2, where E_1 and E_2 are the moduli of the reinforcing and subgrade layers respectively. For a two layered system, the deflections can be obtained from Equation 5-6 or 5-7 shown below, depending on the plate used.

The load applied from tyre to pavement is similar to a flexible plate with a radius "a" and uniform pressure "q". The analysis of a flexible plate is based on the assumption that the load is applied on a flexible plate such as rubber (Figure 5-1a). However, for rigid plates such as that adopted on a plate load test, the deflection is the same for all the points on the plate but the pressure distribution under the plate is not uniform (Figure 5-1b below).

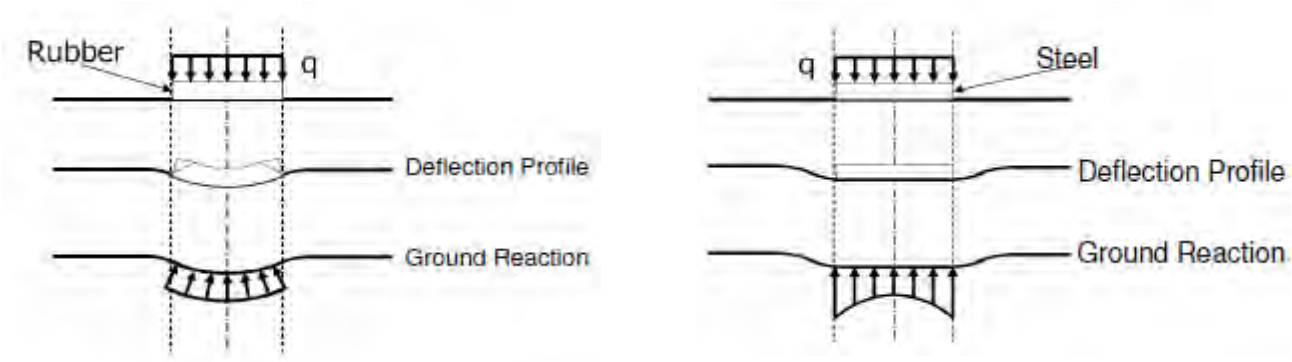

a) b)

Figure 5-1 a) Deflections of flexible plates b) Deflections of Rigid Plates (Yang, 2004)

Flexible Plate	$\Delta = 1.5 \frac{pa}{E_2} F_2$	Equation 5-6
Rigid plate	$\Delta = 1.18 \frac{pa}{E_2} F_2$	Equation 5-7

Where: p = unit load on a circular plate, a = radius of the plate, E_2 =Modulus of Elasticity of lower layer and F_2 =dimensionless factor depending on the ratio of moduli of elasticity of the subgrade and pavement as well as the depth to radius ratio.

5.2.3 Three layered system

The analysis of a three layered system has been made possible with the advent of supercomputers which have simplified the process. The three layered system is comprised of a top bituminous layer, a second layer of unbound road base and subgrade and a third layer representing the subgrade (Figure 5-2).

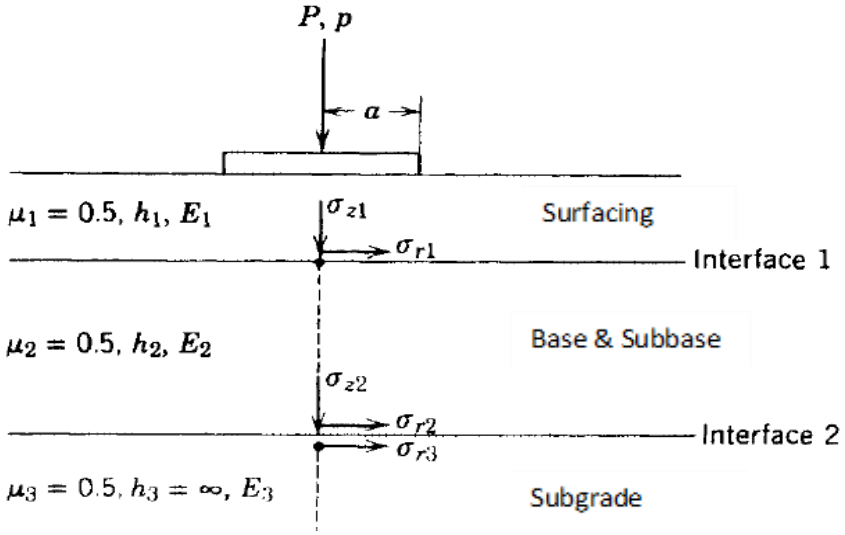

Figure 5-2 Three layer pavement system (Yoder & Witczcak, 1975)

The pavement materials in the three layers are assumed to be elastic and their mechanical properties are controlled by the modulus of elasticity, E. The value of the modulus of elasticity can be obtained from laboratory tests or empirical formula that relates it to the California Bearing Ratio (CBR). The load is assumed to be uniformly distributed over a circular contact area. The more commonly evaluated quantities are (Yoder & Witczcak, 1975):

- The vertical compressive strains and stresses reaching the top of the layer representing the subgrade and unbound layers
- The horizontal and vertical stresses at the bottom of the unbound granular layer.
- The horizontal tensile strain at the bottom of the bituminous bound layer
- Surface deflection.

5.3 EMPIRICAL PAVEMENT DESIGN METHODS

The empirical methods have been developed on the basis of long-term pavement performance for specific traffic loading and environmental conditions. It assumes that if the conditions for which these methods were developed prevail, the performance of the pavement should be satisfactory. These methods have been developed for use in different countries (Bhutta et al, 1998).

5.3.1 The group index method

This method is entirely empirical and it evolved from the plasticity of the subgrade and soil classification methods. The classification of materials enabled judging the suitability of the materials for use as base and subbases (Davis & Jones, 1954). The group index method is defined as:

$$GI = 0.2a + 0.005ac + 0.01bd \qquad \text{Equation 5-8}$$

Where,

GI- Group index

a = That portion of percentage passing the 75µm opening (ASTM #200 sieve) greater than 35% and not exceeding 75%, expressed as a positive integer (1 to 40);

b = That portion of percentage passing the 75µm opening (ASTM #200 sieve) greater than 15% and not exceeding 55%, expressed as a positive integer (1 to 40);

c = That portion of the numerical liquid limit (LL) greater than 40 and not exceeding 60, expressed as a positive integer (1 to 20); and

d = That portion of the numerical plasticity index (PI) greater than 10 and not exceeding 30, expressed as a positive integer (1 to 20).

The obtained GI corresponds to different traffic loading levels which have been formulated in a design chart (Figure 5-3 below) for pavement layer thickness for values of GI. For a given GI and traffic volume value selected, the appropriate curve that represents the combined thickness of surface, base and sub-base is used to give the total thickness of the pavement.

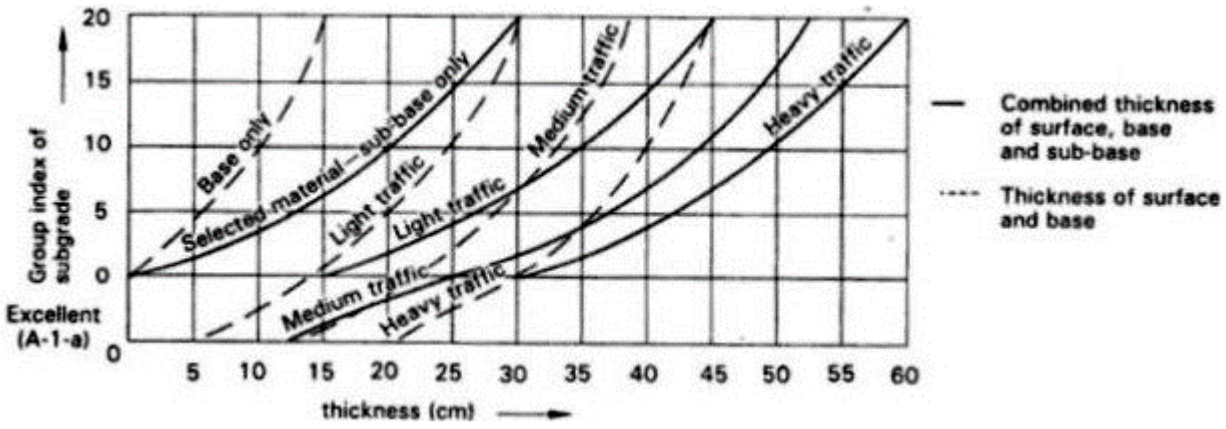

Figure 5-3 Pavement design chart for the Group Index (GI) method

5.3.2 AASHTO design guide

This method was developed from the results of the AASHO Road and is suitable for use in the USA. However, it has widely been adopted for use in tropical countries. Subgrade strength is expressed in terms of the soil support value (group index) and the pavement thickness is expressed as the Structural Number (SN) ranging from 1.0 to 6.0. Traffic loading is expressed as the cumulative standard axles during the design life of a pavement.

The designer is expected to select the thickness of the surfacing, base and subbase which satisfies the Equation 5-11 considering economic and other constraints. This method is further discussed in detail in Section 5.5.4 and Chapter 9.

5.3.3 Other methods

Other methods not discussed include the Road Note 29, Road Note 31 and the Hveem design methods. Road Note 29 is a guide to the structural design of pavements for new roads based on United Kingdom conditions. This method has been used in some tropical countries where the traffic loading was beyond that stipulated in Road Note 31. Road Note 31 was developed by the Transport and Road Research Laboratory (TRRL) for developing countries, and it is a guide for the structural design of bitumen-surfaced roads in tropical and sub-tropical countries.

5.4 MECHANISTIC-EMPIRICAL DESIGN METHOD

Various methods have been developed in the South African road industry for design (SAPEM, 2013; TRH4, 1996); however, the South African Mechanistic-Empirical Design Method (SAMDM) is the most popular method in South Africa (Theyse & Muthen, 2000).

This method analyses the pavement as a mechanism and links mechanistic parameters to the structural capacity through empirical observations of performance. The pavement is analysed as a mechanism material model for the pavement type and calculates engineering parameters such as stresses and strains.

Like other mechanistic-empirical design methods, the South African Mechanistic-Empirical Design Method (SAMDM) estimates the bearing capacity in two stages. In the first stage, the material responses are modelled according to their resilient strength properties with regards to the pavement loading conditions. This has been simplified by software packages such as BISAR, ELSYM5 and mePADs. The stress and strain at critical points in the structure are determined and they are used as input values for the second phase of the design. The second stage involves simulating pavement performance using transfer functions developed and calibrated for specific material types and associated modes of failure. Hence, the structural capacity of the pavement is expressed as the total number of repetitions that a specific layer can withstand before reaching its terminal conditions. Figure 5-4 below illustrates the different steps followed for the mechanistic- empirical design procedure (Ntirenganya, 2014).

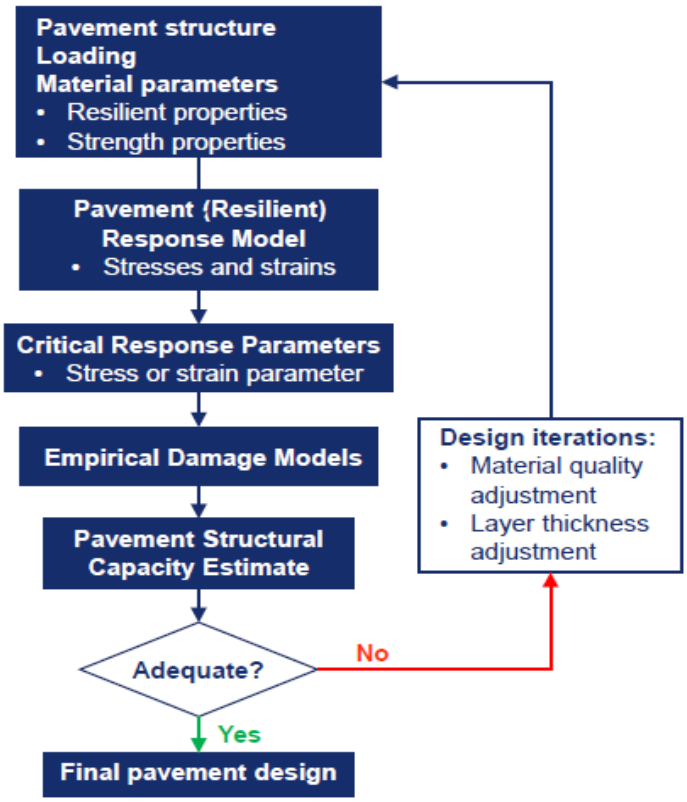

Figure 5-4 Schematic diagram of Mechanistic – Empirical Design procedure (SAPEM, 2013)

This method is purely logical based on the laws of solid mechanics and has no "intelligence" incorporated in the design method. Hence, the resulting pavement design with sufficient structural capacity may not be the optimal design. The "intelligence" in the system is provided by experience and sound engineering practice. Thus, this method requires a sound knowledge of engineering practice to have been captured for an economical design (SAPEM, 2013). Nonetheless, this method is popular due to its ability to accommodate a wide range of local materials and suits different pavement types. Extensive research has been conducted to characterise South African building materials and specifications published as input values for SAMDM (Ntirenganya, 2014).

5.5 DESIGN APPROACHES WITH GEOSYNTHETICS

Various methods have been put forward to address the structural design of reinforced unpaved roads. They have been classified as being either rational methods or empirical, as shown in Table 5-1 below.

Table 5-1 Different design approaches -adopted from Sanjay, (2012)

METHOD	BASIS	EXAMPLES	COMMENTS
Rational Analyses	Static or monotonic loading	Use of spreadsheet programs as developed by Ashmawy & Bourdeau, (1995)	Does not account for repetition of loads by traffic
Empirical Methods	Observation of performance of full scale models or trial road sections	French Method -1981 Swiss Method-1986	Relies on collection of field performance data. Valid for particular materials and conditions
Rational Methods	Reinforcement mechanisms that considers traffic loading	Giroud and Noiray (1981) Oxford method Giroud and Han (2004) AASHTO method (2011)	Drastic simplification of material properties, boundary conditions and traffic loading features. Cyclic nature of traffic considered using empirical equations. Offers the most reliable and versatile design approach.

Considering Table 5-1, the subsequent discussion will focus on the rational methods whose basis is on the reinforcement mechanisms that considers traffic loading. This is because it is holistic as it considers both the static and dynamic aspects of traffic, and is simplified in its approach.

5.5.1 Giroud and Noiray (1981)

This design approach is based on a geotextile placed between the aggregate and the subgrade of an unpaved road based on bearing capacity theory for static loading. The reduction in aggregate thickness provided by the tensile membrane action of the reinforcement is determined based on the static loading. It is developed for larger rut depths; therefore, at small depths, the geotextile resistance is assumed.

The bearing capacity of the soft subgrade is considered to increase from πCu to (π+2)Cu with the inclusion of a geotextile; where Cu is the undrained shear strength (Φu=0) of the subgrade and π is pi. The load transmission angles α_o and α corresponding to the unreinforced and reinforced conditions, respectively, are assumed to both be equal to $\tan^{-1} 0.6$ (Figure 5-5 below). Therefore, this assumes that the geotextile does not significantly influence the load transmission mechanism through the aggregate layer.

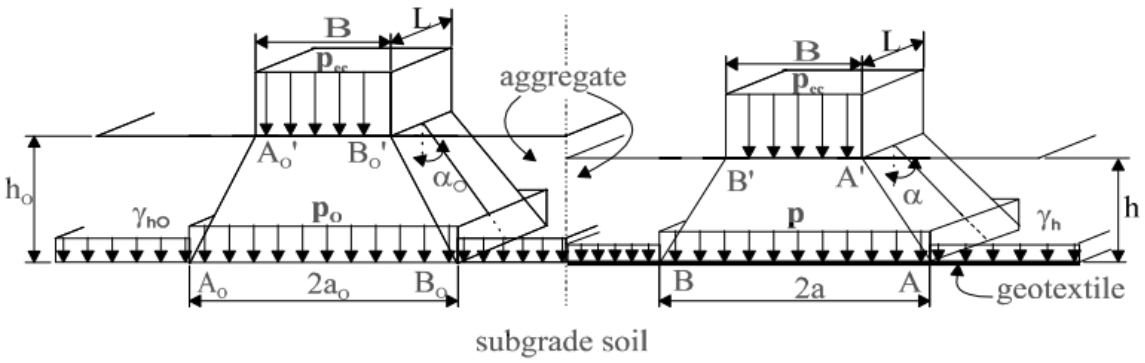

Figure 5-5 Load diffusion model from Giroud and Noiray (1981) and Bearden & Labuz (1999)

Different researchers have investigated the influence of load spread/transmission mechanisms in the subgrade, but the results have not been consistent. However, the prediction of settlement has shown consistency in results for settlements greater than U = 0.2-0.3 (Δ/2B); where Δ= footing settlement, B= half width of the footing, U=dimensionless variable to estimate displacement (Kazimierowicz-Frankowska, 2007).

This method enables the engineer to calculate the required thickness of the aggregate layer and make a proper selection of the geosynthetic to use. The results are presented in the form of a design chart limited to cohesive subgrade soils and roads subjected to traffic of 1-10,000 cycles.

5.5.2 Oxford method

This method considers both the static and cyclic application of loading for unreinforced and reinforced roads by Milligan et al. (1989). Conceptual models have been developed for the geometry of load diffusion and for the equilibrium of the base course wedge located beneath the loaded area in the unreinforced and reinforced case. In the unreinforced scenario, shear stresses induced by traffic load in the granular base develop along the

base-subgrade interface, hence reducing the bearing capacity. If the forces are excessive, sliding may even occur at the interface.

The ultimate or available stress relationship in the subgrade is represented graphically as shown in Figure 5-6:

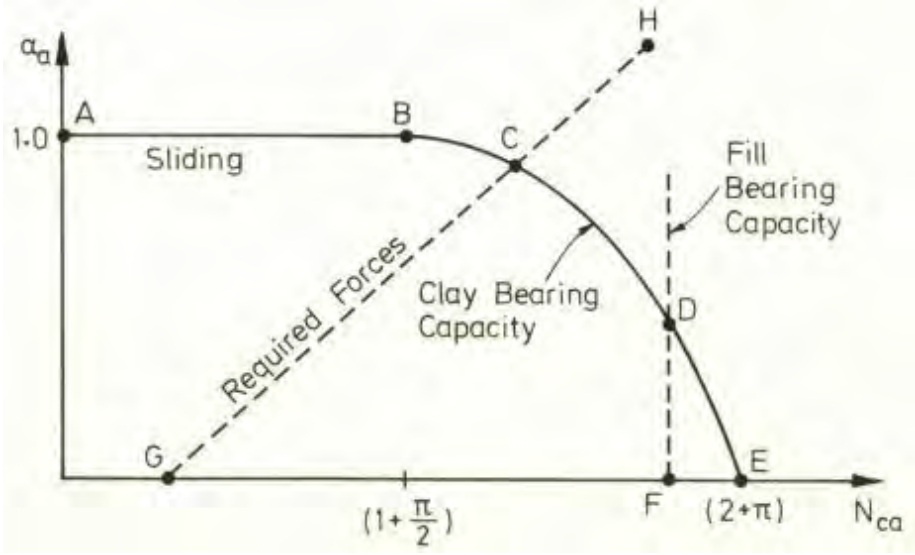

Figure 5-6 Normal and shear stress relationship (Milligan et al., 1989)

The curve in Figure 5-6 represents the locus of ultimate stress conditions for the subgrade, including its bearing capacity and sliding along the interface. At the intersection of this line and the curve (point C), the required and available combination of normal and the shear stresses are compatible with the maximum bearing capacity factor.

The reinforcement function acts by carrying the interface shear stress and thus allowing the subgrade bearing capacity to be maximised. The shear stress developed at the base is transferred to the geosynthetic and the clay subgrade is loaded only by normal vertical stresses. The ultimate state is represented by point E.

For the analysis to be valid,

- There should be a full transfer of shear stress at the interface between the granular course and the reinforcement.
- The resulting elongation should be small such that there is no significant shear stress transfer to the subgrade.

- Also, the bearing capacity of the granular layer should be sufficient to ensure that the bearing capacity failure is not the controlling factor.
- The tensile membrane action is not taken into account, thus it only considers small ruts.

These conditions require that a high interface interaction be achieved between the granular material and the high tensile performance characteristics (modulus and strength) of the geosynthetic.

This method relies principally on the transfer of shear stresses at the interface which leads to enhancement of the confinement of the granular base and improvement of the bearing capacity of the subgrade. Milligan et al. (1989), the authors of the method, intended to show that geosynthetic reinforcement can be effective in unpaved roads without necessarily resulting from large ruts and deflection of the reinforcement as in Giroud and Noiray's (1981) method.

Furthermore, the Oxford method employs empirical corrections to the results of static loading analysis to account for repeated loading. Repeated loading causes deformations that increase as the load cycles increase. There is a poor understanding of the mechanisms that leads to deformation under cyclic loading. For this reason, design methods that consider traffic loading have to employ empirical extensions to static analysis to account for such loading (Houlsby & Burd, 1999).

The Oxford method authors recommended the empirical formulae by De groot et al. (1986), on the basis of full-scale tests of reinforced unpaved road sections under traffic loading:

$$P_N = \frac{P_S}{N^{0.16}} \qquad \text{Equation 5-9}$$

Where: P_N= allowable pressure for N applications of the load for N applications of the load
P_s= allowable static applied surface pressure

5.5.3 Giroud and Han (2004)

This design method was developed for use in geogrid reinforced unpaved roads. It can also be used in geotextile reinforced unpaved roads by neglecting the effects of aggregate interlock and geosynthetic in-plane stiffness. For the design of unreinforced unpaved

structures, the method can be adapted by neglecting the effect of the reinforcement to the subgrade bearing capacity. This method is advantageous because it is theoretically based and experimentally calibrated. The calibration of this design method has been done by the use of field wheel load tests and laboratory plate load tests on unreinforced and reinforced bases (Giroud & Han, 2004).

The load on the granular base is distributed over a circular area as a function of the applied wheel load and tyre inflation pressure. The subgrade is assumed to be fully saturated fine grained soil, with an undrained shear strength and compression modulus related to the CBR coefficient. The rationale for considering this method is that the geosynthetic placement is at the subgrade-base interface. This is because the presence of the reinforcement enables the attainment of the ultimate bearing capacity of the subgrade to be mobilised, hence preventing local shear failure of the subgrade. The ultimate bearing pressure results in better performance than the unreinforced situation arising from smaller deformations.

The aspect of enhanced confinement mechanism due to the interlock between the soil grains and grid is also considered in this analysis. Instead of relying on the overall tensile modulus of the geogrid to quantify the material property, a parameter known as the aperture stability modulus, which is the measure of the local confinement potential, is adopted. The aperture stability modulus is the measure of the in-plane stiffness and stability of the geogrid ribs and junctions. This mechanism is advantageous as it translates to a higher ratio of granular base to subgrade deformation moduli, and increases the stress distribution angle at the interface in comparison to the unreinforced system. Unlike the previous methods, this method integrates the cyclic loading in the formulation. The previous methods develop one static load application whose results are then modified using empirical formulae to account for load repetition.

Giroud and Han's method introduces the effect of traffic as a factor of degradation for some properties of the reinforced system. It considers the decrement of the stress distribution angle with load repetition, which leads to a less and less effective enhanced confinement mechanism. Since the resulting equation is complex; design charts have been produced to simplify the procedure (Figure 5-7 below).

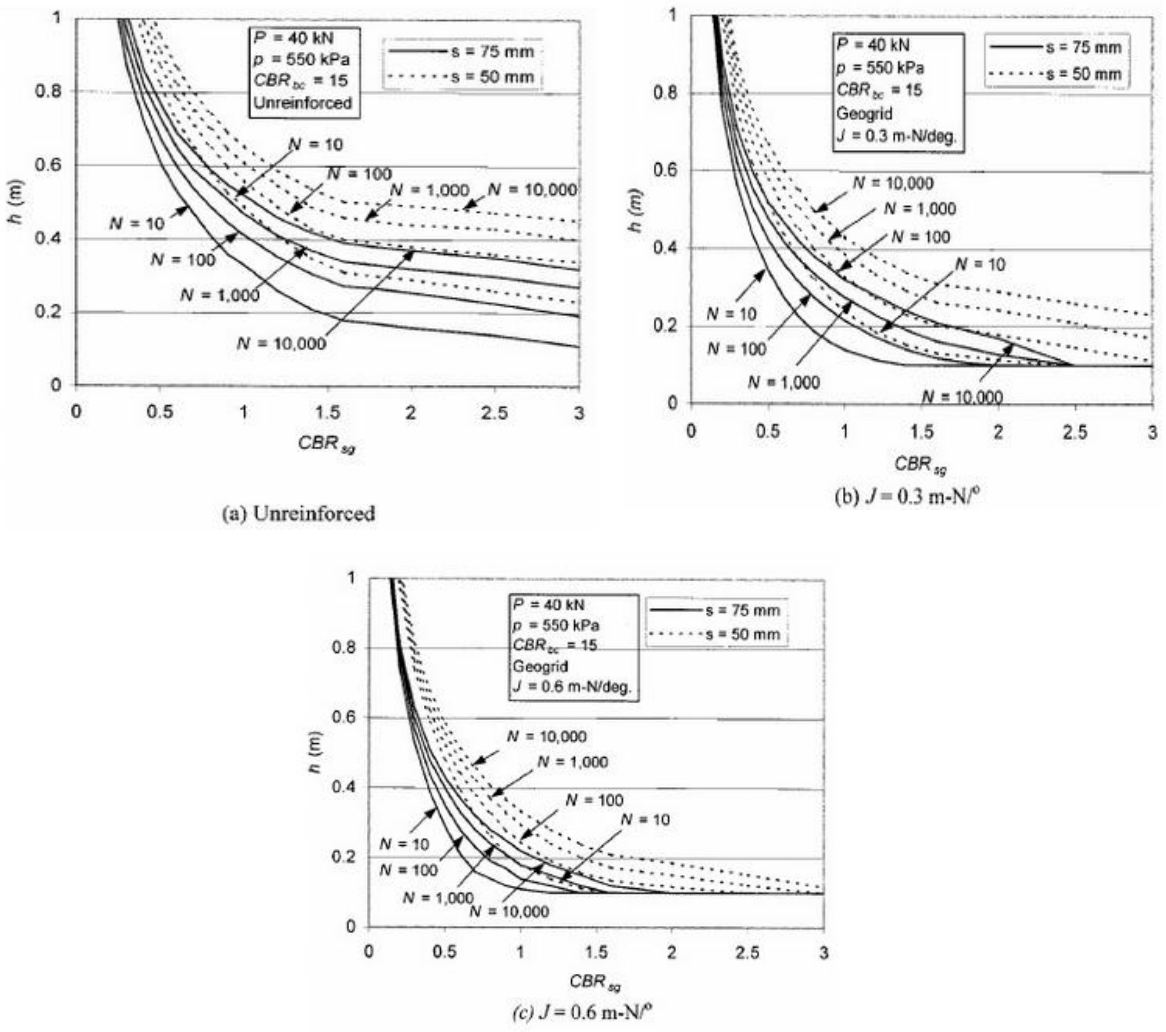

Figure 5-7 Design charts for unreinforced and geogrid reinforced roads (Giroud & Han, 2004-a)

Where P = wheel load; ρ = tyre pressure; CBR_{bc} = California Bearing Ratio of the granular base; CBR_{SG} = California Bearing Ratio of the Subgrade; J=Geogrid aperture stability modulus; S=allowable rut depth; N= Number of load cycles

The charts for the determination of the required base course thickness (Figure 5-6) for unpaved roads were calculated through iteration from the following equation:

$$h = \frac{1.26+(0.96-1.46J^2)(\frac{r}{h})^{1.5}\log N}{f_E}\left[\sqrt{\frac{P}{\pi r^2 m N_c Cu}} - 1\right]r \qquad \text{Equation 5-10}$$

Where h = required base course thickness (m); P = wheel loads in kN, N = Number of passes of axle; J = aperture stability modulus (with J = 0 for unreinforced and geotextile reinforced unpaved roads); and r = radius of equivalent tyre contact area; m = bearing capacity mobilisation coefficient; f_E= modulus ratio factor; R_E = limited modulus ratio and Nc = bearing capacity factor. All these variables have been discussed extensively in Giroud & Han (2004-a).

5.5.4 AASHTO method

The AASHTO design method uses empirical equations developed from AASHTO road tests conducted in Ottawa, Illinois in the late 1950s. The purpose of the tests was to determine a relationship between axle loading and pavement structure on pavement performance. The method considers a pavement as a multilayered system with an overall Structural Number (SN) which is a reflection of the pavement thickness and resilience to traffic loading.

The AASHTO design guide is one of the most widely used design criterion for flexible pavement design. This method considers a pavement as a multilayered elastic system with an overall SN. The SN gives an indication of the combined structural capacity of all the pavement layers overlying the subgrade, and it reflects the total pavement thickness and its resilience to repeated traffic loading (Gupta, 2010). Zornberg (2011) has incorporated the resulting benefits of a geosynthetic in the form of Bearing Capacity Ratio (BCR) and Traffic Benefit Ratio (TBR) to factor SN in an unreinforced case.

The SN is selected such that anticipated traffic loads will be supported without a loss in serviceability no greater than that allowed based on the requirements of the pavement. The SN is determined from a nomograph that solves equation 5-11:

$$\text{Log } W_{18} = Z_R x\, S_o + 9.36\, x \log(SN+1) - 0.2 + \frac{\log\frac{\Delta PSI}{2.7}}{0.4+\frac{1094}{(SN+1)^{5.19}}} + 2.32 \log M_R - 8.07 \qquad \text{Equation 5-11}$$

Where W_{18} is the anticipated cumulative 80kN Equivalent Single-Axle Loads (ESALs) over the design life of the pavements, Z_R is the standard normal deviate for reliability level, S_O is the overall standard deviation, ΔPSI is the allowable loss in serviceability, and M_R is the resilient modulus (stiffness) of the underlying subgrade.

The structural number determines the total number of ESALs (Equivalent Single Axle Loads) that a particular pavement can support. From Equation 5-12 below, the structural number can be determined and the individual pavement layers can be designed through a series of iterations.

$$SN = (a_1 D_1)_{HMA} + (a_2 D_2 M_2)_{Base} + \cdots \quad \text{Equation 5-12}$$

Where a_1 = 1th layer coefficients: D_1 = 1th layer thickness (in inches): M_1 = 1th drainage coefficients

When using geosynthetics for reinforcement, Equations 5-11 and 5-12 have been modified to cater for the benefits achieved by inclusion of geosynthetics to its structure. The improvements to the pavement structure have been measured in terms of Traffic Benefit Ratio (TBR) and Base Course Reduction (BCR).

5.5.4.1 Traffic Benefit Ratio (TBR)

Traffic Benefit Ratio (TBR), also sometimes referred to as a Traffic Impact Factor (TIF), defines the number of load cycles carried by a reinforced section (Nr) at a specific rut depth divided by that of an equivalent unreinforced section (Nu).

$$TBR = \frac{Nr}{Nu} \quad \text{Equation 5-13}$$

The contribution of TBR in pavement design has been included to represent an extended pavement life by (Berg et al., 2000):

$$W_{18}\,(\text{reinforced}) = TBR \times W_{18}\,(\text{unreinforced}) \quad \text{Equation 5-14}$$

And W_{18} = predicted number of 80kN equivalent single axle load applications

The TBR, therefore, can be used to determine the number of traffic passes that a reinforced pavement can withstand as compared to an unreinforced pavement for a given rutting depth (Gupta, 2010).

5.5.4.2 Base Course Reduction factor (BCR)

The Base Course Reduction (BCR) describes the reduction of the base course aggregate allowed for the equivalent service life. It is defined as the percentage reduction of the base

course thickness due to the addition of a reinforcement geosynthetic when compared to an unreinforced thickness. Therefore, the equivalent life, defined in terms of traffic loads, is obtained between the Thinner reinforced pavement (Tr) and the Thicker unreinforced pavement (Tu) (Steven Perkins, 2001).

$$\mathrm{BCR} = \frac{\mathrm{Tr}}{\mathrm{Tu}} \qquad \text{Equation 5-15}$$

BCR, which is sometimes referred to as a Layer Coefficient Ratio (LCR) is applied as a modifier to the SN of the pavement:

$$\mathrm{SN} = (\mathrm{a\ x\ d})_{\mathrm{hma}} + \mathrm{BCR}.\,(\mathrm{a\ x\ d\ x\ m})_{\mathrm{base}} + (\mathrm{a\ x\ d\ x\ m})_{\mathrm{subbase}} \qquad \text{Equation 5-16}$$

The reduced depth of the base course can be computed by inputting the BCR when designing the pavement as follows:

$$\mathrm{d_{Base,(R)}} = \frac{\mathrm{SN_u} - (\mathrm{a\ x\ d})_{\mathrm{hma}} - (\mathrm{a\ x\ d\ x\ m})_{\mathrm{subbase}}}{\mathrm{BCR}.(\mathrm{a\ x\ m})_{\mathrm{base}}} \qquad \text{Equation 5-17}$$

Where $d_{base,\ (R)}$ is the reduced base course thickness due to reinforcement and SNu is the structural number corresponding to the equivalent W_{18} for the unreinforced pavement.

6.0 RESEARCH MATERIALS AND METHODOLOGY

6.1 INTRODUCTION

The testing programme in this study was designed to investigate the improvement arising from the use of geotextiles and geogrids as reinforcement components within the base and at the interface of the base-subgrade. Two categories of tests i.e. static and dynamic loading tests were conducted.

This chapter commences with a detailed description of the various research materials used in this study that includes a granular soil for the base, kaolin clay for the subgrade and geotextile and geogrids as reinforcement components. In addition, the testing apparatus and procedure that was followed are then discussed in detail. Classification tests were conducted on the granular soil for the base and the kaolin clay for the subgrade in order to better understand their behaviour. These tests are summarised in Table 6-1 below together with the corresponding standards. The tests were conducted at the Geotechnical Engineering laboratory at the University of Johannesburg-Kingsway. Details of the classification test results are presented in Chapter 12.

Table 6-1 Soil classification tests

TEST	Parameter	STANDARD
Sieve Analysis	Particle size distribution	ASTM D6913
Hydrometer Test	Particle size distribution	ASTM D422
Atterberg limits:	Liquid limit & plastic limit	BS 1377: Part 2
Standard Proctor test	Optimum moisture content, Maximum dry density	ASTM D1557-12
Modified AASHTO	Optimum moisture content, Maximum dry density	TMH1-Method 7

6.2 MATERIALS PROPERTIES

6.2.1 Granular soil

About 3 tonnes of disturbed granular material was delivered to the materials yard at the Civil Engineering department at the University of Johannesburg. The material was obtained

from a contractor's dump site and it was used for the base course. Its characteristics are as shown in Table 6-2 below.

Table 6-2 Granular soil properties

Property	Soil parameter value
% Passing 0.075mm	42%
Grading Modulus	1.98
Plastic index (PI)	13%
CBR after 4 day soak	18.5%
CBR swell	1.04 mm
Maximum dry density (Mod AASHTO)	2000 Kg/m^3
Optimum Moisture Content (OMC)	13%

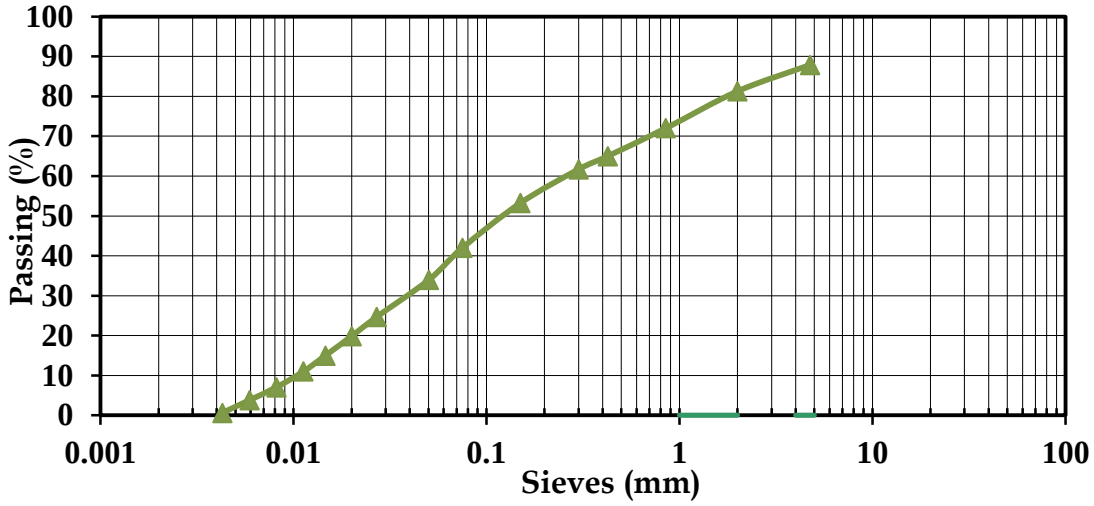

Figure 6-1 Grading curve for the granular base soil

The material is classified as SC, Clayey sand and A-6 according to the unified soil classification system (USCS) and the American Association of State Highway and Transportation Officials (AASHTO) classification system respectively. It has a coefficient of uniformity of 25 and a coefficient of curvature of 0.64, characterising as a poorly graded soil (Figure 6-1 above).

In addition, according to TRH14 (1985), South African standard, the material is classified as a G7 soil. G7 materials are normally used in the lower pavement layers or in the

subgrade. However, quality G7 material can be employed as the subbase materials for sealed roads (Paige-Green 2006).

6.2.2 Kaolin clay

The Kaolin clay material used in this study was acquired from G & W Mineral Resources-Johannesburg and it was packaged in bags of 20 Kgs, and in a dry state. The Grade 3 (G 3) Kaolin was off-white in its natural colour and it had characteristics as shown in Table 6-3 below.

Table 6-3 Kaolin clay properties

Property	Soil parameter value
Plastic index (PI)	17.27 %
Specific gravity	2.62
Maximum dry density (standard proctor)	1520 Kg/m^3
Optimum Moisture Content (OMC)	25.5 %

The soil was classified as a clay of low plasticity (CL) according to the Unified Soil Classification System (USCS) and A-7-5 in the American Association of State Highway and Transportation Officials (AASHTO) classification systems.

The typical mineralogy and Kaolin chemical analysis are as highlighted in Tables 6-4 and 6-5 below, respectively.

Table 6-4 Typical G3 Kaolin mineralogy (G & W Mineral Resources-South Africa, 2015)

Kaolin Mineralogy	Percentage %
Mica	15-20
Quartz	41-50
Kaolinite	29-40
Alunite	1-2

Table 6-5 G3 Kaolin Chemical Analysis (G & W Mineral Resources-South Africa 2015)

Chemical Analysis	Percentage %
SiO2	64.0 – 67.0
Al_2O_3	23.0 – 24.0
Fe_2O_3	0.30 – 0.90
CaO	0.10 – 0.25
MgO	<0.01
K_2O	1.0 – 3.0
TiO_2	0.50 – 0.70
Na_2O	0.20 – 0.35
LOI	5.95 – 6.50

The Kaolin clay was used as a subgrade soil since it is a good representation of problematic soft clays in South Africa. The Kaolin was soft, extremely fine and with a consistency that can easily be controllable, i.e. identical samples could be produced if prepared the same way. Furthermore, Kaolin has been used by different researchers (Love, Burd, Milligan, & Houlsby, 1987; Oriokot, 2014; Qian et al., 2011) who have undertaken similar studies to replicate conditions of a soft subgrade soil.

6.2.3 Geosynthetic material

Two types of geosynthetics materials, woven geotextile and an extruded geogrid, were obtained from Maccaferri Southern Africa-Johannesburg. The geogrid was Macgrid EG 20S commonly used within the pavement layers for reinforcement purposes. The woven geotextile was a Mactex W1 5S and is primarily used for separation in pavements.

6.2.3.1 Extruded geogrid

The extruded geogrid was a biaxial geogrid, black in colour with a smooth surface and square apertures of size 38 mm by 38 mm (Figure 6-2 below). Macgrid EG 20S were manufactured from polypropylene, and the geogrids produced by the punching, extrusion and the bi-axial orientation process. The index and mechanical properties were provided by the manufacturer and are presented in Table 6-6.

Table 6-6 Geosynthetic Properties (Maccaferri Southern Africa, 2015)

Property	**Extruded Geogrid (EG)** ***Macgrid EG 20S***
Tensile Strength MD* (kN/m)	20
Tensile Strength CMD* (kN/m)	20
Strain at maximum strength MD* (%)	13
Strain CMD* (%)	10
Tensile strength at 2% strain, Longitudinal (kN/m)	7
Tensile strength at 5% strain, Longitudinal (kN/m)	14
Tensile strength at 2% strain, Transverse (kN/m)	7
Tensile strength at 5% strain, Transverse (kN/m)	14

MD*=Machine Direction CMD*=Cross Machine Direction

Figure 6-2 Extruded Geogrid

They were characterised by a tensile resistance in both longitudinal and transverse directions and had a high junction strength which ensured a proper distribution of imposed stresses through the entire geogrid. In addition, they had a chemical-biological and U.V. resistance and a low vulnerability to construction damage. These biaxial geogrids are primarily used as reinforcement within the granular layers for base reinforcement and soil stabilisation applications.

6.2.3.2 Woven geotextile

The woven geotextile, Mactex W1 5S was white in colour. The geotextile was a planar woven structure manufactured by weaving in warp and weft directions of polypropylene yarns. The geotextile functions best in soil environments of PH 4 to 9 and temperatures less than 25° C. The index and mechanical properties were provided by the manufacturer and are presented in Table 6-7 below.

Table 6-7 Geosynthetic Properties (Maccaferri Southern Africa 2015)

Property	**Extruded Geogrid (WGx)** ***Mactex W1 5S***
Tensile Strength MD* (kN/m)	50
Tensile Strength CMD* (kN/m)	50
Strain at maximum strength MD* (%)	20
Strain CMD* (%)	13
Tensile strength at 2% strain, Longitudinal (kN/m)	-
Tensile strength at 5% strain, Longitudinal (kN/m)	-
Tensile strength at 2% strain, Transverse (kN/m)	-
Tensile strength at 5% strain, Transverse (kN/m)	-

MD*=Machine Direction CMD*=Cross Machine Direction

Figure 6-3 Woven Geotextile

The Apparent Opening Size (AOS) of the geotextile (O_{90}) was 0.3 mm. This means 90% of the geotextile pores are 0.3 mm or smaller. This concurs with AASHTO M288 standard, which recommends a geotextile with O_{95} < 0.3 mm for a soil with greater than (>) 50% passing the No. 200 (0.075 mm) sieve (Koerner, 2012). This characteristic enabled the geotextile used in this study to be permeable, hence functioning as a filter that allows water but not soil to pass through it, and also as a separator to prevent mixing of the soft soil and granular material. The high strength geotextile used also served as a reinforcement.

6.3 TESTING APPARATUS

6.3.1 Steel test box

The steel box used as a road model was fabricated at the University of Johannesburg-Kingsway. It had dimensions of 1.0 m (length) × 1.0 m (width) × 1.0 m (height) and a thickness of 25 mm as in Figures 6-4 and 6-5 below. It was open at the bottom and top for ease of moving materials in and out of the box. The box was made of steel because of its high strength, low weight, durability, ductility and resistance to corrosion (Buzzle, 2015). The joints were connected by welding; welded structural members are more effective in taking loads since no hole is required as in riveting, hence no reduction of surface area (Civilblog, 2015). In addition, the box was braced on the sides to bolster its strength and prevent any lateral movement of the sides resulting from the applied loading. Lateral movement of the sides of the box would interfere with the results of the study because it would affect the magnitude of the vertical applied load.

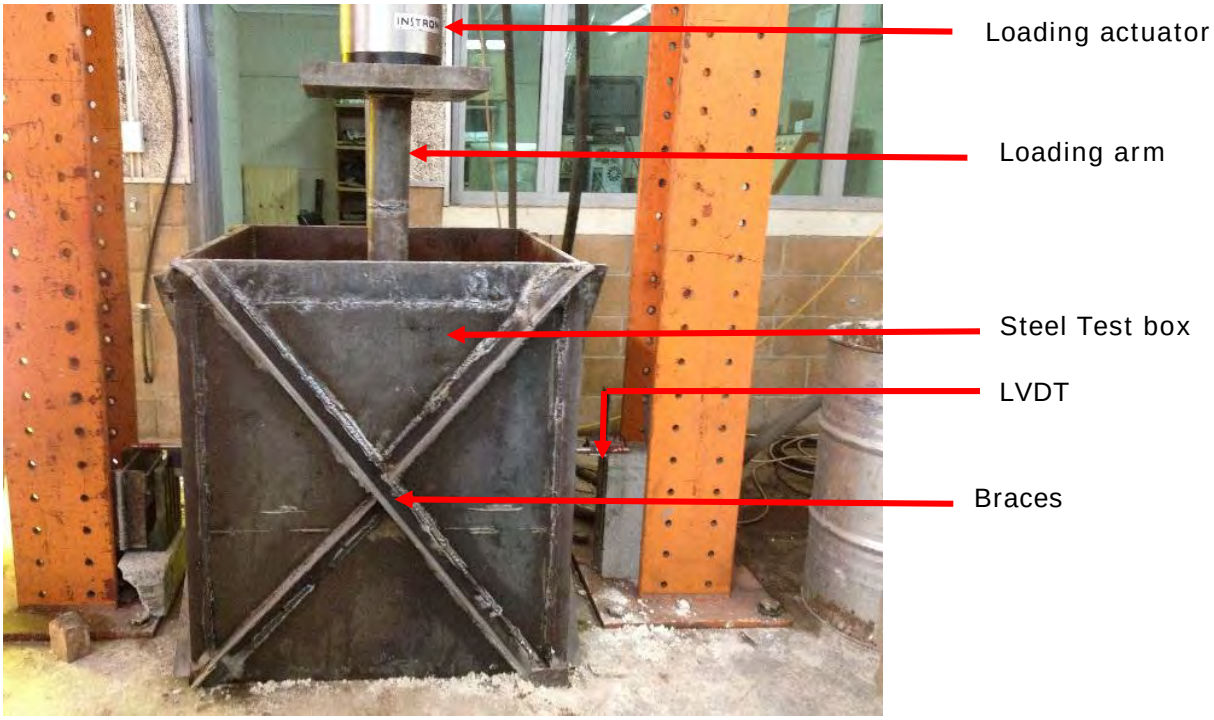

Figure 6-4 Test Box set up

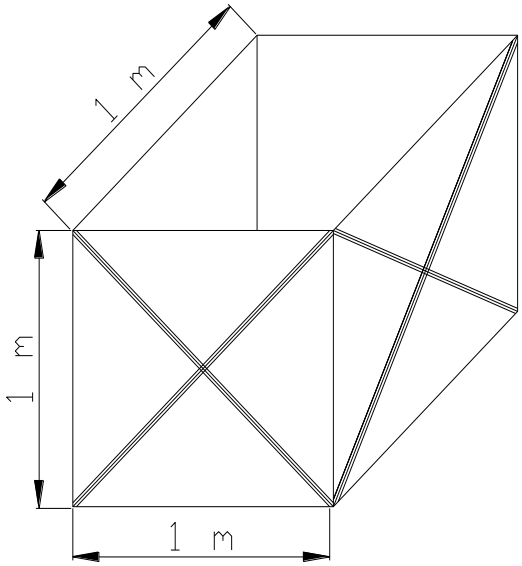

Figure 6-5 Schematic drawing of the test box

For testing in controlled conditions, a size of the test box was required that would minimise boundary effects and maintain a reasonable sample size. Proper sizing of the box was a balance between a large enough box to prevent any absorbing of energy by the sides during loading and space limitation in the laboratory. The eventual sizing was arrived at from the findings of Sawangsuriya et al. (2002) that postulated that boundary effects become negligible for square test boxes with a width greater than 0.6 m using a 300 mm diameter plate. Thus, the measurement configuration of the box was sufficient

6.3.2 Model footing

A steel circular footing of diameter 305 mm and thickness 25 mm was used as a model footing (Figure 6-6 below). It was made out of steel due to the high strength of steel as initially highlighted in Section 6.3.1. An appropriate thickness of the plate was selected; the thickness had to be sufficient to withstand the effects emanating from applied load.

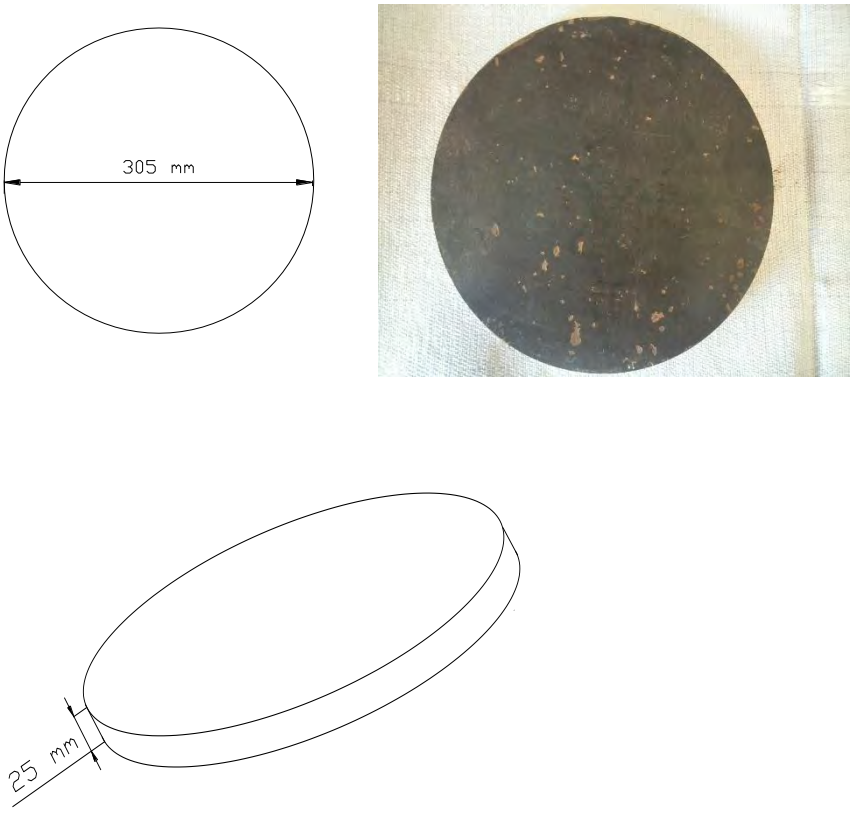

Figure 6-6 Plate of diameter 305 mm

Furthermore, the tests conducted were plate load tests. Different standards i.e. BS 1377 Part 9:1990, ASTM D1196, IS 1888-1982 all stipulated circular plate sizes of diameter between 300−750 mm for plate load tests. Specifically, circular plates have been used to represent the imprint of a wheel on a flexible pavement.

Consideration of the plate diameter was also based on a tyre contact pressure of 550 kPa for a dual wheel load of 40 kN (equal to half an axle load of 80 KN) commonly adopted in current design methods such as AASHTO. This translates to an equivalent diameter of 305 mm from Equation 2-3.

6.3.3 Torvane

A Torvane is a hand held device that is used for rapid determination of shear strength either in the laboratory or field (Figure 6-7 below). The Torvane used was from Durham Geo slope and it had a stress range of 0 to 1 TSP (Total Stress Path), this being an approximate range of torque that can be applied by fingers. It is used in saturated soils whose undrained shear strength is independent of the normal strength. Thus, the stress ranges make them more applicable in clays of soft to stiff consistency.

Table 6-8 Specification for vane sizes (Murthy, 2002; Durham Geo slope indicator)

Type	Diameter (mm)	Soil Type	Maximum strength (kPa)
Large vane	48	Remoulded clays	20
Regular vane (standard)	25	Soft - stiff clays	100
Small vane	19	Stiffer clays	250

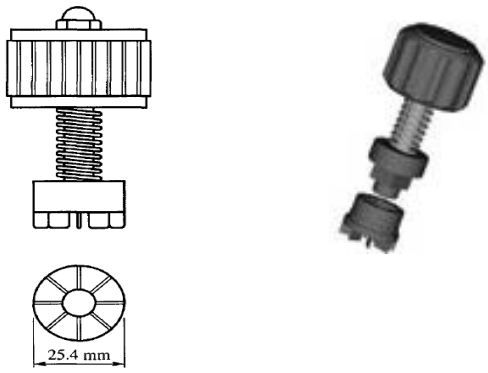

Figure 6-7 Torvane shear device (Murthy, 2002; Durham Geo slope indicator)

The vanes are pressed into the clay to their full depth, whereupon a torque is applied through a calibrated spring until the soil fails in shear. The value at failure is equated to the indicator on the conversion dial. The Torvane set comprised of three vanes as highlighted in Table 6-8.

The standard Torvane was used by Pokharel (1997) to determine the undrained shear strength of the soft subgrade as a function of the CBR using Equation 6-1, which was also used in this study.

$$CBR\ (\%) = \frac{Cu}{20.5} \qquad \text{Equation 6-1}$$

6.4 TESTING PROCEDURE

6.4.1 Soft clay subgrade preparation

100Kg of dry Kaolin was weighed using a scale that had a capacity of 20Kgs. This was then put in an electric PMSA V200 mechanical rotary mixer with a diameter of 1m (Figure 6-9). 31L of water was added to the Kaolin which represented 31% water content. The top of the mixer was covered by a plastic bag to prevent the Kaolin from being blown away once the mixing commenced. The machine was switched on and the mixing was conducted for 5-10 minutes till the Kaolin became a consistent, homogenous mix.

The required thickness of the subgrade was 500 mm, which satisfied the pressure distribution requirement of 1.5B (B-width of the plate), such that all the pressure would be retained within the pavement structure. For a subgrade thickness of 500 mm, it was determined using the density that 700 Kg of Kaolin mixed with 31% water would be required to fill the volume for a CBR of 2%. This represented 92% of the Standard Proctor density.

The mixing was undertaken for each batch and the resulting mix weighed and stored in containers. The containers were covered with plastic bags at the top to retain the moisture of the mix as mixing proceeded until the required weight for the subgrade material was attained.

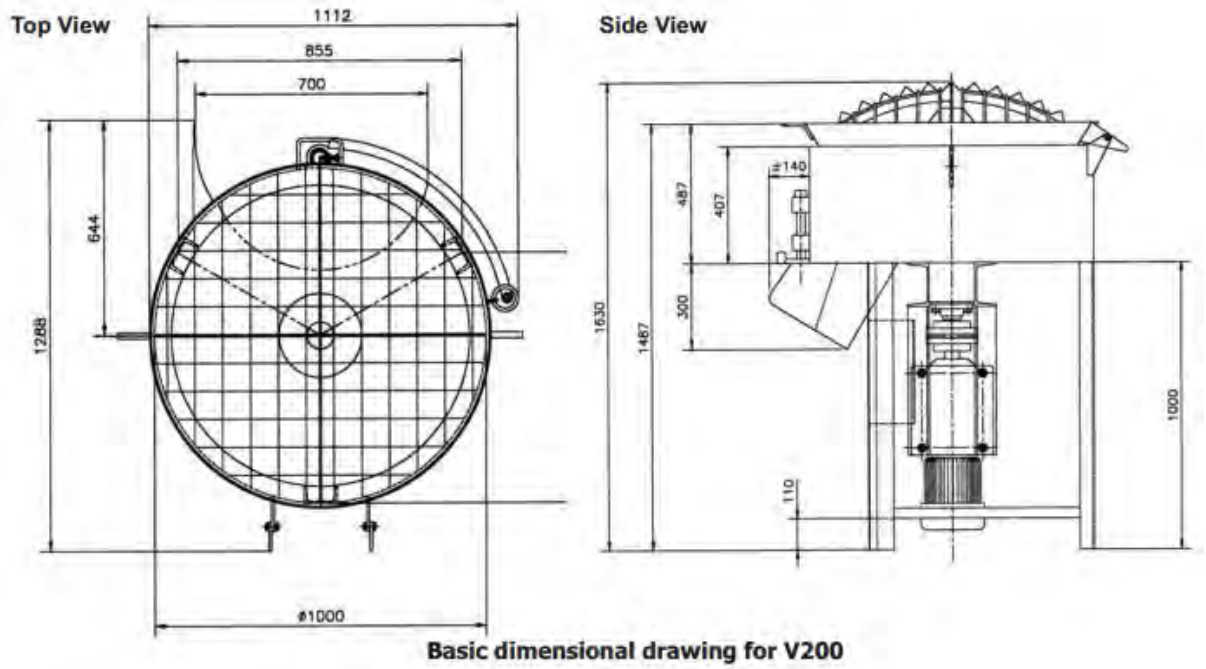

Figure 6-8 Mechanical mixer (PMSA, 2015)

The adopted water content was approximated from a mathematical Equation (6-2 below) developed by Talukdar (2014) that correlates California Bearing Ratio (CBR) value with Maximum Dry Density (MDD), Optimum Moisture Content (OMC), Liquid Limit (LL), Plastic Limit (PL) and Plastic Index (PI).

$$CBR = 0.127\,LL + 0.00\,PL - 0.1598\,PI + 1.405\,MDD - 0.259\,MC + 4.618 \qquad \text{Equation 6-2}$$

Where MDD is in g/cm^3

Talukdar (2014) carried out a comparison of laboratory and computed CBR values from Equation 6-2, which showed a consistency in results (Figure 6-8 below).

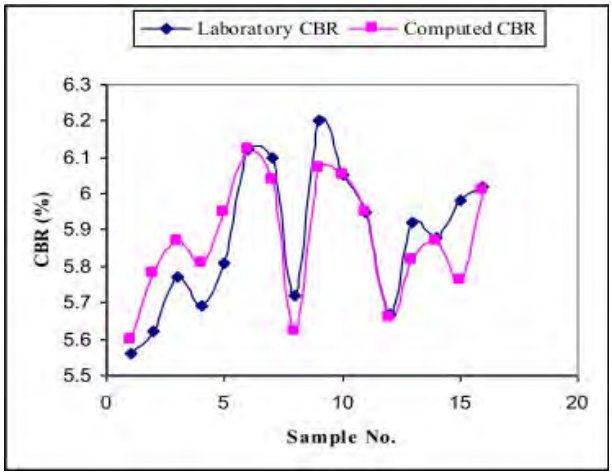

Figure 6-9 Comparison of laboratory and computed CBR values

A moisture content (MC) of 29% was obtained from the computation in Equation 6-2. The derived moisture content was subjected to trial and error by mixing it with Kaolin and a Torvane used to determine its undrained shear strength which was related to the CBR through Equation 6-1. Thus, it was established that a moisture content of 31% would give a more accurate representation of a clay with CBR of about 2%. The moisture content of 31% corresponded to a dry density of 1400 Kg/m^3 in the Kaolin compaction curve in Chapter 12.

Prior to setting of the prepared Kaolin in the test box, a plastic bag as a waterproof material was placed at the bottom. This was to ensure that there was no moisture loss from the subgrade soil through the bottom in the course of the testing.

The Kaolin was then placed inside the box in two lifts (350 Kg each) of the prepared soft clay. A hand tamper (300 mm x 200 mm) with a weight of 11 Kg (Figure 6-10 below) was used for compacting the subgrade. The compaction was commenced from one edge of the box to the other edge whilst standing outside the box on elevated platforms. This was conducted until the determined weight of material filled the volume for the subgrade soil at the 250 mm mark and the surface was evenly level. This process was repeated for the next layer until the entire subgrade layer was uniformly compacted and the surface level was at the 500 mm mark (Figure 6-11 below). Shear tests using the Torvane were

conducted after every lift at eight locations in an evenly distributed manner on the surface. As an exact undrained shear strength value of 41 kPa corresponding to 2.0% CBR was difficult to attain, an undrained shear strength of range 35 kPa to 45 kPa was acceptable.

Figure 6-10 Hand tamper

a) b)

Figure 6-11 a) Preparation of subgrade b) Prepared subgrade

6.4.2 Laying of the geosynthetic

For the reinforced cases, a geotextile or geogrid was placed on top of the subgrade (Figure 6-12 below). For tests that required double reinforcement, the geotextile was placed at the bottom of the base and the geogrid at the midpoint of the granular base. All geosynthetics were cut into 1 m^2 sizes and they were not anchored. The geosynthetic was spread from corner to corner to ensure that it lay flat against clay subgrade.

a)

b)

Figure 6-12 a) Geogrid at the interface b) Geotextile at the interface

6.4.3 Base preparation

The preparation commenced by air-drying the granular material for 7 days in order to bring the soil to an almost equal moisture content for control purposes. Air drying was adopted as an alternative to oven drying due to the large sample size of soil. Furthermore, air drying is a method adopted on-site in road construction (Figure 6-13 below). This is also because drying of soil in temperatures above 35° can cause drastic changes in physical and chemical characteristics of the soil, which could result in increased cementation of the soil, hence altering its grain size distribution (Tan, 1995). The soil was then stored in drums and covered with plastic bags to prevent ingress of moisture.

Figure 6-13 Air drying of base material

The base material was prepared by mixing 100 Kg of the granular soil with 10% of water, which is an equivalent moisture content of 90% of the modified AASHTO, and a density 1800 Kg/m^3. The desired density of 1800 Kg/m^3 was used partly due to the limitation of a soft subgrade which would make it impossible to attain higher densities. Also, Sapem-Pavement design (2013) has adopted the range of compaction of road materials for fills and pavement layers of 90% to 100 % MDD. The material was then placed in the electric PMSA V200 mechanical rotary mixer and the mixing carried out for 5-10 minutes until the material became consistent, homogenous and uniform. A thickness of 300 mm for the base was used in all unreinforced and reinforced pavement models. Using the density of 1800 Kg/m^3, for a 300 mm thick base, 540 Kg of the processed base material would be required. Hence, 540 Kg of material was prepared that would be required to fill the base volume for the attainment of 90% of the modified AASHTO.

The base material was compacted in two lifts of 150 mm each to ensure that the required density was achieved. 270 Kg of material was placed inside the box; compaction using the hand tamper was undertaken from one edge of the box to the opposite edge until a base depth of 150 mm was attained. The next batch of 270 Kg was added and the process repeated until an even level surface was attained at the 300 mm mark (Figure 6-14 below). For the doubly reinforced pavements, geogrid reinforcement was placed after the first lift.

Figure 6-14 Placement of the base material in the box model

This entire process was repeated for two other different densities of 1400 Kg/m^3 and 1600 Kg/m^3 in order to study the implications of varying densities to the performance of

reinforced pavements. This also assisted in informing us of the density at which the base material was placed such that the improvements from the reinforcement geosynthetics would be explored. After the second lift, the pavement model was ready for load application (Figure 6-15 below). Four Linear Variable Differential Transducers (LVDT) were placed at the centre of the outward side of the box in order to monitor the movement of the sides.

Two loading criteria were considered to replicate the loading conditions in a road pavement, albeit at laboratory large scale, since road pavements experience static loading disseminated from the weight of the vehicle and cyclic repetitions of traffic loads, from the moving wheel loads.

6.5 PLATE LOAD TESTS

Two variations of plate load tests were conducted: Static plate load and cyclic plate load tests. Unlike the in situ plate load tests, the tests conducted were bench scale on a 1 m x 1m x 1 m steel box and the boundary conditions assumed to be negligible since the test box had a width greater than 0.6 m (Figure 6-4 above) (Sawangsuriya et al., 2002).

Figure 6-15 Application of load to the composite system

The 305 mm diameter model footing was placed at the centre of the box on top of the prepared base. The base beneath the plate was kept level and horizontal so that there was no stress concentration below the plate during loading. The loading arm was then positioned in the middle of the plate. Seating pressure was then applied through the

loading actuator to the loading arm onto the plate to ensure that the set-up was firm. The loading was applied through a computer controlled INSTRON compression and tensile testing machine with a 250 kN capacity. The settlement was determined as the movement of the loading actuator. The extent of movement of the arm which represented the deformation was set through the computer. In this study, failure of the composite system was measured for a settlement of 75 mm as defined for unpaved roads. Additionally, the improvement from the use of reinforcement geosynthetic was measured against the unreinforced test as a reference point.

6.5.1 Static plate loading test

Static plate load tests were conducted to determine the bearing capacity and deformation of the pavement under loading. This understanding becomes even more important when the pavement is expected to carry heavy loads from vehicles that might result in a load bearing capacity failure. The static load tests were conducted at a rate of 1.2 mm/min for partially drained conditions through the plate (Figure 6-15) (ASTM 3080).

6.5.2 Cyclic plate loading test

Cyclic plate load tests were conducted to determine the improvement in performance of a geosynthetic reinforced pavement under vehicular loads. For laboratory cyclic plate load tests, most authors have adopted a sinusoidal pulse of 40 kN to the 305 mm diameter load plate at a frequency of between 0.67-1 Hz to simulate a single wheel load of 40 kN (equal to half an axle load of 80 kN and a tyre contact pressure of 550 kPa) (Qian et al. 2011; Abu-Farsakh & Chen 2012). These tests have been successfully conducted on either an asphaltic concrete surfacing or a strong aggregate base. However, the loading is not possible for weaker pavements as they experience excessive deformation with the initial load (Tingle & Jersey 2005).

For this study, the base being weak, a dynamic load was applied to the test plate using a computer controlled actuator. The dynamic sinusoidal load wave adopted had a 4 kN seating load that was linearly increased with an incremental load of 4 kN for every 8 cycles at a frequency of 0.2 Hz. Deformation was observed at 75 mm as defined for unpaved roads. In retrospect, as much as all these laboratory frequencies adopted have shortcomings of scale due to their small size of specimens, significant information has been gained with regards to geosynthetic contribution to the pavement (Cox, McCartney, Wood, & Curry, 2010).

6.5.3 Testing schedule

A total of 12 static and 6 dynamic plate load tests were carried out to represent the nature of loading experienced by the pavement structure during vehicular movement. Tests were conducted on the composite laboratory pavement model with (Figure 6-16) and without the geosynthetic (Table 6-9).

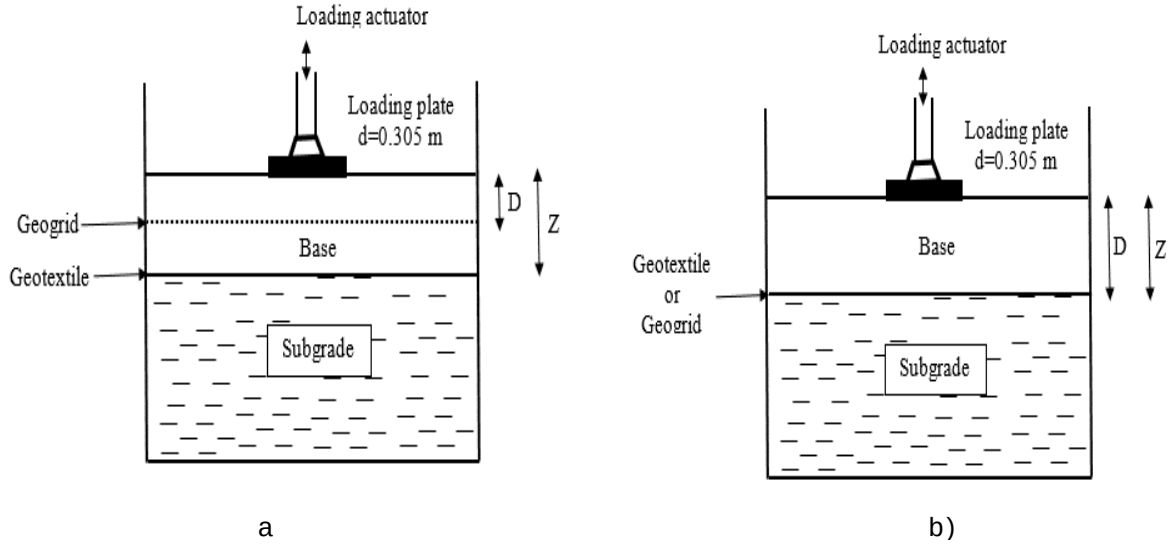

Figure 6-16 a) Geogrid-Geotextile Reinforcement b) Geogrid/Geotextile Reinforcement

Table 6-9 Summary of Testing schedule

Density (kg/m^3)	Thickness of granular materials (Z) (mm)	Depth of placement (D) (mm)	Test Number
Static Loading			
1400	300	300	EG/B305/Z300/D300-1400kg/m^3
1400	300	No Reinforcement	EG/B305/Z300-1400kg/m^3
1600	300	300	EG/B305/Z300/D300-1600kg/m^3
1600	300	No Reinforcement	EG/B305/Z300-1600kg/m^3
1800	300	300	EG/B305/Z300/D300-1800kg/m^3
1800	300	No Reinforcement	EG/B305/Z300-1800kg/m^3
1800	300	No Reinforcement	Unreinforced/B305/Z300
	300	300	WGx/B305/Z300/D300
	300	300	EG/B305/Z300/D300
	300	300	WGx-EG/B305/Z300/D200
Cyclic Loading			
1800	300	No Reinforcement	Unreinforced/B305/Z300
	300	300	WGx/B305/Z300/D300
	300	300	EG/B305/Z300/D300
	300	300	WGx-EG/B305/Z300/D200

7.0 RESULTS AND DISCUSSIONS

7.1 INTRODUCTION

This chapter presents the results of static and cyclic plate load tests performed on a laboratory pavement model to study the benefits of reinforcing a pavement structure using a woven geotextile and an extruded geogrid. The model pavement comprised of a granular base overlying a soft subgrade soil. Reinforcement geosynthetics (geotextile and geogrid) were varied in their location and number.

The trends were observed to determine the effects of the inclusion of a geotextile and geogrid within the pavement model. Additionally, the base soil densities were varied within the pavement model, and the implication of the behaviour of road pavements determined. The tests were repeated in order to ensure that we could have confidence in the results.

7.2 REPEATABILITY OF TEST RESULTS

Repeatability refers to the closeness of the agreement between the results of successive measurements carried out under the same conditions of measurement. Repeatability conditions include the same measurement procedure and the same measuring instrument within a short time interval (Taylor and Kuyatt, 1994). It is an important concept as it gives statistical integrity to test results, hence confidence levels increase with the consistency of the results. Furthermore, a test method can be reliable only if it is able to establish a similar trend within the same test set up. With a known repeatability, it becomes possible for succinct reporting and making of an informed technical decision.

For the tests carried out in this study, the consistency of the methodology was realised through laboratory equipment, materials preparation and application of loading. The repeatability results are as shown Figures 7-1 and 7-2 below.

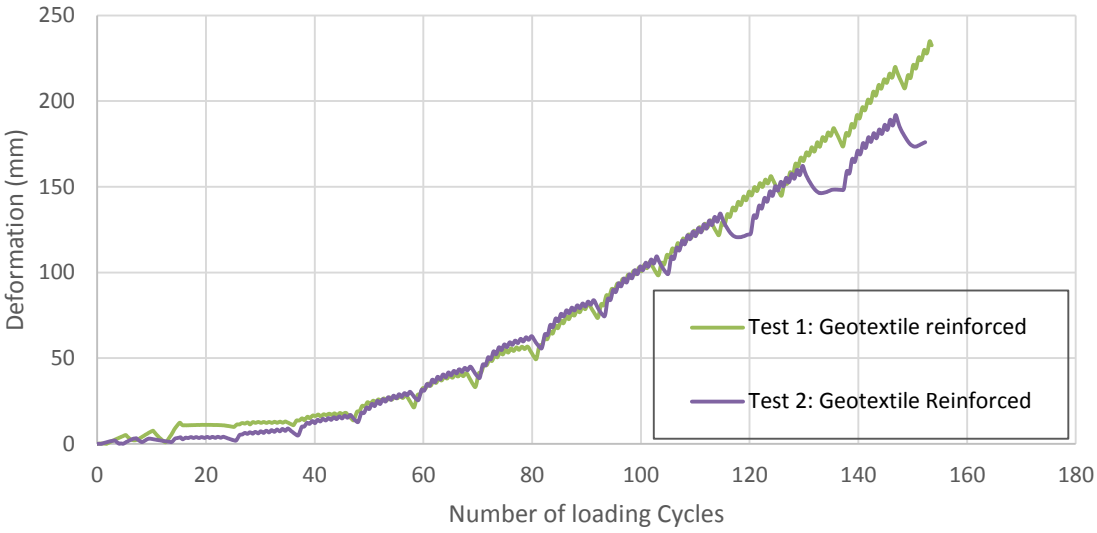

Figure 7-1 Cyclic plate load tests for Geotextile reinforced pavement

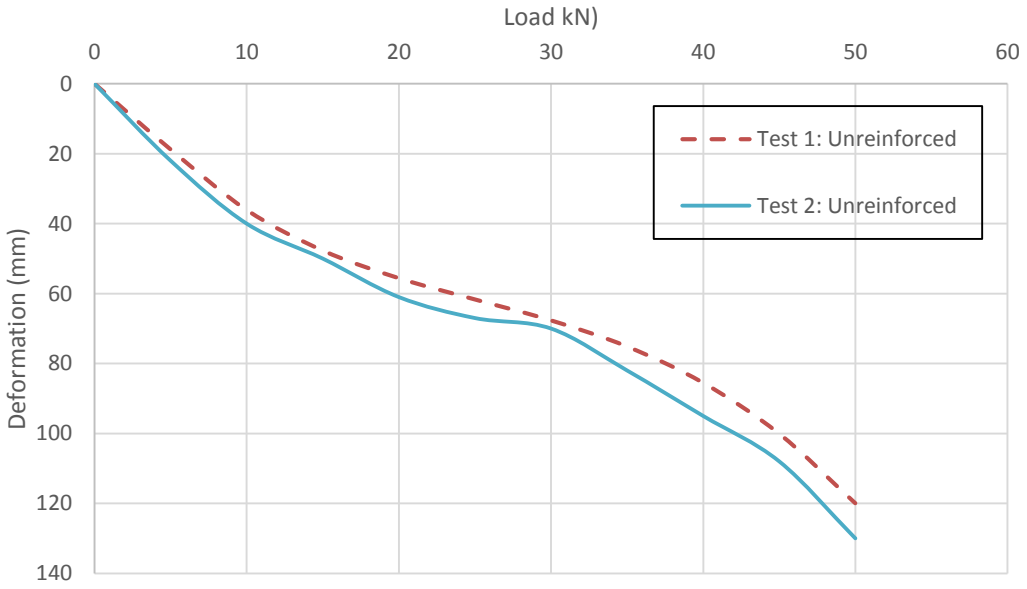

Figure 7-2 Static plate load test for unreinforced pavement

The repeatability results were analysed for standard deviation of the static and cyclic plate load tests. The mean of two similar tests was obtained, and standard deviations were then conducted from the mean. Standard deviations of a minimum 0.5 and a maximum 7 were reported at different deformations. Within this range, it was possible to get a clear distinction in performance between the different cases of reinforced and unreinforced model pavements.

7.3 STATIC LOAD TEST RESULTS

7.3.1 Effect of density

The effect of density was studied by carrying out static plate load tests on unreinforced and geogrid reinforced pavement models. The initial tests were performed on unreinforced and geogrid reinforced pavements at different base densities of 1400 Kg/m^3, 1600 Kg/m^3 and 1800 Kg/m^3 to determine the influence to the performance of road pavements (Figure 7-3 below). The thickness of the base was 300 mm and the geogrid was placed at the interface of the base and subgrade.

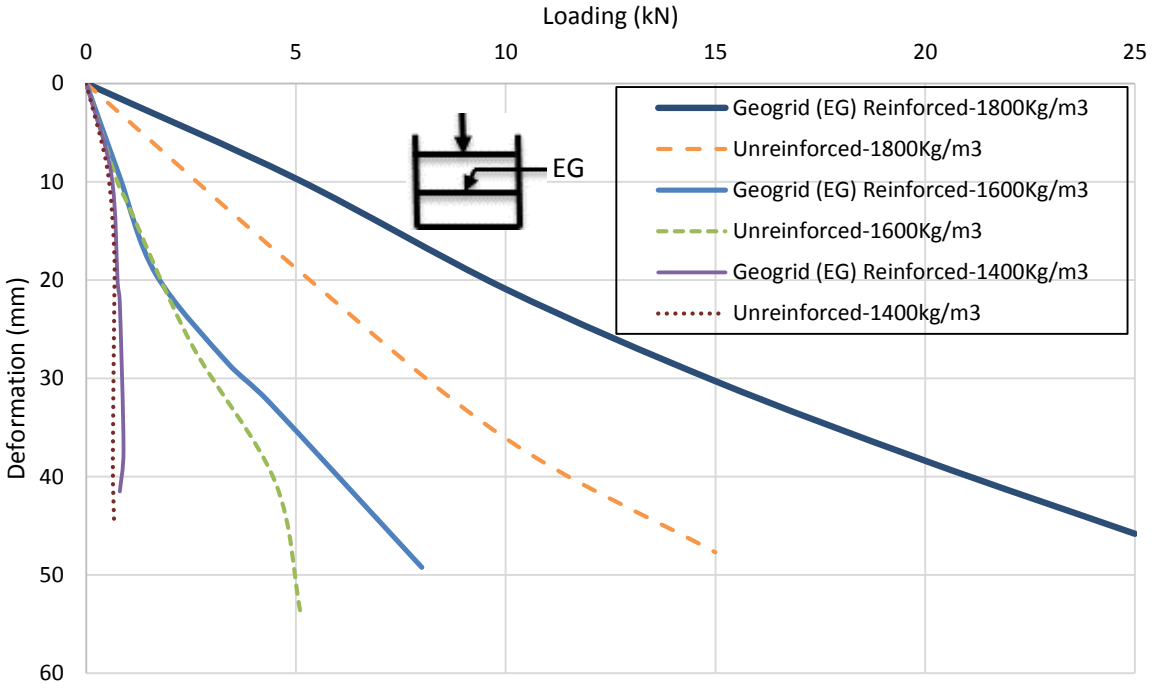

Figure 7-3 Influence of density to performance of road pavement

It was observed that the increase in loading resulted in an increase in deformation. The 1400 Kg/m^3 density base experienced the most deformation while the 1800 Kg/m^3 base experienced the least deformation with loading. The 1600 Kg/m^3 density base showed a deformation pattern that is intermediate between the 1400 Kg/m^3 and the 1800 Kg/m^3 base density. Generally, at each respective density, the geogrid reinforced pavement performed better than the unreinforced pavements as shown by the resistance to loading with each settlement. However, the effect of the reinforcement increased as the density increased. At the lower density of 1400 Kg/m^3, the effect of the reinforcement was minimal, while at the higher 1800 Kg/m^3 density there was a clear distinction in performance between the reinforced and unreinforced pavement model. Moreover, the

intermediate density of 1600 Kg/m^3 showed no reinforcement benefits up to about 2 kN before the difference in performance in the unreinforced and reinforced pavements became apparent. The benefits resulting from the use of reinforcement geosynthetics became apparent with the increase in loading for all the base densities. Therefore, it can be deduced that the best benefits with reinforcement geosynthetics are dependent on the loading regime and the density of the material.

On application of loading to the pavement model, the soil particles were displaced, interparticle contact increased and voids reduced resulting in a dense packing. Thus, the density increased with the frictional resistance leading to a higher shear strength with density increase. Furthermore, the soils become less compressible with an increase of density. As the compactive energy increases, the soil becomes more orientated (dispersed); therefore, the particles are able to effectively interlock within the geogrid with an increase in density. This was reflected in the better performance of the pavement model, with the 1400 Kg/m^3 base having the least performance, the 1600 Kg/m^3 base an intermediate performance and the 1800 Kg/m^3 base having the best performance comparatively. Additionally, the effect of reinforcement increased with increasing densities. This is because as the particle contact increased due to loading, so did the interlock capability of the geogrid which is responsible for the strength of geogrids. For this reason, the reinforcement function was mobilised the least in the 1400 Kg/m^3 base and most in the 1800 Kg/m^3 base.

At the different densities, the reinforced pavement performed better than the unreinforced. Consequently, at lower densities (1400 Kg/m^3 and 1600 Kg/m^3) and loading regimes, there is a similar deformation trend between the reinforced and unreinforced pavement. However, as the loading increases, the deformation trend changes as the reinforcing effect of the geogrid becomes noticeable. The 1400 Kg/m^3 base showed very minimal mobilisation of strength. This is because at this density the soil fabric was open, hence on application of the load, further packing (densification) of the soil occurred. Thus, the tensile strength of the geogrid was not initiated adequately, which could be attributed to partial interlock of the soil particles and the geogrid. At 1600 Kg/m^3 base density, the reinforced and unreinforced pavement performance were similar up to 2 kN, after which the reinforced pavement showed a higher resistance to loading. Before 2 kN, densification of the base was occurring such that the reinforced and unreinforced pavements had the same deformation and loading characteristics. However, after 2 kN, the reinforcement function of the triggered and the geogrid tensile strength mobilised to give a superior performance. As the base density was increased to 1800 Kg/m^3, the performance of the

reinforced and unreinforced pavements increased. The particle to particle contact was sufficiently adequate such that geogrid strength was realised from the onset in comparison to the 1400 Kg/m^3 and 1600 Kg/m^3 bases. This additionally prompted a better reinforced pavement performance in comparison to the unreinforced pavement. Therefore, better reinforcement benefits are realised with higher density bases and at higher loadings.

Overall, the increase of density was observed to be fundamental to the performance of the pavement models, with unreinforced pavements at higher densities manifesting better performance than reinforced pavement models at lower densities. In addition, at lower densities and lower loading regimes, no benefits were realised from the use of the geogrid.

7.3.2 Improvement in bearing capacity

The benefits in bearing capacity improvement and subsequently the reduction in deformation accruing from the inclusion of geosynthetics were investigated through static plate load tests. For the tests, the location was varied, with the geotextile or geogrid at the interface or a placement of geotextile at the interface and geogrid within the base. The plot of deformation against stress is as shown in Figure 7-4 below.

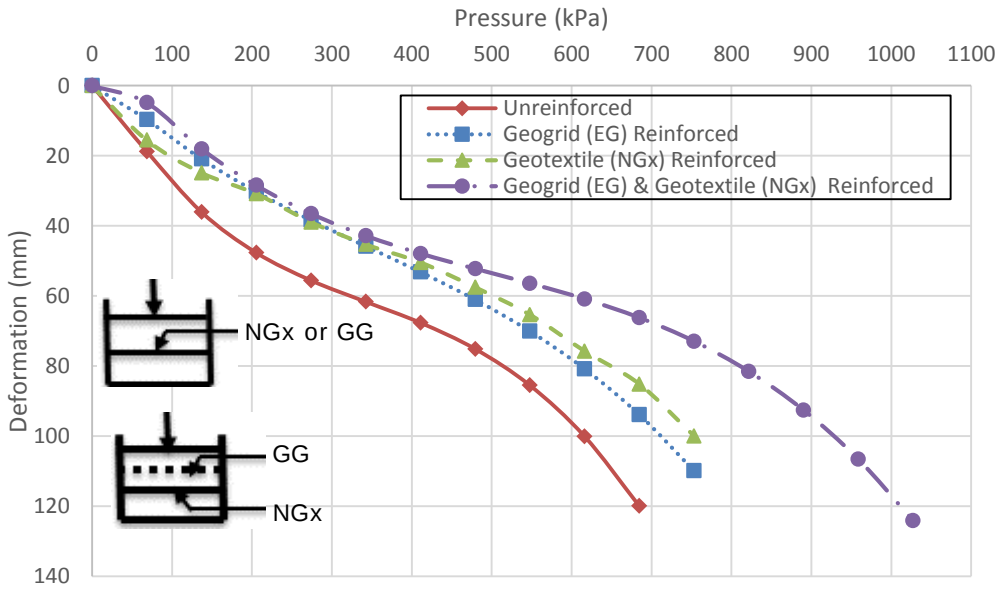

Figure 7-4 Pressure against settlement of the reinforced and unreinforced composite system

There was an overall increase in bearing capacity from the use of geotextile and geogrid within the pavement model. This was shown by increased bearing pressures with reduced deformation for the geosynthetic reinforced bases in relation to the unreinforced pavement model. With geosynthetic reinforcement, at pressures from 0 to about 170 kPa there is a slight deformation (due to low pressure relative to the densification of the materials); between 170 to about 420 kPa, all geosynthetic reinforcements exhibit comparable deformation trends (even with a geotextile-geogrid combination); beyond 420 kPa, the benefits of combining a geotextile and geogrid (as illustrated) are realised. Use of the geogrid or geotextile remains more or less comparable but is significantly better than the reference (without the geosynthetic reinforcement).

Pressures between 0 kPa-170 kPa were marked by a significant settlement of the system with an increment in pressure. In this region, as the load was being applied, compaction of the soil occurred and the soil particles fitted closely. From 170 kPa-420 kPa, there was an increase in resistance to deformation with loading. In this region, the soil was densified such that there was a higher frictional resistance. Beyond a pressure of 420 kPa, significant deformation was achieved with increasing loading, apart from the geotextile-geogrid combination. It was deduced that a deformation bowl (Figure 7-5) had formed in this region (Moghaddas-Nejad & Small, 1996). The base material had been contaminated by the poor subgrade material (Bearden & Labuz, 1999) hence, the base was no longer able to structurally function sufficiently. However, for a combination of geogrid-geotextile in the pavement model, the formation of the deformation bowl occurred beyond 800 kPa. This was because the double reinforcement of the pavement resulted in initialising of the geogrid tensile strength first, followed by the geotextile's strength.

7.3.3 Reduction in deformation

A significant reduction in deformation was realised through the incorporation of geotextile and geogrid within a pavement model as shown in Figure 7-4. The graph showed that the behaviour of the geogrid at smaller strains (0-40 mm) was superior to that of the geotextile, as indicated by the bearing pressure sustained and equivalent reduced deformations.

For the geotextile-geogrid pavement model, at this depth range, the performance exceeded that of geotextile and geogrid. Furthermore, reduced deformation of the geotextile-geogrid pavement was due to the enhanced strength arising from the geogrid mainly due to its proximity to the model footing that favourably allowed triggering of the

tensile strength. In all the cases, the geogrid was able to mobilise its strength at low displacements due to lateral confinement as the soil aggregates interlocked within the grid. Comparatively, the geotextile within this region developed strength through friction between the soil and fibre, but its magnitude was lower than that of the geogrid and geotextile-geogrid pavements.

Figure 7-5 Deformation bowl in a geotextile and geogrid reinforced pavement model

As the strain proceeded (above 40 mm), the performance of the geotextile in both deformation and bearing capacity was comparable to that of the geogrid pavement but was not as significant as the combination of geotextile-geogrid pavement. In this region, sufficient deformation had taken place such that the tensioned membrane effect was the major reinforcing mechanism (U.S Army corps of Engineers, 2002). Thus the geotextile with more than two times the strength of the geogrid resulted in better resistance to deformation. Furthermore, the geotextile functioned primarily as a better separator between the base and soft subgrade than the geogrid, thus maintaining the structural integrity of the base (Koerner, 2012). In contrast, the geotextile-geogrid pavements offered the most reduction in deformation with increase in loading. Generally, the reinforced pavements exhibited better performance than the unreinforced pavements.

7.3.4 Stress-strain relationship

The behaviour of the composite system under static loading was analysed and the stress-strain behaviour was determined, as shown in Figure 7-6 below. The strain was measured as a ratio of the incremental deformation to the overall depth of 0.8 m (0.5 m-subgrade & 0.3 m-Base) of the pavement.

At strain levels between 0 to 0.06, all geosynthetic reinforcement pavements exhibit a similar trend. Beyond the 0.06 level, a combination of geosynthetic reinforcement (geogrid and geotextile) provides a better performance than singular geosynthetic reinforcement systems. The reference (without geosynthetic reinforcement) exhibited the lowest performance.

At lower deformation, the behaviour of the reinforced pavements was defined by the lateral confinement effect, whereby the geogrid and the soil interlocked and there was frictional interaction between the geotextile and the soil resulting in the strength of the composite system in geogrid and geotextile reinforced pavements, respectively. Beyond the strain of 0.06, the strength of the reinforced system was defined by the membrane effect due to the large deformation. A combined geosynthetic reinforcement is capable of sustaining more stress levels at a given strain level than a singular or unreinforced pavement structure.

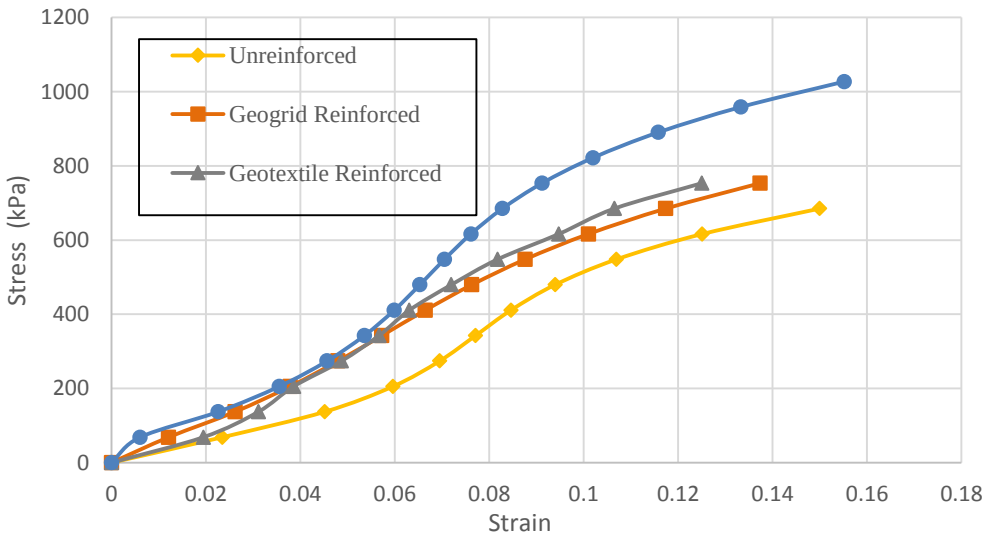

Figure 7-6 Stress-strain relationship

7.4 CYCLIC LOAD TEST RESULTS

Cyclic plate load tests were undertaken on both the reinforced and unreinforced pavement structure. Permanent vertical deformation was recorded in order to study the behaviour of pavements under repeated loads as shown in Figure 7-7 below.

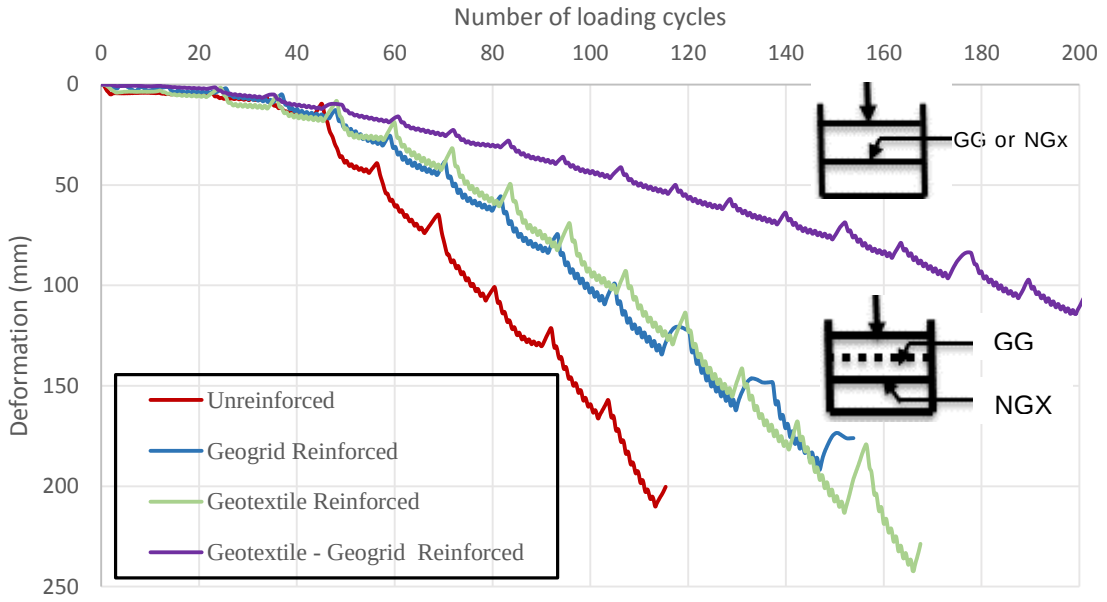

Figure 7-7 Deformation against number of cycles for the reinforced and unreinforced base

7.4.1 Effect of cyclic loading on deformation

The overall results showed that permanent deformation increased with an increased number of cycles for all test cases as shown in Figure 7-7 above. The initial cycles (0-45) offered a high resistance to loading; this was attributed to the additional base compaction arising from the dynamic action. For every cycle, there was an accumulation of plastic non-recoverable deformations.

The rate of deformation was highest for the unreinforced pavement. The geotextile and geogrid reinforced pavement performed better than the unreinforced pavement. The performance of the geogrid reinforced and geotextile reinforced pavement were comparable for all the cycles. The highest benefits were reported for the double combination of geotextile at the interface and geogrid placed within the base of the

pavement. This was at its maximum due to the proximity of the geogrid to the surface that allows a faster mobilisation of the geogrid's tensile strength. From the trends, it is evident that a geosynthetic reinforcement combination (geotextile and geogrid) resulted in the highest resilience to the loading cycles in comparison to the singular systems (geotextile or geogrid) and the unreinforced pavement. Additionally, the singly reinforced systems supported more cycles of load per deformation when compared to the unreinforced pavement.

7.4.2 Effect of type of loading

The method of application of loading in the pavement model was static and dynamic loading. Whereas the static loading was applied at a constant rate of 1.2 mm/min, the dynamic loading was applied at a 0.2 Hz with a 4 kN seating load that was linearly increased with an incremental load of 4 kN for every 8 cycles. The aim of the different modes of load application was to mimic the vehicular load in the road pavement with an objective of understanding the efficacy of geosynthetic reinforced pavements.

From the results of static and cyclic plate load tests as discussed in section 7.3 and 7.4.1, it was apparent that the use of geogrid and geotextile within the pavement resulted in an increase in bearing capacity, reduction in deformation and resilience to loading cycles. The pavement model responded differently under different loadings. When subjected to static loading, the deformation that resulted was gradual where the deformation increased with the loading under cyclic loading, there was an accumulation of small deformations with each load cycle repetition. Thus, the two modes of testing, representing the movement of vehicles in a road pavement, indicated that the use of reinforcement geosynthetics led to a superior performance of the pavement.

There was a general agreement with regard to the performance of the different cases of pavement model regardless of the nature of loading. The geotextile reinforced and geogrid reinforced pavements showed similar trends and were comparable. The geotextile-geogrid reinforced pavement mobilised the highest strengths. Furthermore, for all reinforcement cases, for the static and cyclic loading, at 75 mm the geogrid was observed to rupture and the geotextile stretched as shown in Figure 7-8. The results from static and cyclic plate loading tests showed a similar trend in performance for the different cases of pavement reinforcement.

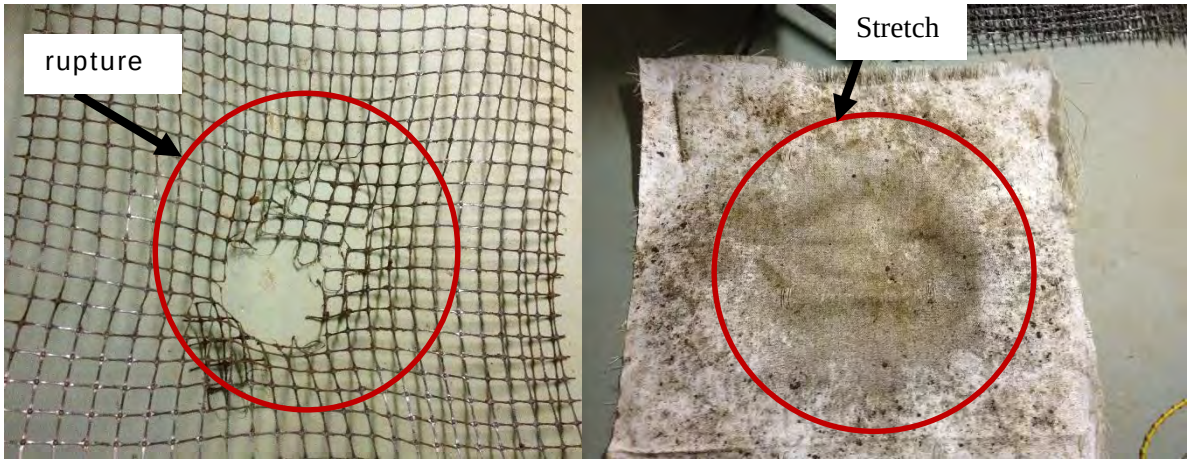

a) b)

Figure 7-8 a) Geogrid rupture after loading b) Geotextile stretched after loading

8.0 ANALYSIS OF RESULTS

8.1 INTRODUCTION

In this chapter, the benefits of considering a reinforcement geosynthetic in a pavement under static and dynamic loading are determined. The inclusion of geotextile and geogrids resulted in an increase in bearing capacity, reduction in deformation and increased resistance to load repetitions. These were represented by the Bearing Capacity Ratio (BCR), Settlement Reduction Factor (SRF) and Traffic Benefit Ratio (TBR) respectively. BCR and SRF were obtained from static plate load tests while the TBR was obtained from the cyclic plate load test.

8.2 BEARING CAPACITY RATIO (BCR)

The improvement in bearing capacity of the reinforced pavement structure from the inclusion of a geosynthetic is quantified through a non-dimensional parameter, the Bearing Capacity Ratio (BCR). It is defined as the ratio of bearing pressure of the reinforced soil (qr) at a given settlement to the bearing capacity of the unreinforced soil (qu) at the same settlement, as seen from Figure 7-4 above.

$$BCR = \frac{q_r}{q_u}$$ Equation 8-1

Table 8-1 Calculated Bearing Capacity Ratio (BCR) at 75 mm deformation

Pavement	Bearing pressure at 75 mm	BCR
Unreinforced (Nu)	480 kPa	1
Geotextile	620 kPa	1.29
Geogrid	580 kPa	1.21
Geotextile & Geogrid	780 kPa	1.63

8.3 SETTLEMENT REDUCTION FACTOR (SRF)

Settlement due to imposed load, also referred to as deformation, is an important factor as it is directly related to pavement serviceability. The reduction in settlement therefore can

be quantified by the Settlement Reduction Factor (SRF) from Figure 7-4. SRF is defined as the percentage reduction in settlement and is expressed as follows:

$$SRF = \frac{S_o - S_r}{S_o}\, x\, 100 \qquad \text{Equation 8-2}$$

Where S_o is the settlement of unreinforced soil at a given footing pressure and S_r the settlement of reinforced soil at the same footing pressure.

The reduction in settlement/deformation was computed from Figure 7-4; pressure against deformation, at a deformation of 75 mm and are as presented in Table 8-2.

Table 8-2 Calculated Settlement Reduction Factor (SRF)

Pavement	Settlement	SRF (%)
Unreinforced (S_o)	75 mm	Control
Geotextile	58 mm	23%
Geogrid	60 mm	18 %
Geotextile & Geogrid	52 mm	31%

8.4 TRAFFIC BENEFIT RATIO (TBR)

Traffic Benefit Ratio (TBR), also referred to as Traffic Impact Factor (TIF), is defined as the number of load cycles carried by a reinforced section (Nr) at a specific rut depth divided by that of an equivalent unreinforced section (Nu).

$$\mathrm{TBR} = \frac{\mathrm{Nr}}{\mathrm{Nu}} \qquad \text{Equation 8-3}$$

In Section 5.5.4.1, the importance of TBR in determining the number of traffic passes that a reinforced pavement can withstand as compared to an unreinforced pavement for a given rutting depth has been highlighted. The calculated TBR values are as shown in Table 8-3 for a 75 mm deformation obtained from Figure 7-7.

Table 8-3 Calculated Traffic Bearing Ratios

Pavement	Number of cycles	TBR
Unreinforced (Nu)	70	1
Geotextile	90	1.29
Geogrid	85	1.21
Geotextile & Geogrid	150	2.14

8.5 SUMMARY OF ANALYSIS OF RESULTS

Based on the computed Traffic Benefit Ratio (TBR), Bearing Capacity Ratio (BCR) and Settlement Reduction Factor (SRF), there was a significant improvement following the use of reinforcement geosynthetics. Results show the use of geosynthetic reinforcements either as a 'combination' or as 'singular' within the pavement structure results in an increase in bearing capacity and resistance to loading repetitions, as well as a reduction in deformation. At 75 mm deformation, an increase of bearing capacity was realised with the use of geotextile and geogrid within the pavement as compared to the unreinforced pavement (referenced pavement type). The combination of geogrid and geotextile within the pavement structure provided the highest overall BCR of 1.63 (see Table 8-1) and settlement reduction factor of 31% (see Table 8-2).

Under cyclic loading, the response trends of the different pavement types compared well with their equivalent under static loading. The geotextile-geogrid pavements showed the highest resilience to the loading repetitions, while the singly reinforced pavements were comparable in performance. For a maximum allowable deformation, the unreinforced case sustained 70 cycles, the geotextile reinforced 90 cycles, the geogrid reinforced 85 cycles and the geotextile-geogrid reinforced pavement 150 cycles. This was represented in Table 8-3 in the form of Traffic Benefit Ratios.

Overall, there was a significant improvement from the use of geotextile and geogrid within the pavement. The combination of geogrid-geotextile reinforced pavement provided additional performance benefits. At 75 mm, both the geotextile and geogrid had stretched and the tensioned membrane effect mobilised. In spite of the geotextile having more than double the strength of the geogrid used, the disparity was not reflected in its performance. This could be attributed to the geogrid's interlocking effect that could have magnified its strength in addition to the tensioned membrane effect.

9.0 AASHTO DESIGN OF GEOSYNTHETIC REINFORCED FLEXIBLE PAVEMENTS

9.1 INTRODUCTION

Different design approaches have been considered in this study i.e. AASHTO method, Giroud & Noiray Method, Oxford method and Giroud and Han method that have been developed for geosynthetic reinforced structures. In this study, the AASHTO method, which incorporates the benefits of geosynthetic reinforcement inclusions, was used to design a pavement, since it is also one of the most widely used design methods for flexible pavement design.

9.2 AASHTO PAVEMENT DESIGN

The procedure for AASHTO design will be discussed in Section 9.2; it incorporates the use of overall structural number which reflects the pavement thickness and resilience to traffic loading. Additionally, the resulting benefits from the use of geosynthetics which are in the form of the Bearing Capacity Ratio (BCR) and Traffic Benefit Ratio (TBR) have been factored in the AASHTO pavement design equations (Sections 8.2 and 8.4).

The important parameters for pavement design are the cumulative 80 kN (18 kip) Equivalent Single Axle Loads (ESALs), reliability, overall standard deviation, road bed resilient modulus and design serviceability loss as shown in AASHTO design Equation 9-3 in determining the pavement's structural number. The choice of the parameters has been highlighted in the Appendix, Section 12.3, and a summary is presented in Table 9-2.

In this design, the ESALs selected was 30000 which corresponded to road category D with a recommended design period of 10 years according to TRH4 (1996). The design pavement comprised of a base as a structural unit and a thin surfacing (HMA) protective layer.

9.3 STRUCTURAL NUMBERS

The Structural Number (SN) is an index value that combines layer thicknesses, structural layer coefficients, and drainage coefficients. The SN for the pavement can be determined using an equation or as a nomograph in Figure 9-1.

$$Log\ W_{18} = Z_R x\ S_o + 9.36\ x\ log(SN+1) - 0.2 + \frac{log\frac{\Delta PSI}{2.7}}{0.4+\frac{1094}{(SN+1)^{5.19}}} + 2.32\ log\ M_R - 8.07 \quad \text{Equation 9-1}$$

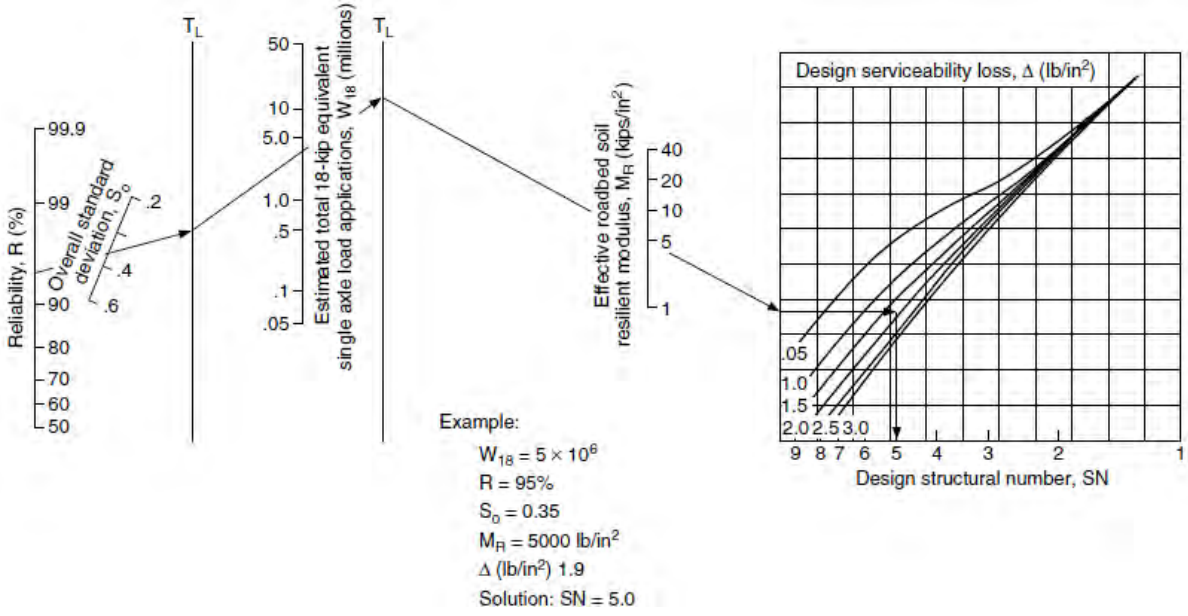

Figure 9-1 Design chart for flexible pavements based on using mean values for each input (AASHTO, 1993).

Using the AASHTO flexible design excel spread sheet, by inputting the different components in Equation 9-1 as summarised in Table 9-1, an overall structure number of 2.19 was obtained for the pavement. The choice of the different parameters is as highlighted in the Appendix Section 12.3.

9.4 SELECTION OF LAYER THICKNESS

Once the SN for a pavement structure is known, the next step is to identify a set of pavement layer thickness which is able to provide a load carrying capacity corresponding to the design SN. The different layers of a pavement can be designed through a series of iterations using the following Equation:

$$SN = (a_1 D_1)_{HMA} + (a_2 D_2 M_2)_{Base} + (a_2 D_2 M_2)_{subbase} \quad \text{Equation 9-2}$$

Where HMA is hot mix asphalt, a is the layer coefficient, D is the actual layer thickness (in inches) and M is the drainage coefficient.

Table 9-1 Summary of Design parameters for unreinforced pavement (TBR and BCR =1)

Parameter	Symbol	Value
Predicted future traffic	W_{18}	30 000 ESALs
Reliability	R	50%
Overall standard deviation	S_o	0.3
Subgrade resilient modulus	MR	3000 psi
Initial serviceability	Po	4.5
Terminal serviceability	P_t	2.5
Layer coefficient	$a_{i\ HMA}$	0.44
	$a_{i\ Base}$	0.1
Drainage coefficient	$m_{i\ (base)}$	0.9

9.5 UNREINFORCED PAVEMENT DESIGN

Considering Equation 9-2 above, a trial and error method was utilised while varying the thickness of the pavement layers to obtain a Structural Number approximate to but greater than 2.19. A thin overlay of 50 mm was maintained in the design in order to improve the ride quality by improving surface smoothness and quality, protect the base from moisture and usage wear, eliminate dust and reduce the loss of surface aggregate.

An unreinforced pavement was adopted with an ESALs of 30000, an asphalt surfacing of 50 mm and a base of 380 mm which yielded a safe design. The overall SN that ensued was 2.23, which is greater than the design Structural Number of 2.19, hence sufficient (Table 9-2).

Table 9-2 Unreinforced pavement structural number

Layer	Material Type	Thickness (mm)	Layer coefficient a^i	Drainage coefficient M^i	Structural Number
1	HMA	50	0.44	1	0.87
2	Base	380	0.1	0.9	1.35
			Overall structural number		2.22
			Design structural number		2.19

The calculated traffic for the unreinforced section based on the AASHTO (1993) equation is 32000 ESALs, which meets the design traffic of 30000 ESALs; thus, the unreinforced section meets the design requirements.

9.6 GEOSYNTHETIC REINFORCED PAVEMENT DESIGN

The use of geosynthetics as reinforcement components within a base results in benefits that have been quantified in the form of the Traffic Benefit Ratio (TBR) and Base Course Reduction (BCR). Improvement of the TBR has been included as a factor of the design Equivalent Standard Axle Loads (ESALs) to represent an extended pavement life. Whereas BCR is applied as a modifier to the Structural Number of the pavement, this results in reduced thickness of the base course.

Two main benefits of the geosynthetic reinforcement have been considered: extended life of the pavement (i.e. additional vehicle passes), and reduced base aggregate thickness (i.e. reduced undercut, aggregate quantities and initial construction cost) as also determined by Holtz et al. (2008).

9.6.1 Extended pavement of life

The contribution of TBR in pavement design is factored into the design ESALs, as shown in Table 9-3 below. The design ESALs in the unreinforced case used was 30 000. After factoring for a reinforced pavement, the computed ESALs were designed for an equivalent unreinforced base. This was to express the benefits of the inclusion of geosynthetics in terms of an equivalent unreinforced base and structural number increment.

$$W_{18}\,(reinforced) = TBR\ x\ W_{18}\,(unreinforced) \qquad \text{Equation 9-3}$$

Table 9-3 Pavement design using the Traffic Benefit Ratio (TBR)

	TBR from model testing	TBR factored ESALs	Structural Number	HMA surfacing	Equivalent unreinforced Base Thickness
Unreinforced (Nu)	1	30 000	2.23	50 mm	380 mm
Geotextile	1.29	38 400	2.32	50 mm	400 mm
Geogrid	1.21	36 300	2.29	50 mm	400 mm
Geotextile & Geogrid	2.14	64 200	2.50	50 mm	460 mm

The calculated traffic for the unreinforced section is 30000 ESALs. Factoring in the TBR, the calculated traffic for the geosynthetic reinforced pavements is 38400 ESALs for geogrid, 36300 for geotextile and 64200 for geotextile-geogrid reinforced pavements. It is evident that for a pavement with the same thickness, the inclusion of reinforcement geosynthetics results in a superior pavement that is able to withstand higher loading repetitions. The double reinforcement of geotextile at the interface and geogrid within the base carries more than twice the equivalent standard axles for the unreinforced pavements.

Moreover, when the loading repetitions are designed for, there is an increase in the SN greater than the unreinforced road. The equivalent unreinforced thickness increases with the inclusion of geosynthetics, conveying that a higher unreinforced base thickness is required to match the increased SN as a result of the inclusion of a geogrid and geotextile.

9.6.2 Reduced base aggregate thickness

Base course reduction factor is a modifier that is applied as a modifier to the SN of the pavement. For ESALs of 30000, the required design SN of an unreinforced pavement is 2.19.

$$SN = (a\ x\ d)_{hma} + BCR.(a\ x\ d\ x\ m)_{base} + \ldots.$$ Equation 9-4

The BCR was factored in the base SN and a new overall SN for reinforced pavements determined. The eventual SN was input in Equation 9-1 to calculate the resulting ESALs. To show the benefit of reinforcement geosynthetic in the pavement, an equivalent unreinforced base thickness for the corrected SN was obtained.

The reduced depth of base course can be computed by inputting the BCR when designing the pavement as follows:

$$d_{Base,(R)} = \frac{SN_u - (a\ x\ d)_{hma} - (a\ x\ d\ x\ m)_{subbase}}{BCR.(a\ x\ m)_{base}}$$ Equation 9-5

Where $d_{base,\ (R)}$ is the reduced base course thickness due to reinforcement and SNu is the Structural Number corresponding to the equivalent W_{18} for the unreinforced pavement.

Table 9-4 Pavement design using the base course reduction (BCR)

	BCR from model testing	Factored SN	Equivalent ESALs	HMA surfacing	Equivalent unreinforced Base	Reduced Base thickness
Unreinforced (Nu)	1	2.19	30 000	50 mm	380 mm	-
Geotextile	1.29	2.62	88 000	50 mm	500 mm	120 mm
Geogrid	1.21	2.50	66 000	50 mm	460 mm	80 mm
Geotextile & Geogrid	1.63	3.08	245 000	50 mm	630 mm	250 mm

The unreinforced thickness of 300 mm, on the inclusion of reinforcement geosynthetic, resulted in reduced base thickness by 31%, 18% and 65% for the geotextile, geogrid and geotextile-geogrid reinforced pavements respectively. In addition, computing the resulting ESALs from the factored SN, showed an increase in the ESALs of up to 8 times the unreinforced ESALs. Furthermore, the corresponding equivalent unreinforced thickness is up to 1.5 times more with the inclusion of geosynthetic reinforcements.

The performance of the geotextile-geogrid reinforcement was better than the singly reinforced pavement with either geogrid or geotextile. The geotextile reinforced pavement sustained more ESALs than the geogrid reinforced pavement. This is attributed to the strength of the geotextile used being more than twice the strength of the geogrid.

9.6.3 Cost savings analysis

The cost saving was calculated from the obtained improvements which were considered in the AASHTO design for reinforced and unreinforced pavements. The economy is obtained from the reduction in the thickness of the base. The width of the road pavement was assumed to be 7 m and the cost savings were computed over a 1 Km length. The cost of materials is as shown in Table 9-5 below.

Table 9-5 Cost of materials

	Material Type	Cost
Granular base	G7 material	300 Rands/m^3
Geogrid	Macgrid EG 20S	15 Rand/m^2
Geotextile	Mactex W1 5S	19 Rand/m^2

Cost saving from the use of geotextile and geogrid reinforcement will vary from project to project depending on the subgrade conditions and the base material properties used. From the design adopted, it was determined that there was a reduction in the thickness of the granular base. The advantages of increasing base thickness were considered vis-à-vis the cost of using a geotextile and geogrid within the pavement, as shown in Table 9-6 below. The outcome showed that there were savings from the cost of the reinforcement geosynthetics versus the additional base materials. This was represented as a percentage saving in cost of base materials of 47%, 38% and 55% for the geotextile, geogrid and geotextile-geogrid pavements respectively (Table 9-6).

Table 9-6 Summary of cost savings for 7 m wide, 1 Km Pavement

Pavement	Equivalent unreinforced Base	Reduced Base thickness	Cost of geosynthetics over 1 Km	Savings in base thickness reduction	Percentage saving in cost
Unreinforced (Nu)	380 mm	-	-	-	-
Geotextile	500 mm	120 mm	R133 000	R252 000	47%
Geogrid	460 mm	80 mm	R105 000	R168 000	38%
Geotextile & Geogrid	630 mm	250 mm	R238 000	R525 000	55%

10.0 CONCLUSION AND RECOMMENDATIONS

The effectiveness of the use of geotextile and geogrid as reinforcement inclusions within the road pavement with a granular base overlying a soft subgrade was evaluated in this research study. The tests conducted were in static and dynamic loading with the intention of representing the effects of vehicular motion on a road. Rutting failure was considered at a depth of 75 mm, as in unpaved roads.

The results from static plate load tests and dynamic plate tests clearly demonstrated the benefits of geotextile and geogrid reinforcement in terms of increased bearing capacity, wider stress distribution and reduced permanent deformation. The results were then included in the AASHTO design method for a pavement, with a thin protective surfacing of 50 mm that is expected to experience an ESAL repetition of 30 000.

10.1 CONCLUSIONS

The following conclusions can be drawn from the present study:

1. There was minimal difference between the performance of geogrid and geotextile reinforced models, even though the tensile strength of the geotextile is twice that of the geogrid.
2. The ultimate tensile strength of a geosynthetic is not the governing performance indicator, since the inherent characteristic of geogrid to interlock with soil results in a comparable performance as a geotextile with double the geogrid's ultimate strength.
3. There was an increase in the bearing capacity of the reinforced composite systems by up to 60% of the unreinforced systems, with the best performance recorded for the arrangement of geotextile at the interface between the subgrade and base as well as having a geogrid within the base.
4. There was a reduction in permanent deformation by up to 31% due to the use of geosynthetics within the road pavement. This maximum reduction in deformation was observed in the double reinforcement of geotextile at the interface between the base layer and subgrade as well as having a geogrid within the base layer.
5. The design of a reinforced pavements showed that it was capable of supporting more than twice the Equivalent Standard Axles (ESALs) of an unreinforced pavement. Also, there was a reduction of the thickness of the base layer owing to

from the inclusion of reinforcement geosynthetics by up to 40% of the unreinforced base thickness.

6. There are cost savings attributed to use of the reinforcement geosynthetics of up to 55%; this was based on the cost of the geosynthetic materials relative to the additional thickness of the base layer.

10.2 RECOMMENDATIONS

The experimental work conducted in the study focused on both the static and dynamic effects of loading on model pavements. The benefit of including geosynthetic reinforcements (geogrid and geotextile) was illustrated through laboratory cyclic and static plate load tests.

However, there are limitations that come with laboratory testing. Unlike the cyclic plate load test, real traffic is comprised of moving loads with wander. As such, the performance of reinforced bases due to real traffic could be different from the stationary cyclic plate load test. Furthermore, traffic experiences higher dynamic frequencies that cannot be adequately replicated in the laboratory. Moreover, the anticipated traffic loading occurring from the vehicular weight can be of a higher magnitude than that reflected in the experimental study. Additionally, scale can only be minimised with larger models, but the accurate conditions can only be obtained through field measurements under variable weather conditions. Thus, experimental results should not be used directly without establishing a correspondence with the full scale field data. For this fact, it is recommended that full scale field experiments be conducted to assess the suitability of using geosynthetics as reinforcement membranes in a pavement structure under vehicular loading and environmental conditions.

It is also important to understand fully the mechanisms of interaction between the geosynthetic and the soil. Hence, fully instrumented experiments both in the laboratory and in the field should be conducted with load cells and strain cells in order to better evaluate the typical load distribution and ascertain the failure mechanism in reinforced pavements compared to the unreinforced types. Theoretical modelling calibrated using the field acquired test data could be extended to evaluate the actual failure criterion and provide reliable parameters for the design of pavements using geosynthetics.

The results have also shown that the best performance can be obtained with reinforcement arrangement of geotextile at the interface of base-subgrade and geogrid within the base. This comes with the challenge of laying the second reinforcement (geogrid) in the field, as the geogrid becomes more susceptible to damage in the process. Therefore, a

methodology should be formulated to address the challenge of laying a geosynthetic within the base in such a manner that damage is minimised.

11.0 BIBLIOGRAPHY

American Association of State Highway and Transportation Officials (AASHTO) (1993). Guide for Design of Pavement Structures, Washington, D.C.

Abu-Farsakh, M., & Chen, Q. (2011). Evaluation of geogrid base reinforcement in flexible pavement using cyclic plate load testing. *International Journal of Pavement Engineering*, *12*(3), 275–288.

Abu-Farsakh, M., & Chen, Q. (2012). Evaluation of the Base/Subgrade Soil under Repeated Loading: Phase II–In-Box and ALF Cyclic Plate Load Tests, (2).

Abu-Farsakh, M., Chen, Q., & Sharma, R. (2013). An experimental evaluation of the behavior of footings on geosynthetic-reinforced sand. *Soils and Foundations*, *53*(2), 335–348.

Abu-farsakh, M., Chen, Q., Sharma, R., & Zhang, X. (2008). Large-Scale Model Footing Tests on Geogrid-Reinforced Foundation and Marginal Embankment Soils, *31*(5), 1–11.

Al-Hunaidi, M. O., Rainer, J. H., & Tremblay, M. (1996). Control of traffic-induced vibration in buildings using vehicle suspension systems. *Soil Dynamics and Earthquake Engineering*,

Asha, M., & Madhavi, L. G. (2010). Modified CBR Tests on Geosynthetic Reinforced Soil-aggregate Systems. In *Indian geotechnical conference,Geotrendz* (pp. 2–5).

Ashmawy, A. ., & Bourdeau, P. (1995). Geosynthetic-reinforced soils under repeated loading: a review and comparative design study. *Geosynthetics …*, *2*(4), 643–668.

Bearden, J. B., & Labuz, J. F. (1999). *Fabric for Reinforcement and Separation in Unpaved Roads*. Minnesota.

Berg, R. R., Christopher, B. R., & Perkins, S. (2000). *Geosynthetic reinforcement of the aggregate base/subbase courses of pavement structures*.

Bhutta, S. A., Brandon, T. L., Reifsnider, K. L., Trani, A. A., & Walker, R. D. (1998). Mechanistic-Empirical Pavement Design Procedure For Geosynthetically Stabilized Flexible Pavements.

Bjerrum, L. (1967). Engineering Geology of Norwegian Normally-Consolidated Marine Clays as Related to Settlements of Buildings. *Géotechnique*, *17*(2), 83–118.

Bloise, N., & Ucciardo, S. (2000). On site test of reinforced freeway with high-strength geosynthetics, 5–7.

Bourdeau, P. L., Chapuis, J., & Holtz, R. D. (1988). Effect of anchorage and modulus in geotextile-reinforced unpaved roads. *Geotextiles and Geomembranes*, *7*(3), 221–230.

Brokenbrough, Ro. L., & BoedeckerKenneth J. (2004). *Highway Engineering Handbook*.

Buzzle. (2015). Physical properties of steel. Retrieved from http://www.buzzle.com/articles/physical-properties-of-steel.html

Carotti, A., & Rimoldi, P. (1998). A nonlinear model for the seismic response analysis of geosynthetic-reinforced soil structures. *Geosynthetics International*, *5*(March), 167–201.

Cebon, D. (1999). *Handbook of Vehicle-Road Interaction*. Lisse,Netherlands: Swets &Zeilinger Publishers.

Cerato, A. B. (2005). *Scale effects of shallow foundation bearing capacity on granular fill*.

Cerato, A. B., & Lutenegger, A. J. (2007). Scale effects of shallow foundation bearing capacity on granular material. *Journal of Geotechnical and Geoenvironmental Engineering*, *133*(10), 1192–1202.

Chen, Q. (2007). An experimental study on characteristics and behavior of reinforced soil foundation. PHD Thesis, Louisiana State University.

Christopher, B. R., Schwartz, C., & Boudreau, R. (2006). *Geotechnical Aspects of Pavements Reference Manual / Participant Workbook*.

Civilblog. (2015). Advantages and disadvantages of welding joints. http://civilblog.org/2015/01/24/what-are-the-advantages-and-disadvantages-of-welding-joints/

Coleman, D. M. (1990). Use of Geogrids in Railroad Track: A literature review and synopsis.

Collin, J. G., Kinney, T. ., & FU, X. (1996). Full scale highway load test of flexible pavement systems with geogrid reinforced base courses, *3*(4), 537–549.

Cox, B. R., McCartney, J. S., Wood, C., & Curry, B. (2010). performance evaluation of full scale geosynthetic reinforced flexible pavements using field cyclic plate load tests. In *Transportation Research Board 89th Annual Meeting* (p. Paper #10–1764). Washington DC: Transport Research Board.

Craig, R. (2004). *Craig's Soil Mechanics* (7th Editio.). Taylor & Francis Group.

CSIR. (1997). *THE DAMAGING EFFECTS OF OVERLOADED HEAVY VEHICLES ON ROADS*. doi: ISBN: 1-86844-285-3

Das, B. M., & Sobhan, K. (2013). *Principles of Geotechnical Engineering*. Cengage Learning.

Davis, W. C., & Jones, W. G. (1954). FLEXIBLE-PAVEMENT DESIGN BY THE GROUP INDEX METHOD. In *33rd Annual Conference of the Highway Research Board*.

de Beer, M., Fisher, C., & Kannemeyer, L. (2004). Tyre-pavement interface contact stresses on flexible pavements - Quo vadis? *8th Conference on Asphalt Pavements for Southern Africa*, (September), 681–702.

Delft Technical University. (1989). Traffic loadings and road roughness. *Traffic*, 92–115.

Diop, S., Stapelberg, F., Tegegn, K., Ngubelanga, S., & Heath, L. (2011). *A review on Problem Soils in South Africa*. Cape Town.

Duffy, O. C., & Wright, G. (2016). *Fundamentals of Medium-Heavy Duty Commercial Vehicle Systems*. Burlington,Massachusetts: Jones & Bartlett Publishers.

Erdem, C., 2007. Relationship between Resilient Modulus and soil index properties of unbound materials. MIDDLE EAST TECHNICAL UNIVERSITY.

Erlingsson, S. (2013). Failure modes in pavements. *KTH AF2903 Road Construction and MaintenanceAF2903 Road Construction and Maintenance*.

Fannin, R. J., & Sigurdsson, O. (1996). Field Observations on Stabilization of Unpaved Roads with Geosynthetics. *Journal of Geotechnical Engineering*, *122*(7), 544–553.

Federal highway administration. (2006). EPS Geofoam: Demonstrating a Lightweight Soil Alternative - September 2006 - FHWA-HRT-06-029 - Focus | Federal Highway Administration. *FHWA-HRT-06-029*. Retrieved January 15, 2016,

Franki Book. (2008). *A guide to practical Geotechnical Engineering in Southern Africa* (4th Editio.). Vivo Design Associates.

Fwa, T. (2005). *The Handbook of Highway Engineering*. Taylor & Francis Group.

Geoffroy, D. N. (1998). *Thin-surfaced Pavements*. Transportation Research Board.

Giroud, J. , & Han, J. (2004). Design Method for Geogrid-Reinforced Unpaved Roads.I. Development of Design Method. *JOURNAL OF GEOTECHNICAL AND GEOENVIRONMENTAL ENGINEERING -ASCE*, (a).

Giroud, J., & Noiray, L. (1981). Geotextile Reinforced Unpaved Road Design. *Journal of Geotechnical Engineering Division, ASCE, Vol. 107,*(No. GT9,), pp. 1233–1254. 8.

Giroud, J. P., Ah-Line, C., & Bonaparte, R. (1985). Design of unpaved roads and trafficked areas with geogrids. *Polymer Grid Reinforcement*.

Graham, J., Crooks, J., & Bell, A. L. (1983). TIME EFFECTS ON STRESS-STRAIN BEHAVIOUR OF NATURAL SOFT CLAYS. *Geotechnique*, *33*(3). Retrieved from

Gupta, R. (2010). *A study of geosynthetic reinforced flexible pavement system*. University of Texas at Austin.

Haeri, S. , Noorzad, R., & Oskoorouchi, A. (2000). Effect of geotextile reinforcement on the mechanical behaviour of sand. *Geotextiles and Geomembranes*, *18*(6), 385–402. doi:10.1016/S0266-1144(00)00005-4

Hammitt, G. M. (1970). *Thickness requirement for unsurfaced roads and airfields, bare base support, Project 3782-65*.

Hjort, M., Haraldsson, M., & Jansen, J. M. (2008). *Road wear from Heavy Vehicles*.

Hobbs, N. B. (1987). A note on the classification of peat. *Géotechnique*, *37*(3), 405–407. doi:10.1680/geot.1987.37.3.405

Holtz, R., Christopher, B., & Berg, R. (1998). *Geosynthetic design and construction guideline*. Minnesota.

Holtz, R., Christopher, B. R., & Berg, R. R. (2008). *Geosynthetic Design & Construction Guidelines Reference Manual*.

Houlsby, G. T., & Burd, H. J. (1999). *Understanding the behaviour of unpaved roads on soft clay*. Department of Engineering Science,Oxford University,U.K.

Huang, P.-T., Patel, M., Santagata, M. C., & Bobet, A. (2009). Classification of Organic Soils. *Soil Science Society of America Journal*, *B7*(1), 108.

Hufenus, R., Rueegger, R., Banjac, R., Mayor, P., Springman, S., & Bronniamann, R. (2006). Full-scale field tests on geosynthetic reinforced unpaved roads on soft subgrade. *Geotextiles and Geomembranes*, *24*(1), 21–37.

Jenkins, K. (2013). *Hitchhiker's guide to Pavement Engineering: Pavement material I*. Stellenbosch.

Jones, G. A., and Davies, P. 1985. Soft clays: problem soils in South Africa-state of the art. Civil Engineer in South Africa. Siviele Ingenieur in Suid-Afrika, 27(7), 355-357.

Jung, Y. H., Choi, C. Y., & Nsabimana, E. (2012). Modeling Shakedown Plastic Strains of Subballast and Subgrade Materials in the Concrete Slab Track System of High-Speed Trains. In *11th International conference on computational structures Technology* (pp. 1–14).

Kazimierowicz-Frankowska, K. (2007). Influence of geosynthetic reinforcement on the load-settlement characteristics of two-layer subgrade. *Geotextiles and Geomembranes*, *25*(6), 366–376

Kim, W., Edil, T. B., & Benson, C. H. (2006). Deflection of prototype geosynthetic-reinforced working platforms over soft subgrade. *Transportation Research Record*, (Paper No #06-2285), 1–25.

Kiron, M. I. (2016). Types of Geotextile | Geotextile of Woven Fabrics, Non-woven Fabrics and Knitted Fabrics - Textile Learner

Koerner, R. M. (2012). *Designing with Geosynthetics* (6th Editio.). New Jersey: Pearson Prentice Hall, Upper Saddle River.

Kupec, J., & McGown, A. (2004). The Biaxial load-strain behaviour of Biaxial Geogrids. In *Geoasia04*.

Latha, G. M., & Somwanshi, A. (2009). Bearing capacity of square footings on geosynthetic reinforced sand. *Geotextiles and Geomembranes*, *27*(4), 281–294.

Lau, C. K., & Bolton, M. D. (2011). The bearing capacity of footings on granular soils . II : Experimental evidence. *Geotechnique*, *61*(8), 639–650

Lee, K. W., Marcus, A. S., Mooney, K., Vajjhala, S., Kraus, E., & Park, K. (2003). *DEVELOPMENT OF FLEXIBLE PAVEMENT DESIGN PARAMETERS FOR USE WITH THE 1993 AASHTO PAVEMENT DESIGN PROCEDURES*.

Lekarp, F., Isacsson, U., & Dawson, A. (2000). State of the Art. I: Resilient Response of Unbound Aggregates. *Journal of Transportation Engineering*, *126*(1), 66–75.

Leng, J. (2002). *Characteristics and behaviour of geogrid-reinforced aggregate under cyclic load*. North Carolina State University.

Look, B. G. (2014). *Handbook of Geotechnical Engineering Investigation and Design Tables* (second edition.). CRC Press,Taylor & Francis Group.

Love, J. ., Burd, H. ., Milligan, W. ., & Houlsby, G. (1987). Analytical and model studies of reinforcement of a layer of granular fill on a soft clay subgrade.pdf.

Malla R., & Joshi S. (2006). Establish subgrade support values for typical soils in New England. Prepared for The New England Transportation Consortium. Project No. 02-3

Mallik, R. B., & El-Korchi, T. (2013). *PAVEMENT ENGINEERING-Principles and Practice* (2nd Editio.). New York: CRC Press,Taylor & Francis Group.

Mandal, J. N., & Das, B. M. (1993). Ultimate bearing capacity of shallow foundation on geogrid-reinforced sand Capacité portante maximale de fondations superficielles avec armature géogrille, (2), 1397–1400.

Mawer, B. (2013). *Thesis : Reinforcement of soft clay soils using geotextiles*. University of Cape Town.

Maxwell, S., Kim, W., Edil, T. B., & Benson, C. H. (2005). EFFECTIVENESS OF GEOSYNTHETICS IN STABILIZING SOFT SUBGRADES By.

Milligan, G. W. ., Jewell, R. A., Houlsby, G. ., & Burd, H. . (1989). A New Approach to the Design of Unpaved Roads - Part II. *Ground Engineering*, *Vol. 22*(No. 8).

Moayed, R., & Nazari, M. (2011). Effect of Utilization of Geosynthetic on Reducing the Required Thickness of Subbase Layer of a Two Layered Soil. *World Academy of Science, Engineering and …*, 963–967

Moayedi, H., Kazemian, S., Prasad, A., & Huat, B. (2009). Effect of geogrid reinforcement location in paved road improvement. *Electronic Journal of Geotechnical Engineering*, *14 P*, 1–11.

Moghaddas-Nejad, F., & Small, J. (1996). Effect of geogrid reinforcement in model track tests on pavements. *Journal of Transportation …*, (December), 468–474

Montanelli, F., Zhao, A., & Rimoldi, P. (1997). Geosynthetic-reinforced pavement system: testing & design. In *Proceeding of Geosynthetics* (Vol. 97, pp. 619–632).

Morton, B., Luttig, E., Horak, E., & Visser, A. (2004). The Effect of Axle Load Spectra and Tyre Inflation Pressures on Standard Pavement Design Methods. In *8th Conference on Asphalt pavements for Southern Africa*. Sun City,South Africa

Mukabi, J. , & Tatsuoka, F. (1999). Influence of reconsolidation stress history and strain rate on the behaviour of kaolin over a wide range of strain. In *Geotechnics for Developing Africa: Proceedings of the 12th regional conference for Africa on soil mechanics and geotechnical engineering, Durban, South Africa, 25-27 October 1999* (p. 698). CRC Press

Munfakh, G., Arman, A., Collin, J. G., Hung, J. C. J., and Brouillette, R. P. 2001. Shallow foundations reference manual. National Highway Institute, Federal Highway Administration, US Department of Transportation, Washington, DC, 222.

Murray, H. H. (1999). Applied clay mineralogy today and tomorrow. *Clay Minerals*, *34*, 39–49. doi:10.1180/000985599546055

Murthy, V. N. (2002). *Geotechnical Engineering. Principles and practices of Soils Mechanics and Foundation Engineering*.

Nordengen, P. (2009). National Transport Month Opinion Piece. *Council for Scientific and Industrial Research (CSIR)*.

Ntirenganya, N. (2014). *An Investigation of the Interlayer Adhesion Strength between the Granular Base and Lightly Cemented Subbase and Its Influence on the Pavement Performance*. Stellenbosch University.

Oh, W. T., & Vanapalli, S. K. (2013). Scale Effect of Plate Load Tests in Unsaturated Soils. *International Journal of Geomaterials*, *4*(2), 585–594.

Oloo, S. Y., Fredlund, D. G., & Gan, J. K.-M. (1997). Bearing capacity of unpaved roads. *Canadian Geotechnical Journal*, *34*(1981), 398–407

Oriokot, J. (2014). *Reinforcement of pavement subgrade using granular fill and a Geosynthetic layer.* University of Cape Town.

Ovesen, N. (1975). Centrifugal Testing Applied to Bearing Capacity Problems of Footings on Sand. *Geotechnique.*, *Vol. 25*(No. 2.), 394–401.

Paige-Green, P. (2004). THE GEOLOGY AND ENGINEERING GEOLOGY. In *Proceedings of the 23rd Southern African Transport conference (SATC 2004)*. Pretoria.

Paige-Green, P., (2006). Appropriate Roads for Rural Access. *Gulf Conference on Roads, Proceedings of the Third*, pp.1–10.

Paige-Green, P. (2008). Dealing with Road Subgrade Problems in Southern Africa. In *The 12th International Conference of International Association for Computer Methods and Advances in Geomechanics (IACMAG)*. Goa,India.

Palmeira, E. M., & Cunha, M. G. (1993). A study of the mechanics of unpaved roads with reference to the effects of surface maintenance. *Geotextiles and Geomembranes*, *12*(2), 109–131

Patra, C. R., Das, B. M., & Atalar, C. (2005). Bearing capacity of embedded strip foundation on geogrid-reinforced sand. *Geotextiles and Geomembranes*, *23*(5), 454–462. doi:10.1016/j.geotexmem.2005.02.001

Pavement interactive. (2015). Pavement Interactive | Your destination for all things pavement. Retrieved February 1, 2016, from http://www.pavementinteractive.org/

Perkins, S. (1999). Mechanical response of geosynthetic-reinforced flexible pavements. *Geosynthetics International*, *6*(5), 347–382

Perkins, S. (2000). Constitutive modelling of geosynthetics. *Geotextiles and Geomembranes*, *18*(August 1999), 273–292. doi:10.1016/S0266-1144(99)00021-7

Perkins, S. (2001). *Mechanistic-Empirical Modeling and Design Model Development of Geosynthetic Reinforced Flexible Pavements*. Montana.

Perkins, S., & Ismeik, M. (1997). A synthesis and evaluation of geosynthetic-reinforced base layers in flexible pavements: Part I. *Geosynthetics …*, *4*(6), 605–621

Pham, T. (2009). *INVESTIGATING COMPOSITE BEHAVIOR OF GEOSYNTHETIC-REINFORCED SOIL (GRS) MASS*. University of Colorado Denver.

PMSA. (2015). V200/V300 mixers. Retrieved from http://www.pmsa.com/images/V200/V200 & V300 SPEC SHEET.pdf

Pokharel, S. K. (1997). *Experimental Study on Geocell-Reinforced Bases under Static and Dynamic Loading*. University of Kansas.

Propex. (2011). Geotextile Functions in Paved and Unpaved Roads. *ENGINEERING BULLETIN EB-101*.

Public works South Africa. (2007). *Identification of problematic soils in Southern Africa*. Pretoria,South Africa.

Qian, Y., Han, J., Pokharel, S. K., & Parsons, R. L. (2011). Stress Analysis on Triangular-Aperture Geogrid-Reinforced Bases over Weak Subgrade Under Cyclic Loading. *Transportation Research Record: Journal of the Transportation Research Board*, *2204*(-1), 83–91. doi:10.3141/2204-11

Redlight-Gbarnga-Liberia, (2012). Output and Performance-Based Road Contract (OPRC)(Road Asset Management Contract) for the Design, Rehabilitation and Maintenance

Ruiken, A., & Ziegler, M. (2008). Effect of reinforcement on the load bearing capacity of geosynthetic reinforced soil. *EuroGeo4*.

Sanjay, K. S. (2012). *Handbook of Geosynthetic Engineering* (Second Edi.). ICE Publishing.

Sapem-Materials testing. (2013). *South African Pavement Engineering manual- Chapter 3*.

Sapem-Pavement design. (2013). *South African Pavement Engineering manual- Chapter 10*.

Sarsby, R. (2007). *Geosynthetics in Civil Engineering*. CRC Press.

Sawangsuriya, A., Bosscher, P. J., & Edil, T. B. (2002). Laboratory Evaluation of the Soil Stiffness Gauge. *Transportation Research Board*, (November 2015).

Scholosser, F., & Long, N. T. (1972). Comportement de al terre armée dans les ouvrages de soutènement. In*: Proceedings of the European Conference on Soil Mechanics and Foundation Engineering,Vol. 1* (pp. 299−306). Madrid.

Shukla, S., & Yin, J. (2006). *Fundamentals of geosynthetic engineering*. Taylor & Francis Group

Siddique, M. S. A., Tanaka, T., Tatsuoka, F., Tani, K., & Morimoto, T. (1999). Numerical Simulation of Bearing Capacity Characteristics of Strip Footing on Sand. *Soils and Foundations*. doi:10.3208/sandf.39.4_93

Siripun, K., Jitsangiam, P., & Nikraz, H. (2011). Dynamic Response Improvement of Crushed Rock With Cement Modification. In *Deformation Characteristics of Geomaterials: Proceedings of the Fifth International Symposium on Deformation Characteristics of Geomaterials, IS-Seoul 2011, 1-3 September 2011, Seoul, Korea* (pp. 754 – 761).

Slocombe, B. (2001). *Deep compaction of problematic soils,Problematic soils*. Thomas Telford Ltd

Som, N., & Sahu, R. (1999). Bearing capacity of a geotextile-reinforced unpaved road as a function of deformation: a model study. *Geosynthetics International*, *6*(1), 1–17.

South Africa Department of Transportation. (2012). *Unproclaimed roads & road maintenance budgets: Department of Transport briefing*

Suppes, T., McConnell, R. L., Dennehy, E. B., Abel, D. C., & McConnell, R. L. (2013). *Environmental Geology Today*. Jones & Bartlett Publishers

Tafreshi, S. N. M., & Dawson, a. R. (2010). Behaviour of footings on reinforced sand subjected to repeated loading – Comparing use of 3D and planar geotextile. *Geotextiles and Geomembranes*, *28*(5), 434–447.

Talukdar, D. K. (2014). A Study of Correlation Between California Bearing Ratio (CBR) Value With Other Properties of Soil, *4*(1), 559–562.

Tan, kim H. (1995). *Soil Sampling, Preparation, and Analysis*. CRC Press,Taylor & Francis Group.

Tencate. (2014). *Application of the Giroud – Han Design Method for Geosynthetic Reinforced Unpaved Roads with TenCate Mirafi ® Geosynthetics*

Tencate mirafi. (2010a). Geosynthetic Reinforcement of the Aggregate Base / Subbase courses of pavement structures, 1–7.

Tencate, (2010b). *Benefits of Subgrade Stabilization Using Geosynthetics Versus Lime*.

Theyse, H., & Muthen, M. (2000). Pavement Analysis and Design Software (PADS) Based on the South African Mechanistic-Empirical Design Method. In *South African Transport Conference (SATC). Action in Transport for the new Millennium*.

Tingle, J., & Jersey, S. (2005). Cyclic Plate Load Testing of Geosynthetic-Reinforced Unbound Aggregate Roads. *Transportation Research Record*, *1936*(1), 60–69.

Toyosawa, Y., Itoh, K., Kikkawa, N., Yang, J.-J., & Liu, F. (2013). Influence of model footing diameter and embedded depth on particle size effect in centrifugal bearing capacity tests. *Soils and Foundations*, *53*(2), 349–356.

TRH4. (1996). *Structural design of flexible pavements for interurban and rural roads*. Pretoria,South Africa. doi:ISBN 1-86844-21 8-7

U.S Army corps of Engineers. (2002). *Use of geogrids in pavement construction* (Vol. Engineer T). Washington DC.

US Geological survey. (1999). Environmental Characteristics of Clays and Clay Mineral Deposits

US. Army. (1974). *Planning and Design of Roads, Airbases, and Heliports in the Theater of Operations*. Departments of the Army and Air Force

Webster, S. L. (1992). *Geogrid Reinforced Base Course for Flexible Pavements for Light Aircraft: Test Section Construction, Behavior under Traffic, Laboratory Test, and Design Criteria*.

Weng, L. K. (2003). *ANCHORED AND PRETENSIONED GEOTEXTILES FOR UNPAVED ROAD STABILISATION*. National University of Singapore

Werkmeister, S., Dawson, A. R., & Wellner, F. (2005). Permanent Deformation Behaviour of Granular Materials. *Road Materials and Pavement Design*, *6*(1), 31–51.

Widodo, S. (2013). *ANALYSIS OF DYNAMIC LOADING BEHAVIOUR FOR PAVEMENT ON SOFT SOIL*. Technische Universitat Bergakademie Freiberg.

Yang, H. H. (2004). *Pavement analysis and design* (2nd Editio.). Kentucky: Pearson Education, inc.

Yetimoglu, T., Wu, J., & Saglamer, A. (1994). Bearing capacity of rectangular footings on geogrid-reinforced sand. *Journal of Geotechnical …*, *120*(12), 2083–2099

Yoder, E.J. (1959). Principles of pavement design. John Wiley and Sons, Inc. New York.

Yoder, E. J., & Witczcak, M. (1975). *Principle of Pavement Design*. John Wiley & Sons.

Yu, H., McDowell, G., Dawson, A. R., & Thom, N. (2008). *Advances in Transportation Geotechnics: Proceedings of the International Conference held in Nottingham, UK, 25-27 August 2008*. CRC Press.

Zhan, C., & Yin, J. H. (2001). Elastic Analysis of Soil-Geosynthetic Interaction. *Geosynthetics International*, *8*(1), 27–48.

Zornberg, J. (2011). Advances in the use of Geosynthetics in Pavement design. In *Geosynthetics India'11,IIT Madras,Chennai* (pp. 23–24)

12.0 APPENDIX

12.1 SOFT CLAY SUBGRADE CHARACTERISATION TESTS

Atterberg limits - Kaolin clay

a) Liquid limit

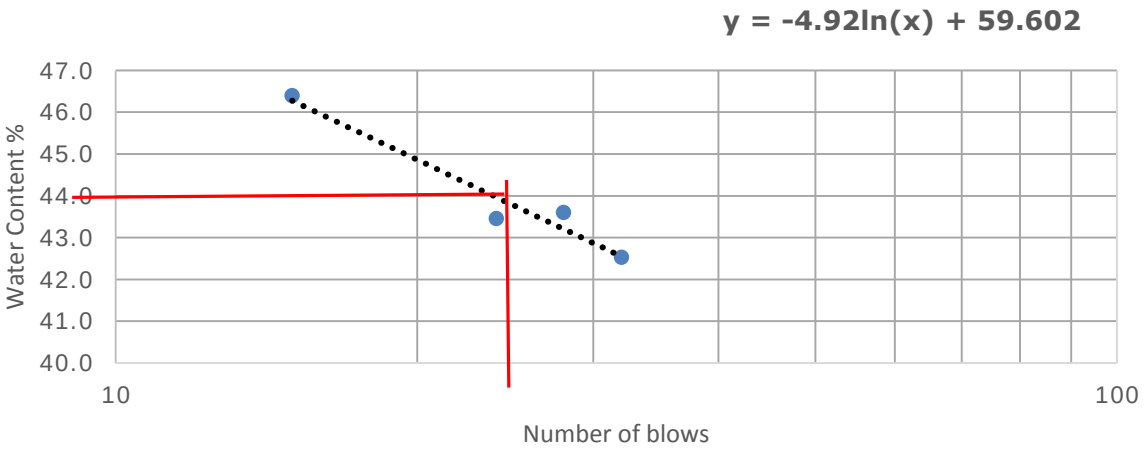

b) Plastic limit

Sample Number	1	2	3
Mass of container(g)	16.34	16.11	16.74
Mass of container + wet soil	19.61	19.67	19.64
Mass of container + dry soil (g)	18.92	18.92	18.83
Mass of water (g)	2.58	2.81	3.05
Mass of dry soil (g)	0.69	0.75	0.81
Moisture content (%)	26.7	26.7	26.6
	26.7		

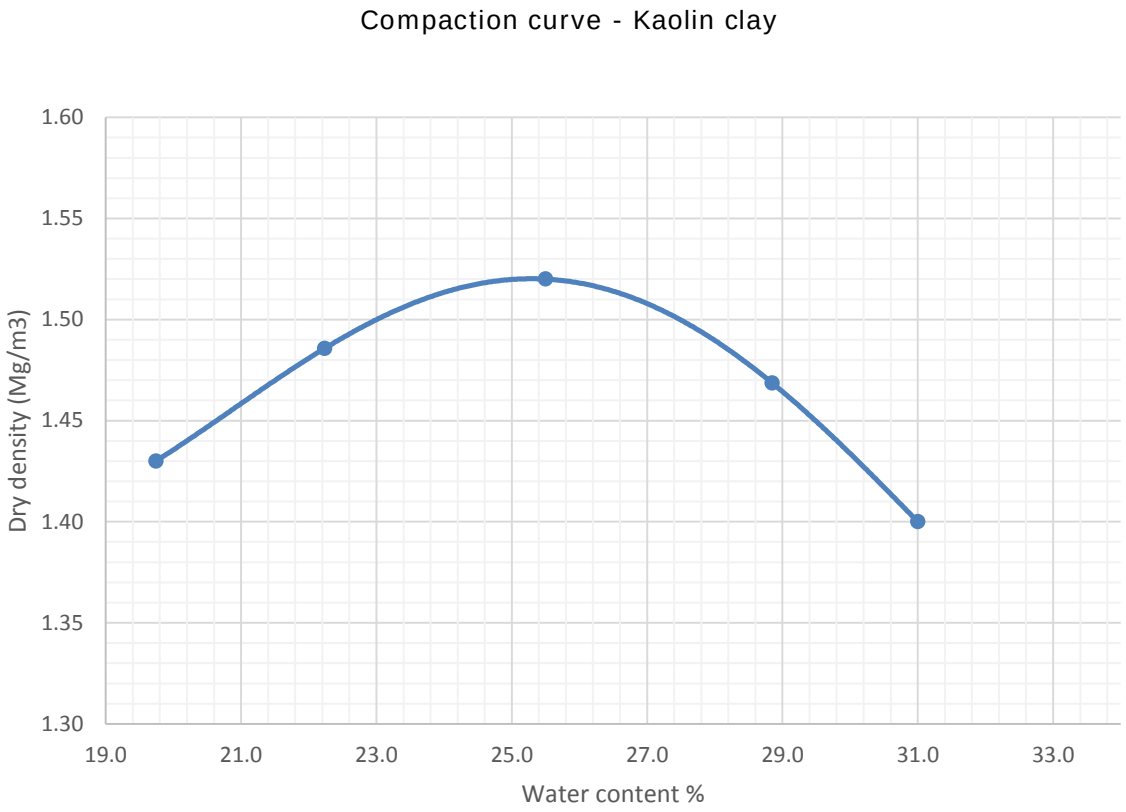

12.2 GRANULAR BASE CHARACTERISATION TESTS

Atterberg limits - G7 Base soil

a) Liquid limit

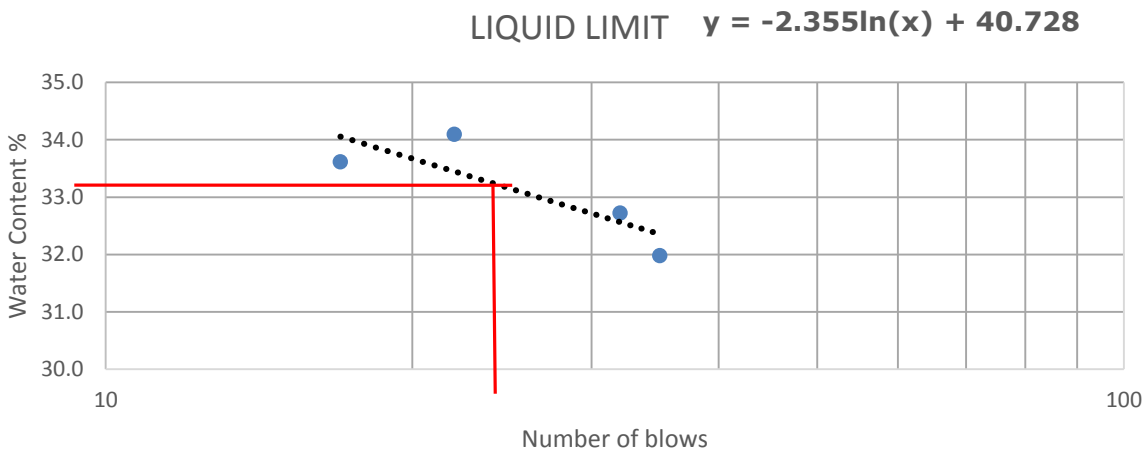

b) Plastic limit

Sample Number	1	2	3
Mass of container(g)	16.7	16.31	16.9
Mass of container + wet soil	19.12	19.41	19.77
Mass of container + dry soil (g)	18.72	18.9	19.12
Mass of water (g)	2.02	2.59	3.16
Mass of dry soil (g)	0.4	0.51	0.65
Moisture content (%)	19.8	19.7	20.6
	20.0		

Compaction curve - G7 Base material

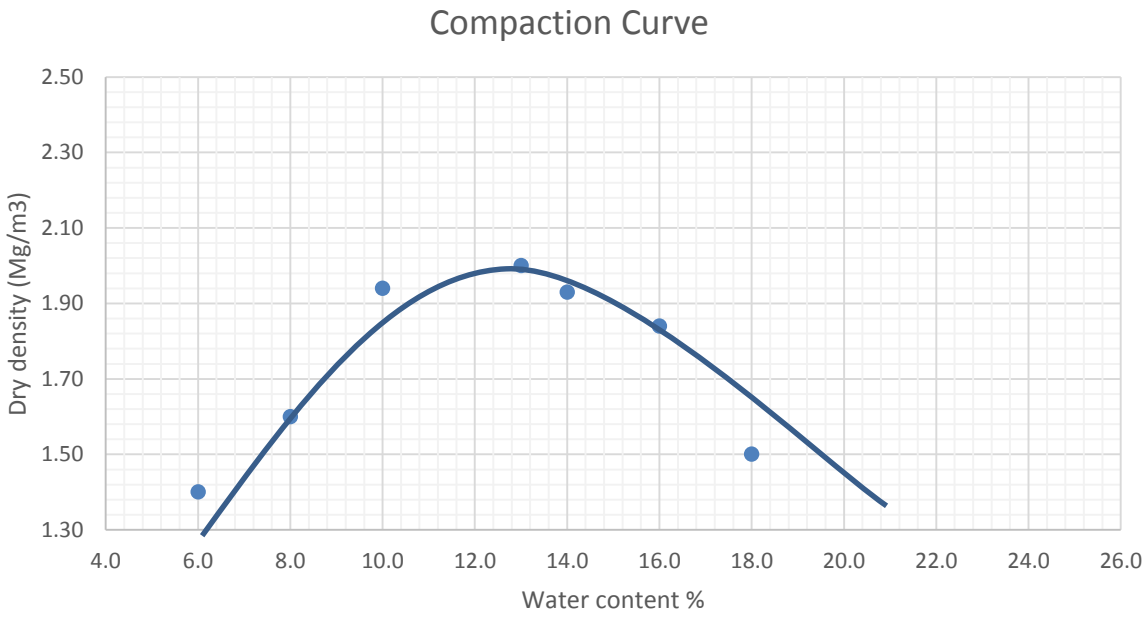

CBR for G7 base material

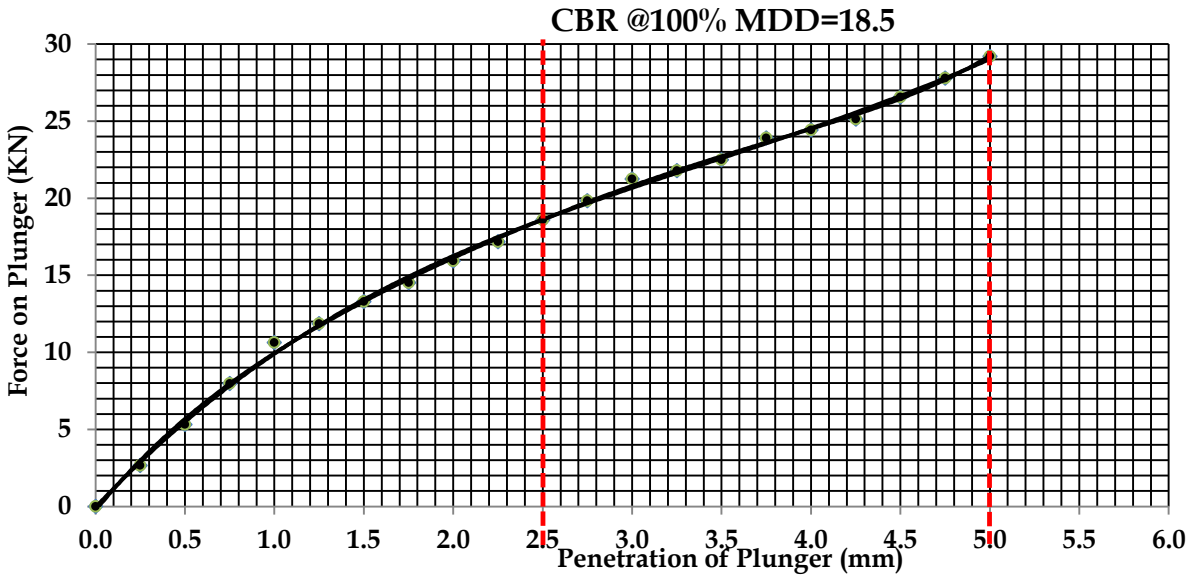

12.3 CHOICE OF DESIGN PARAMETERS

The main objective of design is to determine a satisfactory thickness of the pavement layers that is able to satisfy serviceability, cost-effectiveness, load carrying capacity and limited deterioration over the design period requirements. The following are the criteria that informed the choice of parameters such as predicted future traffic, reliability, overall standard deviation, road bed resilient modulus, design serviceability loss, drainage coefficient and layer coefficient required for the AASHTO design.

12.3.1 Predicted future traffic (W_{18})

Pavements are normally designed to accommodate cumulative traffic for several years into the future. Because of the mix of traffic i.e. passenger cars, buses, trucks with different axle configurations, the accumulated traffic has to be standardised by presenting it in terms of Equivalent Single Axle Loads (ESALs). AASHTO defines ESAL as 80KN, and it is denoted in literature by the symbol W_{18}.

The 1993 AASHTO guide developed Equivalent Axle Load Factors (EALF) to relate the damage resulting from different load magnitudes and axle configurations to the standard

axle. Conversion factors of axle loads other than 80 kN are available in the appendix of the AASHTO design guide for design pavement structures.

In this design, 80 kN ESAL repetitions (W_{18}) of 30 000 will be assumed considering a road founded on a soft soil with a granular base.

12.3.2 Reliability

AASHTO uses the reliability concept to account for design uncertainties. Uncertainties in pavement design problems can arise from traffic prediction, material characterisation and behaviour modelling, environmental conditions, etc. as well as variability during construction and maintenance. Also, the lack of input parameters required to better characterise the traffic results in uncertainties. Therefore, the factor was introduced in the design equation to account for these uncertainties.

Reliability of a pavement design-performance process is generally defined as the probability that a pavement section designed using the process will perform satisfactorily over the traffic and environmental conditions for the design period (1993 AASHTO Guide Part 1- Chapter 4-4.11). The selection of appropriate level of reliability for the design of a particular facility depends primarily upon the projected level of usage and the consequences associated with constructing an initially thinner pavement structure.

A design reliability of 50% by the Transport Research Board (TRB) for low volume roads has been recommended because of the relatively low usage and associated low level of risk.

Table 12-1 Suggested levels of reliability for various highway classes (AASHTO 1993)

Functional classification	**Recommended level of reliability**	
	Urban	**Rural**
Interstate and freeways	85-99.9	80-99.9
Principal arterials	80-99	75-95
Collectors	80-95	75-95
Locals	50-80	50-80

12.3.3 Overall standard deviation

The overall standard deviation takes into consideration the variability of all input data. AASHTO 1993 design guide recommends a range of 0.3-0.5 for flexible pavements. An overall standard deviation (S_o) is thus selected by the designer in this range.

12.3.4 Roadbed soil resilient modulus

All materials experience deformation (strain) when subjected to loading (stress). Failure does not occur for as long as the stress is less than the strength of the material. The relationship between stress and strain can be expressed as resilient modulus (MR). The resilient modulus of a roadbed is determined in the laboratory according to AASHTO T307 method (AASHTO, 2004). Resilient modulus is dependent on the moisture content; therefore, different resilient moduli will be obtained in different seasons depending on the amount of rain. Thus, a value that is representative of the different seasons depending on the amount of rainfall is required.

Since laboratory tests are time consuming, empirical correlations between MR and CBR have been developed as an estimate. The resilient modulus for this study will be considered as determined by the Equation below from the AASHTO design guideline.

$$M_R\ (psi) = 1500.CBR \qquad \text{Equation 12-1}$$

12.3.5 Design serviceability loss (Δpsi)

Serviceability is the ability of a road section to serve traffic in its existing condition. The serviceability loss is the difference between the initial serviceability index P_o and the terminal serviceability index P_t.

$$\Delta PSI = P_o - P_t \qquad \text{Equation 12-2}$$

PSI ranges from 0 to 5 where 0 means the existing road condition is impossible for driving, and 5 means the road is in perfect condition for driving. A value of P_t of 2.5 or higher is used for the design of major highways while a P_t of 2.0 is adopted for low volume roads. The typical P_o value for a new pavement is 4.6 or 4.5. Considering a P_o of 4.5 and a P_t of 2.0, a ΔPSI of 2.5 is used for this design problem.

12.3.1 Drainage coefficient (mi)

Drainage coefficient is an indicative value of the quality of drainage and availability of moisture in the granular base and sub-base. The drainage coefficient for the untreated base and subbase has been recommended by AASHTO (1993). For good drainage, it is assumed that when the pavement is exposed to moisture levels nearing saturation, the base should be able to drain within one day, and a coefficient value of 0.9 is adopted (Fwa, 2005).

12.3.1 Layer coefficient (a_i)

The structural layer coefficient refers to the measure of the relative ability of a unit thickness of a given material to function as a structural component of the pavement. AASHTO design has categorised the different values that are applicable as the layer coefficient for the different types of pavement materials. A layer coefficient of 0.1 will be used for the base which has been determined for sand, and a value of 0.44 for HMA.

12.4 EBE Faculty: Assessment of Ethics in Research Projects

Any person planning to undertake research in the Faculty of Engineering and the Built Environment at the University of Cape Town is required to complete this form before collecting or analysing data. When completed it should be submitted to the supervisor (where applicable) and from there to the Head of Department. If any of the questions below have been answered YES, and the applicant is NOT a fourth year student, the Head should forward this form for approval by the Faculty EIR committee: submit to Ms Zakiya Chikte (**Zakiya.chikte@uct.ac.za)**; New EBE Building, Ph 021 650 5739).

Students must include a copy of the completed form with the dissertation/thesis when it is submitted for examination.

Name of Principal Researcher/Student: **Department:** Civil Engineering

If a Student: **Degree:** **Supervisor:** Dr Denis Kalumba

Dennis K. Kiptoo Msc. Civil Engineering,specialising in geotechnical Engineering

If a Research Contract indicate source of funding/sponsorship: None

Research Project Title: AN INVESTIGATION OF THE EFFECT OF STATIC AND DYNAMIC LOADING TO GEOSYNTHETIC REINFORCED PAVEMENTS OVERLYING A SOFT SUBGRADE

Overview of ethics issues in your research project:

Question 1: Is there a possibility that your research could cause harm to a third party (i.e. a person not involved in your project)?	YES	**NO** ✓
Question 2: Is your research making use of human subjects as sources of data? If your answer is YES, please complete Addendum 2.	YES	**NO** ✓
Question 3: Does your research involve the participation of or provision of services to communities? If your answer is YES, please complete Addendum 3.	YES	**NO** ✓
Question 4: If your research is sponsored, is there any potential for conflicts of interest? If your answer is YES, please complete Addendum 4.	YES	**NO** ✓

If you have answered YES to any of the above questions, please append a copy of your research proposal, as well as any interview schedules or questionnaires (Addendum 1) and please complete further addenda as appropriate.

I hereby undertake to carry out my research in such a way that

- there is no apparent legal objection to the nature or the method of research; and
- the research will not compromise staff or students or the other responsibilities of the University;
- the stated objective will be achieved, and the findings will have a high degree of validity;
- limitations and alternative interpretations will be considered;
- the findings could be subject to peer review and publicly available; and
- I will comply with the conventions of copyright and avoid any practice that would constitute plagiarism.

Signed by:

	Full name and signature	Date
Principal Researcher/Student:	Dennis K. Kiptoo Signed by candidate	16th Feb 2016

This application is approved by:

Supervisor (if applicable):	Dr Denis Kalumba	16th Feb 2016
HOD (or delegated nominee): Final authority for all assessments with NO to all questions and for all undergraduate research.		16 FEB 16
Chair : Faculty EIR Committee For applicants other than undergraduate students who have answered YES to any of the above questions.		